C.P. No. 959

C.P. No. 959

MINISTRY OF TECHNOLOGY

AERONAUTICAL RESEARCH COUNCIL

CURRENT PAPERS

The Influence of Gas Streams and Magnetic Fields on Electric Discharges

Part 3. Arcs in Transverse Magnetic Fields at Atmospheric Pressure

by

V. W. Adams

LONDON: HER MAJESTY'S STATIONERY OFFICE

1967

PRICE 15s Od NET

C.P. No.959*
December 1965

THE INFLUENCE OF GAS STREAMS AND MAGNETIC FIELDS ON ELECTRIC DISCHARGES
PART 3. ARCS IN TRANSVERSE MAGNETIC FIELDS AT ATMOSPHERIC PRESSURE

by

V. W. Adams

SUMMARY

Experimental results in air at a pressure of one atmosphere on the bohaviour of arcs under the action of applied magnetic fields are given for two electrode materials (graphite and brass) and different electrode configurations. These results extend earlier work, in annular gaps using graphite, to larger electrode path lengths on graphite and brass, and also include results for a pair of long straight electrodes. The *range* of arc current has been extended to 3700 amps and the applied magnetic field to 0·49 Wb/m^2 for experiments on a pair of straight electrodes.

The results are analysed using a simple model for the arc motion assuming that the arc behaves in the same way as a body in a gas stream. Some comments are made on a major difference between results for brass and graphite electrodes in experiments where the arc wake might affect the arc motion (annular gaps). Arc drag areas are calculated for results where the arc wake does not affect the motion (pair of open-ended rail electrodes) and are found to be about one half of the maximum luminous frontal areas of the arc determined photographically. A tentative picture of the arc's cross-sectional shape is also given.

Finally, the results are analysed according to a theory for convection-stabilised arc columns and smoothed-out results for arcs moving through stationary air at constant temperature are shown to agree qualitatively with this theory.

However, a direct analogy between an arc and a heated solid body in a transverse gas flow is shown to be inadequate.

---

* Replaces R.A.E. Technical Report No.65273 - A.R.C.28072

CONTENTS

ILLUSTRATIONS

ILLUSTRATIONS (Contd)

1 INTRODUCTION

This Paper is a continuation of the work discussed previously[1] and is concerned with the behaviour of direct-current arc discharges in air at a pressure of *one* atmosphere propelled along electrode systems by external magnetic fields. The experiments of the previous reports are confined to arcs moving round *annular* gaps with graphite as the electrode material, and because of the short electrode path length round which the arc moves and the speed of the arc it is difficult to define the state of the ambient gas; the arc moves in its own wake. Three extensions of this work have been studied:-

(a) The motion of arcs around annular gaps with longer electrode path lengths (circumference) where the wake effects would be expected to diminish.

(b) The motion of arcs immediately after initiation and along a pair of open-ended *rail* electrodes *where* the *arc* does not *move in* its own wake.

(c) The motion of arcs on brass electrodes. Brass and copper were considered as suitable materials, brass finally being chosen because a large amount of work had already been done with this material at very small gaps [2,3,4]. Earlier work indicated that results with copper electrodes *were* unpredictable and widely scattered[2].

With annular brass electrodes, it was fairly easy to increase the path length *to* 1·12m, which was the limit imposed by the existing field coil, while with graphite the convenient limit was 0·48m. In addition, by making use of an apparatus primarily intended for studying a different aspect of the arc motion over straight electrodes (namely arc shape) it was possible to increase the path length to 2·19m, but it should be noted that in this case the path although mostly uniform and straight was interrupted by two sharp bends, see Fig.1(a). This apparatus also permitted the use of larger arc currents and magnetic fields than did the annular electrodes and existing field coil, and some work on the initial motion i.e., before moving into the wake, was possible. No work with graphite has been done with this shape of electrode path.

Most of the results on the initial motion were obtained for both brass and graphite on pairs of open-ended rail electrodes (Figs.1(b) and (c)). This permitted the use of even larger arc currents because overheating of the electrodes became a minor problem except at low velocities, and the rotating machines providing the arc power could be overloaded for the short duration of the *arc.* The maximum *arc* velocity recorded was 435 m/sec (Mach number 1·24) with an arc current of 3600 amp and an applied magnetic field of 0·49 Wb/m^2.

The experimental results are presented in graphical form showing relationships between arc velocity, U, electrode path length, applied magnetic field, B, arc current, I, and arc voltage, V.

The analysis of the results is concerned with two main aspects relating to:-

(i) motion of the arc (velocity measurements)

(ii) heat transfer to the surrounding air (voltage measurements).

In the first case, we are concerned with relations between U end electrode path length at constant B and I and also relations between U, B and I with a fixed path length. We use a simple model of the arc column similar to that used earlier and based on a flexible conducting body moving in a transverse magnetic field where the electromagnetic driving force and the aerodynamic retarding force arc equated[1,5,6,7,8]. In the second case, we are concerned with relations between V (or more exactly E, the column voltage gradient), B, I and U and we use parameters suggested by a theoretical treatment [8,9] of the convective and radiative heat losses from an arc column held stationary in a gas flow by means of an external magnetic field.

The ranges over which the effects of the parameters B, I, U and E were explored were restricted by practical considerations such as (1) size and range of power supplies available, (2) the fact that very-high-current arcs could not be propelled at low velocities because of overheating of the electrodes (small diameter uncooled metal electrodes could not be used for arcs rotating round annular gaps and only the apparatus providing the longest path length could be used for high current arcs on uncooled brass electrodes), (3) the fact that very long arcs could not be propelled over long distances because of instability due to external disturbances (e.g. natural convection).

2 DESCRIPTION OF APPARATUS AND METHODS OF MEASUREMENT

2.1 Field coils and electrical supplies

The experiments with annular gap electrodes were made using a solenoid 0·45m inside diameter and 0·45m long consisting of 180 turns of 100 amp "PREN" cable wound on an existing wooden former. This imposed the limit on the maximum diameter of electrodes used and hence on the electrode path length for arc motion. The maximum value of magnetic field obtainable for short periods was 0·1 Wb/m^2 at the centre of the coil.

The electromagnet providing the transverse driving fields for experiments using straight electrodes was constructed from copper bar (10 x 0·6 cm) and produced a vertical uniform field over a horizontal plane 1·5m long and 0·1m wide; it was designed for use with a long cylindrical pressure vessel[10] and a general view is shown in Fig.2. The maximum value of the magnetic field was, until recently, limited by the power supply available; a 12 volt 1200 amp d.c. generator giving a field of 0·12 Wb/m^2. However, a new power supply consisting of a 3-phase transformer and solid state rectifiers capable of providing 10000 amp at 120 volts has recently become available and has to date been used at $\frac{1}{4}$ maximum power giving a field of 0·47 Wb/m^2.

The arcs were supplied from four Ward-Leonard 600 volt, 600 amp d.c. motor generator sets each with a series stabilising resistance consisting of two groups of one hundred 1 kW, 50 ohm radiant fire bar elements connected in parallel, and arranged so that these groups could be used in either series or parallel. The generators had separate excitation controls and circuit breakers and were used in parallel for very large arc currents, each machine being switched in consecutively. In order to propel very high current arcs along a pair of straight open-ended rail electrodes a circuit breaker capable of switching all four machines together was used.

2.2 Electrodes

(a) Graphite

Two electrodes configurations were employed:-

(i) Circular electrodes of various diameters forming annular gaps with different path lengths. These electrodes were described in Ref.1 where results were given for path lengths up to 0·315m with a 0·7 cm gap. New electrodes have been made to increase the path length to 0·48m by making use of a fabricated outer electrode made in sections clamped between two brass rings.

(ii) A pair of open-ended rail electrodes 1·2m x 0·055m x 0·025m with electrical connections to one end were used for work on the initial motion of arcs as shown in Fig.1(c). The arcs were started at one end by fusing a short length of 20 swg copper wire connected across the electrodes, and the magnetic field was applied so that it was added to the field due to the arc current in the electrodes (calculated as in Appendix A). It was evident from the tracks left by the arcs on the electrodes that the arc roots wandered over the top surfaces, and in an attempt to prevent this happening in subsequent work using metal electrodes it was decided to sandwich them between layers of refractory insulating material.

(b) Brass

Three electrode configurations, made with 10 swg (0·325 cm) brass sandwiched between refractory insulating material so that the arc roots were restricted to a thin edge, have been used:-

(i) Circular electrodes of various diameters were made so that results for arcs rotating round 'annular gaps with different path lengths could be obtained. Three pairs of electrodes were used with a gap width of 1·27 cm for inner electrode radii of 6·35 cm, 12·7 cm and 17 · 8 cm as shown in Fig.3(a). A shorter track length using electrode radii of 2·54 cm and 3·81 cm was also obtained using the simple design of water cooled electrodes shown in Fig.3(b) where each electrode was isolated by rubber hose from the mains water supply. It is planned to continue some work with these electrodes and eventually incorporate water-cooled electrodes in a pressure vessel. The electrical connections to the inner electrode (cathode) were made via equal stabilising resistances to each end of the central rod or tube support so that there was no resultant magnetic field due to the arc current. The connections to the outer electrodes were made to both ends of the three equally spaced bars or tubes used for supporting the electrode.

(ii) Two electrodes, intended primarily for studying *arc* shapes by high speed photography over a relatively long time interval enabled the electrode path length to be increased to 2·19m as shown *in* Fig.1(a). Electrode spacings of 1·27 cm, 2·54 cm and 3·81 cm were used, and *one* set of electrodes 0·63 cm thick, with a 1·27 cm spacing were also made for high arc currents.

(iii) A pair of open-ended rail electrodes, 1·2m x 0·038m with electrical connections to one end as shown in Fig.1(b). The additional field due to the arc current in the electrodes was calculated as in Appendix A.

For the above electrode configurations (i) and (ii) the arcs were started by using a piece of folded metal foil pushed between the electrodes; it was found that this did not melt but acted as a moving connection which was ejected from the electrode system thus forming an arc in a distance of less than 15 cm. The arcs on the pair of open-ended rails (iii) *were* started by fusing a short length of wire.

2.3 Measuring equipment and methods

Measurements of the mean arc velocity or frequency of rotation (depending on which electrode configuration was used), the total arc voltage, arc current and applied magnetic field were made. In the case of the circular electrodes

with annular gaps and the brass electrodes of Fig.1(a) the measurements were made for a period corresponding to several cycles of the arc. For the open-ended rail electrodes the measurements were taken over an electrode distance of 0·5m. Tektronix oscilloscopes type 502 together with a Thompson Land type 410 camera and a Dumont type 302 camera were used to record the arc velocity, voltage and current.

Optical probes, consisting of miniature photo-diodes mounted in one end of a 15 cm length of hypodermic tubing 0·128 cm internal diameter to serve as a collimator, were used to provide voltage pulses for the measurement of arc velocity. For the annular gap experiments and the electrodes of Fig.1(a) a single optical probe pointing at a position midway between the electrodes was used to measure the frequency of arc rotation and hence the mean velocity. In this case the oscilloscopes were triggered from an external circuit operated manually once the arc was established. A check was also made to ensure that this method gave identical results to the earlier method used for graphite electrodes [1] i.e., a small search coil in the applied magnetic field so that a voltage was induced in it which was in phase with the rotation of the arc+ For the rail experiments two probes were fixed 0·5 ± 0·001m apart with the ends of the tubes about 3 cm above the electrode surfaces and pointing vertically down to a point midway between the electrodes. A third optical probe, placed 25 cm in front of the first of the two measuring probes and 20 cm from the starting position of the arc, was used to trigger the oscilloscopes. In this way any effects due to the initial starting period of the arc were avoided.

The arc currents and voltages were measured by using either a 2000 amp, 1000 amp or 600 amp, 50 mV shunt in series with one electrode and a Toktronix type 6017 ten times attenuation probe connected across the electrodes, the electrode common to both measuring circuits being earthed. It was found that the current records contained a large high frequency noise signal which may have been amplified because of the inductance of the measuring shunts, or may have been the result of actual variations in the arc. No such variations were observed in the amplitude of the applied magnetic field and they were reduced when a non-inductive shunt was used. Only the mean d.c. current was recorded and this was obtained by using a low pass filter with a cut off frequency of 320 c/s. The oscilloscope time baso and amplifiers were nominally calibrated to within an accuracy of ±3%, but since the measurements were taken from photographic records and because of fluctuations in the arc current and voltage it is estimated that the experimental values of arc current and voltage are accurate to within ±10% and the arc velocity to within ±5%. The arc gaps were measured to within ±0·05 cm.

The applied magnetic fields in all cases were taken from calibration curves of coil current against magnetic field obtained by using a search coil and a Cambridge Insts. Fluxmeter. The measured fields were accurate to within ±4%. When circular electrodes of different radii were used the magnetic fields were measured at the appropriate positions in the solenoid. In the case of the experiments using open-ended rail electrodes the applied fields were corrected for the field due to the arc current in the electrodes (for method of calculation see Appendix A).

Typical observation errors based on the above are shown in the plotted experimental results and a list of errors for all parameters used is given after the list of symbols.

Examples of the oscilloscope records are shown in Fig.4.

In order to obtain some idea of the arc size and shape a number of high speed photographs of the arcs on the straight electrodes (Fig.1) were obtained using a Fastax rotating prism camera in conjunction with either (i) a neutral density filter with brass electrodes or (ii) a narrow band filter (5855 Å to 5925 Å) or a neutral density filter with carbon electrodes. When the electrodes of Fig.?(a) were used, so that the arc moved continuously for a few seconds, many circuits of the discharge were photographed. When a pair of open-ended rail electrodes was used the arc was photographed over a distance of 0·35m and synchronisation of the camera was obviated by replacing the film spools by small plastic wheels and running a 0·48m closed loop of film over them, which was driven in the normal way by the toothed drive wheel. Thus, by allowing the loop to revolve at high speed for two or three seconds, the arc could easily be photographed since its total starting and transit time was much less than this (approximately 400 millisec for lowest velocity recorded). To use the camera in this way it was necessary to remove the timing marker light source ; the framing rate was thus estimated from the' arc velocity to be 7000 frames/second. With this method both panchromatic and colour films were used successfully and an exposure of $1 \cdot 6 \times 10^{-5}$ sec per frame at f/22 with a 0·5 neutral density filter was typical for both PANF and Ektachrome films.

Examples of the high speed ciné films are shown in Figs.5,6 and 7.

3 EXPERIMENTAL RESULTS

For convenience the measured experimental results are collected together in Figs.8 to 27 in the form of graphical plots. Figs.8 to 10 are for graphite electrodes, Figs.11 to 14 are for circular brass electrodes, Figs.15 to 20 are for the electrodes of Fig.1(a) and are referred to as continuously operated

arcs on brass electrodes and Figs.21 to 26 are for a pair of open ended brass rails. Fig.27 gives arc velocity against electrode gap width for all the electrode configurations.

The photographic evidence shows that the shape of the arc column fluctuates as it moves along the electrodes. The inclination to the electrodes can vary from point to point and the arc can form bends and, for long arcs, even loops during its somewhat erratic journey. In general, the corresponding fluctuations in arc current and voltage increased as the electrode separation was increased. Nevertheless, by measuring average values of arc velocity and current, and minimum values of arc voltage over an electrode distance of 0·5m or for many cycles of arcs operating continuously, consistent results have been obtained and analysed. It is assumed that the minimum values of arc voltage correspond to arc lengths equal to the electrode gap width. For the unshrouded graphite electrodes the fluctuations in arc current and voltage were greater than for the brass electrodes sandwiched between refractory insulating material.

We will now consider the results for each electrode configuration in turn before discussing them in detail in a later section.

3.1 Circular graphite electrodes

These results were confined to fixed values of arc current and applied magnetic field in order to compare them with those roported earlier'. The earlier'results where the electrode path length was varied but the arc gap kept constant by using electrodes of different radii, showed that an increase in path length resulted in a decrease in the arc velocity. In addition it was indicated that with the same applied magnetic field and electrode spacing one would expect a limiting velocity to be reached for very long track lengths. The path length has now been extended to 0·48m and the results are shown in Fig.8 together with corresponding values of velocity for a pair of open-ended graphite rails where the arc moves once along the electrodes. The velocities were calculated from the measured frequencies of rotation and circumferences of the inner electrodes and are thus values for the cathode root velocity.

3.2 Straight graphite electrodes

These electrodes were, for practical reasons, made fairly large in cross section (7·5cm x 2·5 cm), and it was at first thought that the arc roots would remain on the inside vertical surfaces. However, the oscilloscope records showed that the arc voltage and current varied considerably during the motion along the electrodes, thus making it impossible to obtain results at a constant

arc current, and the high speed photographs (see below) indicated that the arc motion was very erratic. It was therefore decided to explore the arc's motion for a range of magnetic field using a constant total voltage (500V) applied across the electrodes and series stabilising resistance. This gave arc currents in the range 250 to 350 amp for magnetic fields between 0·0070 and 0·086 Wb/m^2 and an electrode spacing of 3 cm. These results together with those for electrode spacings of 0·7 cm and 1·5 cm are shown in Fig.9. The measured arc voltages plotted against the applied magnetic field are shown in Fig.10, the total variation in the recorded voltages being also shown.

The high-speed photographic records of the arc revealed that its motion was erratic and its shape continually changing. A mirror was arranged along the eleotrodes so that two image3 were recorded; one from a direction transverse to both the elec trodes and the arc, and the other via the mirror, from a direction at right angles to the field and across the upper surfaces of the electrodes in order to see if any part of the discharge came above the upper electrode surfacos. It was evident from the films (e.g. see Fig.5) and the tracks left on the electrodes that the arc roots wandered over the top electrode surfaces in directions other than that of the magnetic driving force, and that sometimes the luminous discharge was almost completely above tho electrodes.

3.3 Circular brass electrode3

Circular brass electrode3 of various diameters as described in section 2.2 were used so that results for arcs rotating round annular gaps with different path lengths but the same gap width were obtained. The inner (cathode) root velocities were calculated from the measured frequencies of rotation and circumferences of the inner electrodes. The electrodes were sprayed with aluminium oxide in order to confine the arc3 to the edges (0·33 om wide).

The measured arc velocities are plotted against arc current in Pig.11 and against applied magnetic field in Fig.12. It is seen from Fig.12 that changes in the electrode path length did not significantly alter the arc velocity. This till be discussed in a later section. The minimum values of the arc voltage are plotted against arc current in Fig.13 and against magnetic field in Fig.14. It should be noted that the voltage is approximately independent of the arc current and increases slightly with increase of magnetic field.

3.4 Brass electrodes with long closed path length

This electrode configuration (Fig.1(a)) was made so that a very long path length could be used and arcs could be photographed over straight electrodes without having to modify the camera. In addition a large number of photographs could be obtained for statistical studies of arc shapes.

Two types of refractory insulator were used to sandwich these electrodes, and no difference could be detected for results using either material (i.e. 0·63 cm thick "Sindanyo" or a thin sprayed coating of aluminium oxide). The majority of results were obtained on electrodes 0·33 cm thick but some results were also obtained for a thicker set of electrodes (0·63 cm) with a 1·27 cm gap; no difference could be detected between them.

It was found that the mean arc velocity measured by using a single probe to *record* the number of circuits of the arc over a fixed time interval was less than the velocity of the arc along the straight portions of the track i.e., measured by placing two probes 0·5m apart as for the rail experiments. In addition, the velocity along the straight portions for the initial circuit of the arc was also measured (before it has moved into its own wake), and was found to be the same as for arcs moving along a pair of straight open-ended rails as given in the next section. A similar result has been confirmed for arcs rotating round annular gaps, i.e. Bronfman[11] has found that the velocity of an arc during its first revolution round a 0·1 cm annular gap between copper electrodes was the same as given in published literature [12] for straight parallel electrodes *and was* higher by a factor of 2 or 3 for subsequent revolutions.

The measured arc velocities are plotted against arc current in Fig.15 and against magnetic field in Fig.16 for an electrode gap of 1·27 cm. Results of velocities obtained along one side of the track are also shown in Fig.15, and they are seen to be higher than those obtained from the number of arc circuits per sec at the same magnetic field. The minimum values of arc voltage *are* plotted against arc current in Fig.17 and against applied magnetic field in Fig.18 for two electrode spacings. It should be noted that the voltage is approximately independent of the arc current and increases with magnetic field. An attempt was made to obtain voltage gradients, E, for a range of magnetic fields by plotting mean values of V (the minimum arc voltage) against the electrode gap, d, as shown in Fig.19. For this purpose, only three gap widths were used, the spread at the largest gap being ±8 volts. If we assume that the lengths of the non-uniform parts of the column and the electrode fall

regions are small compared with the length of the uniform column, then the slopes of Fig.99 give values for the column voltage gradient, i.e.

$$V = v + Ed \qquad (1)$$

where V is the minimum arc voltage
v is the sum of the electrode fall voltages and the voltages of the non-uniform parts of the column near the electrodes
E is the column voltage gradient
d is the gap width

It should be noted that for high-current arcs in small gaps the above assumptions are unlikely to apply and consequently our values for E are mean values for the electric field in the arc. The values of electric field are plotted against the applied magnetic field in Fig.20 and are seen to vary between 14 v/cm and 30 v/cm.

The high-speed photographic records showed that the luminous arc column was very nearly straight when the arc moved along the straight portions of the electrodes, and varied about a mean position perpendicular to the electrodes. A statistical analysis of the inclinations of the luminous column to the eleotrodes has shown the most probable position was perpendicular to them[13]. Over the curved parts of the electrodes the arc's motion was more interesting and the formation of a curved arc, similar to that already observed in annular gaps', was in general, observed. In addition, it was found that the arc velocity over the inner electrode decreased when negotiating the sharp bends at the ends of the system, and this accounts for the difference in velocity mentioned earlier and shown on Fig.15. Examples of the high speed photographs are shown in Fig.6, and the transition from the "straight" to the "curved" shape can be seen as the arc moves round the curved ends of the electrode track.

3.5 Straight open-ended brass electrodes

These electrodes enabled a study of the motion of arcs through cold, stationary air to be made. They were sandwiched between refractory insulating material 0·66 cm thick in order to confine the arc roots to an edge 0·33 cm wide (big.1 (b)).

It was found that the velocities were cons&tent only after sevorcl runs had been made, (more than ten), and visible tracks built up on the electrodes. Because of this and for comparison with the work on arcs moving continuously round electrode systems (sections 3.3 and 3.4), the results are for the same pair of electrodes used many times (between 10 and 150 runs).

The mean arc velocities (measured over a distance of 0·5m) are plotted against arc current in Fig.21 and against magnetic field in Fig.22 for an electrode gap of 1·27 cm, the values of the magnetic driving field having been corrected for the arc current in the electrodes. At fields below 0·04 Wb/m^2 the field due to the electrodes makes the presentation of results at fixed magnetic fields (Fig.21) difficult i.e., the variation in B is > ±25% for an arc current range up to 1200 amp. The results for 3700 amp and magnetic fields below 0·1 Wb/m^2 are necessarily for arcs driven to a large extent by the self field due to the current in the electrodes, and it is possible that the divergence of these results (Fig.22) is due to the fact that the driving field cannot be accurately determined at the position of the arc because of an asymmetric current distribution in the electrodes. In calculating the corrections for the self field a uniform current density in the electrodes was assumed (Appendix A).

The minimum values of arc voltage are plotted against arc current in Fig.23 and against applied magnetic field in Fig.24 for three electrode spacings. As noted before, the voltage is approximately independent of arc current and increases with magnetic field. Estimates of the voltage gradient, E, were made as before (section 3.4) by plotting mean values of V (the minimum arc voltage) against d and using equation (I), see Fig.25. The same remarks about high current arcs in small gaps made in section 3.4 also apply so that our values for E are mean values for the arc. The values of electric field are plotted against the applied magnetic field in Fig.26 and are seen to vary between 16 v/cm and 26 v/cm. An additional experiment was carried out to try and confirm the estimated value of E at an applied field of 0·12 Wb/m^2 by measuring the voltages of arcs moving along either a diverging or converging electrode gap and measuring the gradient $\Delta V/\Delta d$ from oscilloscope records. This was done for various values of Ad and a plot of the gradient against Ad showed that $\Delta V/\Delta d$ tended to the value of E obtained for parallel electrodes as Ad tended to zero.

The high-speed photographic records showed that the luminous column behaved in the same way as for arcs over the straight portions of the electrodes with a long path length (section 3.4) i.e., was very nearly straight and varied about a mean position perpendicular to the electrodes as shown by the example in Fig.7(a). High-speed cine films were also taken in a direction along the direction of motion of the arc (e.g. Fig.7(b) and it is seen that the luminous width of the arc transverse to the direction of motion is greater than the total thickness of the electrodes and insulation. From the limited number of

film records made in both this direction and looking down on to the electrode gap width it is estimated that the luminous width of the arc parallel to the direction of motion and transverse to the driving field (approximately 0·5 cm to 1·5 cm) tended to be less than the luminous width transverse to the direction of motion and parallel to the magnetic field (approximately 1 cm to 2·5 cm). This will be discussed in a later section.

4 DISCUSSION

The results described in the previous section will now be considered in more detail and we discuss two main aspects:-

(i) Motion of the arc through the surrounding air, and, where applicable, through its own wake. This will be confined to an analysis of the velocity measurements.

(ii) Heat losses from the arc to the surrounding air. This will include an analysis of the voltage gradient measurements and we will use parameters suggested by Lord [8,9].

4.1 Motion of arc (velocity measurements)

We make use of a simple model of the arc motion similar to that used in previous papers [1,5,6,7] where the conducting column is taken to be a body moving with velocity U through a surrounding gas, causing a displacement of the external gas. It is assumed that this displacement does not close downstream of the arc and that a wake is formed, which is related to an aerodynamic drag force on the arc and can be written in the form:-

$$\text{Drag force} = \tfrac{1}{2} \rho U^2 A \,, \qquad (2)$$

where ρ is the density of the external gas

and A is the effective frontal area of the body presented to the gas, i.e. the "effective drag area"

To produce a uniform motion of the body, the drag force and the overall body force, BId, on the arc due to the magnetic field must be in equilibrium. Hence their magnitudes obey the relation:-

$$\tfrac{1}{2} \rho U^2 A = BId \,, \qquad (3)$$

where d is the distance between the electrodes-

This expression can only be applied to two-dimensional straight arcs or elements of curved arcs. However, for experiments reported here, in which circular electrodes have been used and curved arc shapes would be expected

(e.g. involutes') the electrode spacing was kept small (1·27 cm) compared with the periphery of the inner electrodes (16 cm to 112 cm) so that, the arcs may be considered as approximately radial. In addition, because of electrode plasma jets within the arc column it is likely that the arc would in any case be straight over gaps less than about 1·5 cm, and suggested by earlier experiments on carbon electrodes'. In this case, it must be remembered that the motion may not be governed by equation (3) and that equilibrium between centrifugal and magnetic centripetal forces might be produced. For the present we will ignore the effects of any plasma jets (which may be intermittent) and assume that equation (3) is applicable, and express the arc velocity in terms of the measured quantities B, I and d:-

$$U = (2\,BId/\rho A)^{\frac{1}{2}} . \qquad (4)$$

Previous considerations using the above model [1,5,8] have shown that the arc size *increases* with arc current and decreases with increase of arc velocity, so that A is a function of I, U and hence of B. In addition, the effective area A would depend on (a) arc velocity, particularly for velocities comparable with the speed of sound, and (b) the Reynolds number. In the special case where the arc runs through its own wake as in the annular gap experiments, the density ρ would change due to heating and contamination of the gas, and the arc would also tend to produce circulation of the gas around the annulus so that the velocity relative to the electrodes would differ from the velocity relative to the surrounding gas.

We now consider the experimental results in detail and will analyse them using the simple model above.

4.1.1 Effect of arc wake

We deal first with the motion induced in the surrounding gas by the passage of the arc. It has been reported [14] that, for an arc rotating round an annular gap in the open atmosphere, the velocity of the induced motion of the gas in the annulus is one or two orders of magnitude less than the velocity of the arc. Further, a calculation given in Appendix B assuming (i) all the gas in the annulus rotates under the action of the applied electromagnetic torque and (ii) the shortest electrode path length used', where the effect would be greatest, is in agreement with the results of this report. We shall therefore ignore this effect for the present.

Consider now the effect on the density of the surrounding gas due to contamination and heating by repeated passage of the arc. Contamination of the

air in the annulus by gases derived from electrode materials could only be assessed by spectroscopic methods, but two remarks can be made concerning the present results. For carbon electrodes most of the likely contaminants, except carbon vapour, would not have a density much less than that of air. For brass electrodes, and most metals likely to be used, the metal vapours *are* more dense than air but neither the density nor the amount of contamination is likely to make this significant,

An effect of temperature *on* the gas density seems more likely to be significant because if the temperature through which the arc is moving is raised from room temperature to say, 1200°K then the arc velocity would be increased by at least a factor of two. We now consider experimental results *in* which only the electrode path length varied and *in* which B, I and d were kept constant. For these conditions equation (3) becomes:-

$$\tfrac{1}{2}\ \rho A U^2 = (\text{const}) \qquad (5)$$

so that any variation of U with electrode path length must be a consequence of variations in ρ and A. These results for the annular gap experiments *are* shown in Fig.28 where the arc velocity, calculated from the measured frequency of rotation and the radius of the inner electrode, is plotted against the periphery of the inner electrode. It is seen that there is a major difference between results for the two materials. With brass the velocity is approximately independent of path length and is comparable with the value, U_i, for the initial motion (before the ara traverses its own wake). With carbon, on the other hand, the velocity decreases with increasing path length and tends to the value for the initial motion. Now, by comparing the velocities for different path lengths with the velocity for the initial motion through still air at room temperature we obtain,

$$U_r/U_i = (A_i\ \rho_i/A_r\ \rho_r)^{\frac{1}{2}} \qquad (6)$$

where the subscripts r and i refer to values for arcs rotating in annular gaps and for the initial motion, respectively. If perfect gas laws are assumed to apply,

$$A_i\ T_r/A_r\ Ti = (U_r/U_i)^2 \qquad (7)$$

where T is the temperature of the surrounding gas ($T_i = 300°K$). By substitution of the values of U_r and Ui given in Fig.28 into equation (7), the ratio ($A_i\ T_r/A_r$ Ti) has been calculated for each electrode size used. The

results are plotted in Fig.29 and it is seen that for carbon electrodes the ratio approaches unity for long path lengths, while for brass electrodes the ratio increases slightly with path length but that the values are all close to unity. There are three possible reasons why the ratio $A_i T_r/A_r$ Ti might depend on electrode path length:-

(i) the effective drag area depend? on the velocity,

(ii) the temperature in the wake decreases as the velocity decreases,

(iii) the temperature of the electrodes and thus the wake temperature depend on the path length.

Now, since with brass electrodes $U_r \simeq$ Ui and the ratio ($A_i T_r/A_r$ Ti) is approximately unity, this may be interpreted to mean that the wake temperature does not change much with path length. In the case of carbon electrodes, the ratio ($A_i T_r/A_r T_i$) approaches unity as the arc velocity, U_r, approaches the initial value, U_i, at the longer path lengths. If we ignore the change in drag area, A, over the velocity range 45 to 180 m/s, then the decrease in arc velocity with path length may be wholly accounted for by a fall in wake temperature as the path length is increased. This temperature decrease would havo to be from 2300°K to 300°K for electrode path lengths ranging from 0·044m to 0·48m, (inner electrode radii 0·0065m to 0·0765m).

The above difference in the results for the two electrode materiels is not surprising when we consider the following:-

(a) carbon electrodes operate at a higher temperature than brass,

(b) the thermal conductivity of the carbon used is an order of magnitude smaller than that of brass,

(c) the outer carbon electrodes were 1·9 cm thick and the brass electrodes only 0·33 cm thick,

(d) the arc velocities for brass electrodes were in general greater than those for carbon.

These differences could have caused the wake temperatures for the two materials to differ but in order to resolve this, wake studies will have to be made. It is also possible that an electrode effect not accounted for by the simple model could result in different effects for different materials, and it must be remembered that the emission mechanisms for carbon and brass are different. It was reported earlier' for carbon electrodes that a steady arc rotation was not always immediately established but took a short time (up to a few seconds for very long arcs) to reach a steady frequency. This was never observed with

brass electrodes and could have been the result of some conditioning period for thermionically emitting cathodes (e.g. carbon), which my be accounted for by a necessity for heating up the cathode track before a smooth arc motion is possible.

4.1.2 Variation of velocity with drag area, current and magnetic field

We consider next the experimental results for arcs moving over constant electrode path lengths and along the open-ended rail electrodes with a fixed electrode spacing (1·27 cm). For these conditions equation (4) becomes

$$u = (\text{const})_2 \left(\frac{BI}{\rho A}\right)^6 \qquad (8)$$

where the constant equals $(2d)^{\frac{1}{2}}$.

Now, since the effective drag area has not been measured and can only be calculated for known values of p, (see section 4.1.3), and in order to make a comparison with previously published results [1,2,3,4,5,11] we choose to obtain empirical relations of the form

$$U \simeq K I^{n_1} B^{n_2} , \qquad (9)$$

where the dependence of (ρA) on I and B is included in the indices n_1 and n_2 (not equal to $\frac{1}{2}$) and a modified constant, K. Relations of this form have been obtained by plotting $\log_{10}U$ against $\log_{10}B$ at constant I, and $\log_{10}U$ against $\log_{10}I$ at constant B (Figs.30 and 31). The values of K, n_1 and n_2 are given in Table 1 together with the values *given* in the above references.

We now obtain relations between the parameters ρA, I and B by comparing equations (4) and (9)

i.e.
$$\rho A \simeq \frac{2}{K^2} I^{(1-2n_1)} B^{(1-2n_2)} . \qquad (10)$$

This gives a different dependence of ρA on I and B for each electrode configuration as shown in Table 2. It should be noted that for the experiments where ρ is constant (using a pair of open-ended rails) this also gives the dependence of A on I and B.

4.1.3 Arc size and shape

We now consider how the effective drag area, A, changes with arc velocity, U, and also from photographic evidence compare the luminous arc widths and consequent luminous frontal areas of the arc with values of A as defined by equation (3),

i.e. $$A = 2BId/\rho U^2 \quad . \qquad (11)$$

In order to have unambiguous values for ρ, it is necessary to choose data from experiments in which the arc has moved through undisturbed air Of known temperature and pressure. This condition is satisfied by the experiments using a pair of open-ended rails (Fig.1(b)), and a plot of calculated values of A against U for the results of Figs.21 and 22 is shown in Fig.32.

High-speed ciné films were taken in directions along the arc axis and along the direction of motion for two arc currents. As noted earlier in section 3.5 the luminous width parallel to the direction of motion (approximately 0·5 cm to 1·5 cm) was less than that transverse to the direction of motion (approximately 1 cm to 2·5 cm). This gives a range of values for luminous frontal area of the arcs from 1·27 cm^2 to 3·2 cm^2. Note that these are maximum values taken to be the product of the luminous width and electrode separation (d = 1·27 cm). Two points representing the maximum luminous areas from the photographic records are also shown in Fig.32 and it is seen that they are about twice the calculated values of A. It should be noted that the observed luminous areas need not be the main current-carrying path of the arc and if we assume that there is a hotter central cone, then equations (3) and (11) may only apply to this central core, Some evidence is already emerging from spectroscopic work[15] that the conducting width of the arc, assumed here to be the hotter central core, is smaller than the photographic width and the total radiating width transverse to the direction of motion. Theoretical work[16] on the flow about an arc transverse to an airstream using potential flow methods discusses the possibility of the arc periphery being porous, and in order to arrive at a satisfactory solution compatible with experiment an inner impermeable boundary is suggested for the arc.

Taking the above considerations into account we have the result that the arc might be represented by an impervious body whose effective drag area is less than the luminous area and we therefore briefly consider this possibility. In order to take the discussion a stage further, we draw an analogy betwcon the arc and a solid body of uniform cross-section. For such a body we may put

$$A = C_D D d \qquad (12)$$

where C_D is the drag coefficient
D is the geometrical width
d is the length.

Now, if we take D and a to be the width and length of the conducting column of the arc, then the *results in* Fig.52 imply that:-

(i) if D decreases with *increase* of U, (as suggested in Refs.1,5 and 8), then there is a compensating increase in C_D which accounts for the observed increase in A with U,

(ii) if D decreases with increase of I, (as suggested in Refs.1,5 and 8), then either this increase is small or C_D diminishes with increase of I at constant U.

Consider now the dotted curves in Fig.32 which are for solid cylinders of different diameters in a transverse flow. These curves give the variation of effective drag area with stream velocity and are obtained from recorded aerodynamic data[17]. Note that in the case of the cylinders, A has values which bracket those for the arcs, but that the upward trend of A is never as great. It is possible that changes in the geometry of the arc with velocity could cause a further *increase in* A with U than would occur with *constant* cross-section (e.g. if the arc was considered to be approximately elliptical in cross-section, changes in the ratio major axis/minor axis would affect the drag), but these are unlikely to account for the continued upward trend of A between Mach 0·1 and 1·2. A similar result i.e., that the variation of CD with Reynolds number for arcs differs from that for solid bodies of constant cross-section, has been found for arcs rotating in annular gaps[18]. Thus, it is evident that the solid-body analogy for the arc is inadequate, although the calculated values of A are comparable with those of solid bodies about one half of the luminous arc size determined photographically.

It is, however, possible to present a tentative picture of the arc's size and shape based on the photographic records and the calculated values of A. This is represented by a body of luminous gas whose width is greater when measured transverse to the direction of motion than along the direction of motion, as shown schematically in Fig.33. The dashed lines indicate the total extent of the luminous gas and in practice the shape varies with the motion of the arc. It is possible that the outer luminous regions are the result of colliding plasma jets[19,1] from the constricted arc roots, but a more precise picture could possibly be given when the spectrographic work is completed.

4.1.4 Effect of electrode spacing and shape

Finally, we discuss two other aspects of the arc motion which *were* observed:-

(i) The variation of arc velocity with electrode spacing as shown in Fig.27. It can be seen that the velocity tends to become independent of the gap width as this is increased for constant values of current and magnetic field. The arc velocity would be independent of the gap width if the conducting column was uniform along its length so that the effective drag area, A, in equation *(3)* was proportional to the gap width, d. Hence the experimental results indicate that as the arc length is increased by increasing the electrode spacing, then the arc shape becomes uniform along its length. However, as the gap was increased the arcs were more unstable, greater fluctuations occurred in the arc current and voltage and hence the results were less reproducible so that the applicability of the model becomes doubtful.

(ii) The motion of arcs round the sharp bends of the electrode configuration shown in Fig.1(a), as described in section *3.4.* A study of the photographic records of the arc when changing its shape as shown in Fig.6, (i.e. from a "straight" arc to a "curved" arc similar in shape to that already found for arcs in annular gaps'), showed that the velocity of the inner electrode arc root changed in the following way. Referring to the inset diagrams in Fig.6 where the end of the electrode system is shown divided up into regions numbered 1 to 5, the motion was from region 1 to *region 5.* The velocity of the inner arc root began to decrease at the end of region 2, was slowest in regions *3* and 4, and finally increased to the velocity attained on the straight portions of the electrodes by the end of region 5. In addition, when the inner electrode was made the cathode the arc root travelled slower relative to the column resulting in the behaviour shown in frames 29 to *33* of Fig.6. This had the effect of always producing an arc with a lagging cathode root over region 4. Although the decrease in velocity also occurred when the inner electrode was made the anode the above effect producing a lagging root over region 4 was absent. This behaviour cannot be explained by our simple model and the following reasons are suggested as possible explanations

(a) in negotiating a sharp bend the arc is, in effect, restricted by a wall where the electrode surface is transverse to the general motion of the arc,

(b) a local increase in pressure occurs in the sharp bend due to motion of gas induced by the arc,

(c) the formation of eddies between the curved parts of the electrodes impedes the arc's motion,

(d) a centrifugal force on the arc causes a reduction in the arc velocity. This could account for a decrease of velocity in region 4 due to a change in the velocity distribution over the gap when the arc re-enters a straight region of the electrodes; (an analogy could be made here with fluid flow in curved pipes).

4.2 Heat losses from arc (voltage measurements)

In this section we are concerned with the overall energy balance for the arc column and hence consider the heat input per unit length, given by EI watts/m. For this purpose we use the estimated values for E given in Figs.20 and 26 and it must be remembered that these are mean values for the total electric field in the arc. The electric field varies along the arc length because the anode and cathode regions are constricted, and the measured voltage gradients will only correspond to the uniform column voltage gradient if the lengths of the non-uniform parts of the column are small (equation (1)). The estimated values for E were found to be approximately independent of arc current but, by plotting $\log_{10}E$ against $\log_{10}B$, were found to obey simple power laws with the magnetic field as shown in Table 3.

First we will consider the results using well known similarity relations derived from the energy balance equation when radiation is neglected [8,20,21]. The treatment assumes that the arc column is axisymmetric, uniform and in thermal and chemical equilibrium. Magneto-hydrodynamic effects are assumed to be small and the arc column optically thin. The power input per unit length is equated to the amount of heat conducted to the arc periphery:-

$$EI = -\frac{1}{r}\frac{d}{dr}\left(r k T \frac{dT}{dr}\right) \qquad (13)$$

where r is the radial distance from the column axis,
k is the local thermal conductivity,
and T is the local column temperature.

From this equation it is readily shown that (e.g. Refs.8, 20 and 21) arc columns may be characterised by values of $E\hat{r}$, $I/\hat{r}$ or EI independent of the absolute values of E, $\hat{r}$ and I, where $\hat{r}$ is the radius of the arc column, and that

$$E\hat{r} = f_1(EI) \qquad (14)$$

$$I/\hat{r} = f_2(EI) \qquad (15)$$

therefore

$$E\hat{r} = f_3(I/\hat{r}) \qquad (16)$$

Now, if for an arc moving in a gas stream under the action of a transverse magnetic field, we assume that the heat transfer to the gas is a function of the product of the arc velocity U and the arc radius $\hat{r}$, (e.g. for a heated solid cylinder the Nusselt number is a function of the Reynolds number), it may be shown[8,9] that $\hat{r}$ in equations (14) to (16) is replaced by U^{-1} so that equation (16) becomes

$$E/U = f_4(IU) \quad . \tag{17}$$

This relation only applies for arcs with a constant ambient temperature and pressure and it should be noted that it does not necessarily apply to arcs rotating in annular gaps because of wake effects (section 4.1.1).

We now consider the experimental results for our three electrode configurations and plot E/U against IU (Fig.34). It is seen that all the results very approximately follow curves of the form

$$E/U = (\text{const})(IU)^{-n_4} \tag{18}$$

where the constant depends on the electrode material and configuration. The values of E for circular brass electrodes were assumed to be the same as those for continuously operated arcs on the brass electrodes of long path length. This may be justified by comparing the measured arc voltages in Figs.13 and 14 with those in Figs.17 and 18 for an arc gap of 1·27 cm. Due to observation errors the values of E/U and IU are accurate to within ±11%. By plotting on logarithmic scales (Fig.35) n_4 is found to be about 0·4. The results for rotating arcs on brass electrodes are too limited to be of interest but fall within the limits of those for arcs on the brass electrodes with a long path length. The considerable scatter of experimental results presents a difficulty in analysing them further, and in what follows smoothed-out results are used. However, Fig.35 demonstrates that all the results follow a trend which yields an approximate equation for arcs moving along the three electrode configurations used:-

$$E/U \propto (IU)^{-0\cdot4 \pm 0\cdot1} \quad . \tag{19}$$

In the above analysis heat lost by radiation was neglected and in an attempt to account for some of the unduly large scatter in Figs.34 and 35 we now consider the effect of radiation. An analysis by Lord[9] for an arc held stationary in a gas stream by a magnetic field yields a useful form of voltage gradient - current characteristic in terms of non-dimensional parameters. A characteristic equation is derived which relates the non-dimensional forms

of EI, I/E and a radiation parameter which is proportional to $1/U^2$. This equation applies when the thermal conductivity, or more specifically the heat flux potential $\left(\text{defined by } \int_0^T k\,dT\right)$, the electrical conductivity and radiation power density of the arc column obey certain power laws specified in Ref.9, and may be written

$$EI = f_5\left(\frac{P^2 U^2 I}{E}\right) + \frac{1}{P^{2-m} U^2} f_6\left(\frac{P^2 U^2 I}{E}\right) \qquad (20)$$

where P is the ambient pressure. The L.H.S. of equation (22) is the heat input, the first term of the R.H.S. is the heat lost by conduction to the arc periphery and thence by forced convection to the external surroundings, and the second term on the R.H.S. is the heat lost by radiation, per unit time per unit length of arc column. For the purpose of analysing the experimental results we may rewrite equation (20) in terms of EI, U^{-2} and U^2 I/E if we assume the ambient temperature and pressure are constant.

i.e. $$EI = f_7\left(\frac{U^2 I}{E}\right) + (\text{const})\, U^{-2} f_8\left(\frac{U^2 I}{E}\right). \qquad (21)$$

Thus, by plotting EI against $U^2 I/E$ for different values of U a series of curves might be obtained, the dependence on U being given by the third term (radiation loss) of equation (21) i.e., the radiation loss and hence the total input power EI increases as the velocity decreases. By smoothing out the results for low Mach numbers in Figs.15 and 21 and using values for E from Figs.20 and 26 for brass electrodes, plots of EI against $U^2 I/E$ have been made (Figs.36 and 37). From Fig.36 it can be seen that results for arcs moving through stationary air at a constant ambient temperature are approximately represented by a series of smooth curves at constant values of U, where EI increases as U decreases. However, it should be noted that because of the experimental error there is some overlap in the scatter for each line drawn through points of constant velocity. Due to this and the uncertainty in the values used for the voltage gradient it is considered unwise to proceed with the analysis suggested by equation (21). On the other hand, from Fig.37 for results of arcs moving through previously heated gas and where the ambient temperature might be expected to change with U and I, it can be seen that there are discontinuities in curves joining points of constant velocity and that EI decreases as U decreases. It is interesting to note however that these results may be approximately represented by a series of smooth curves relating EI and $U^2 I/E$ at constant values of E or B,

i.e. $$EI = f_9(E \text{ or } B)\, f_{10}(U^2 I/E) . \qquad (22)$$

From the above it is seen that only the results for arcs moving through stationary air at constant temperature agree qualitatively with Lord's theoretical work. This is only to be expected since the theoretical work assumes a constant ambient temperature for the external gas and hence does not necessarily apply to arc's traversing their own wake.

Next, we consider a method of analysing experimental results which is independent of the form of the radiation loss. It may be shown[18] that if both the drag coefficient and the Nusselt number for the arc depend only on the Reynolds number (as they would for a solid cylinder at low Mach numbers) then the parameter BI/U depends only on $U^2 I/E$. It is suggested [18] that a plot of BI/U against $U^2 I/E$ may prove illuminating in the analysis of experimental results. These plots are shown in Figs.38 and 39 for the smoothed out results on a pair of brass rails and the electrodes of Fig.1(a), respectively. The full significance of these plots is not evident but it is of interest that they may be approximately represented by a series of smooth curves at constant values of E or B, and that BI/U increases with E or B for both sets of experiments. These results may thus be approximately represented by equations of the form

$$BI/U = f_{11}(E \text{ or } B)\, f_{12}(U^2 I/E) . \qquad (23)$$

Finally, we consider the effect of using slightly different values for the column voltage gradient. Let us consider an element of the arc at the centre of the electrode gap and assume we are free from electrode effects. In this case the voltage gradient in the element would be equal to that obtained from a plot of arc voltage against arc length for large electrode spacings i.e., the lower curve of Fig.26 for straight brass electrodes. If we use these values of E and again plot EI against $U^2 I/E$ then a closer approximation to a single curve is obtained. In addition, by extrapolating the E against B relation for large gaps the results for velocities comparable with the speed of sound have been included (Fig.40). It is seen that all the results for arcs moving through stationary air at a constant ambient temperature may be approximately represented by a simple power law

i.e. $$EI \simeq 1{\cdot}35 \times 10^4 (U^2 I/E)^{0{\cdot}57} . \qquad (24)$$

This collapse of experimental data is in accordance with the theory (equation (21)) if the radiation term is neglected. A plot of BI/U against U^2I/E using the values of E for large gaps and including all the results is shown in Fig.41. As before, these may be approximately represented by relations of the form of equation (23), and it should be noted that at constant values of velocity BI/U is approximately constant.

It is evident from the above that the analysis of the experimental data is very dependent upon the accuracy of the estimated values for the column voltage gradient. However, the results would indicate (Figs.36 and 40) that either

(i) the radiation term expressed as in equation (21), is small for arcs in air at atmospheric pressure

or (ii) the theoretical model is inadequate. The results shown in Figs.38 and 41 demonstrate that BI/U does not depend only on U^2I/E, as would be the case for a solid cylinder at low Mach numbers, and we conclude that the analogy with a solid body is inadequate.

5 CONCLUDING REMARKS

It has been demonstrated that for the range of conditions used an arc moving in a transverse magnetic field does not proceed in a uniform manner and that fluctuations occur in the arc velocity, the current flow between the electrodes and the shape of the conducting path. In the analysis of results these fluctuations have been ignored. All results are based on mean values of arc velocity and current and minimum values of arc voltage, measured over large electrode distances (0·5 metre minimum) in a uniform external magnetic field. In this way, results have been obtained which could be analysed, as summarised below.

(1) A major difference between results *for* carbon and brass electrodes using annular gaps was observed. As the electrode path length (at constant applied magnetic field, arc current and electrode spacing) was increased the arc velocity *on* carbon decreased and tended to the value obtained for the initial motion (or along a pair of open-ended rails). On brass electrodes the arc velocity was approximately independent of path length and comparable with that for the initial motion. In order to explain this difference, wake effects, electrode effects, or both, need to be studied.

(2) Approximate relations between the arc velocity, arc current and applied magnetic field have been obtained for three electrode configurations

and two electrode materials. These relations are summarised *in* Table 1 together with similar relations obtained from other results[1,2,3,4,5,11]. From Table 1 further relations between the parameter ρA, (product of the density of the surrounding gas and the effective drag area), arc current and applied magnetic field were derived using a simple model for the arc motion. These relations are shown in Table 2.

(3) The effective drag area using a simple model for the arc has been calculated for a range of arc currents and velocities using results where the arc wake does not affect the arc motion, and is shown to be about one half of the maximum luminous frontal area of the arc determined photographically. The variation of drag area with velocity is shown to be incompatible with that for a solid body. A tentative picture of the arc's cross-sectional shape based on photographic evidence is given, in which the width measured along a direction parallel to the driving field or transverse to the arc's motion is greater than the width measured along a direction parallel to the arc's motion.

(4) Values for the voltage gradient were estimated and found to be approximately independent of arc current, but obeying a simple power law with the applied magnetic field as shown in Table 3.

(5) An approximate power relation between E/U and IU was obtained for all the results as shown in Table 3, where the constant of proportionality differs for each electrode configuration. By using smoothed out results for a pair of open-ended brass rails relations between EI and IU^2/E were obtained which agree qualitatively with theoretical work for convection-stabilised arc columns [9].

The simple model used for the analysis of results has proved to be useful but a direct comparison between an arc and a solid body in transverse flows is inadequate, a result in agreement with calculations by Lord and Broadbent[18].

ACKNOWLEDGEMENT

The author wishes to acknowledge the help of Mr. P. Fethney of Aerodynamics Department in designing and making the optical probes.

Appendix A

CALCULATION OF THE MAGNETIC FIELD DUE TO THE ARC CURRENT IN THE ELECTRODES

In correcting the applied magnetic field for the self-field due to the arc current in the electrodes it is not possible to consider the current to be concentrated into a single filament at the centre, and their profile must be taken into account. The field of such a distributed current oanbe found by the superposition of the fields of an infinite number of line current elements.

Let each electrode be infinitely long and have a cross section 2a x 2b as shown in Fig.42 where the current I is norm&Lout of the paper. If we consider any element of cross-section $dx_1\ dy_1$ at coordinates (x_1, y_1) then the current in the element is $(I/4ab)\ dx_1\ dy_1$, and the vector potential function of this line current is given by

$$A = -\frac{\mu_o I}{8\pi a b} \log r\ dx_1\ dy_1 \quad . \tag{A1}$$

The field of all elements in the electrode is found by integrating over the rectangular section of the electrode and, at any point (x,y) distance r from any element (x_1, y_1), is thus given by,

$$A = -\frac{\mu_o I}{8\pi a b} \int_{-a}^{a} \int_{-b}^{b} \log r\ dx_1\ dy_1 . \tag{A2}$$

Substituting for r,

$$A = -\frac{\mu_o I}{16\pi a b} \int_{-a}^{a} \int_{-b}^{b} \log[(x_1-x)^2 + (y_1-y)^2]\ dx_1\ dy_1 . \tag{A3}$$

This can be integrated in terms of simple functions, and the result has been given by Strutt[22] in the form

$$A = -\frac{\mu_o I}{16\pi a b}\Bigg\{\begin{aligned}&(a-x)(b-y)\log[(a-x)^2+(b-y)^2]\\&+(a+x)(b-y)\log[(a+x)^2+(b-y)^2]\\&+(a-x)(b-y)\log[(a+x)^2+(b-y)^2]\\&+(a-x)(b+y)\log[(a-x)^2+(b+y)^2]\\&+(a+x)(b+y)\log[(a+x)^2+(b+y)^2]\\&+(a-x)^2\left[\tan^{-1}\frac{b-y}{a-x}+\tan^{-1}\frac{b+y}{a-x}\right]\\&+(a+x)^2\left[\tan^{-1}\frac{b-y}{a+x}+\tan^{-1}\frac{b+y}{a+x}\right]\\&+(b-y)^2\left[\tan^{-1}\frac{a-x}{b-y}+\tan^{-1}\frac{a+x}{b-y}\right]\\&+(b+y)^2\left[\tan^{-1}\frac{a-x}{b+y}+\tan^{-1}\frac{a+x}{b+y}\right].\end{aligned}\Bigg\} \quad (A4)$$

This expression is the flux function of the field and the field components, B_x and B_Y, are given by

$$B_x = \frac{\partial A}{\partial y} \quad \text{and} \quad B_Y = \frac{\partial A}{\partial x}.$$

We are concerned with the component B_Y when $y = 0$ (i.e. the self-field in the arc gap) and this is given by

$$B_{y\,(y=0)} = \frac{\mu_o I}{8\pi a b}\left\{b\log\left[\frac{b^2+(x+a)^2}{b^2+(x-a)^2}\right]+2(x+a)\tan^{-1}\frac{b}{x+a}-2(x-a)\tan^{-1}\frac{b}{x-a}\right\} \quad \ldots (A5)$$

for each electrode. For a pair of long electrodes with the current terminated in an arc near the centre the total self-field at the centre of the arc gap, d, is given by B_Y when $y = 0$ and $x = (a+d/2)$; this expression was used to evaluate the corrections added to the applied magnetic field for the experiments using a pair of open-ended rail electrodes of rectangular cross-section:-

$$B_{corr} = \frac{\mu_o I}{8\pi a b}\left\{b\log\left[\frac{b^2+(2a+d/2)^2}{b^2+d^2/4}\right]+(4a+d)\tan^{-1}\frac{b}{2a+d/2}-d\tan^{-1}\frac{2b}{d}\right\} \quad \ldots (A6)$$

Appendix B

CALCULATION OF THE MOTION OF GAS INDUCED BY ARCS MAGNETICALLY PROPELLED ROUND ANNULAR GAPS

We will assume that the gas in the annular space between the electrodes is forced to rotate under the action of the total electromagnetic driving torque at an angular velocity, ω.

Now, for a disc rotating in a gas at an angular velocity ω, the shear stress at a radius, r, is according to Streeter [23], given by,

$$\text{Shear stress} = 0{\cdot}616\,\rho(\nu\omega^3)^{\frac{1}{2}}\,r \qquad \text{(B1)}$$

where ρ is the gas density and v its kinematic viscosity. Neglecting edge effects the total moment of a rotating annular disc of inner and outer radii r_1 and r_2 is given by

$$\text{Moment} = -2 \times 0{\cdot}616 \int_{r_1}^{r_2} 2\pi r^2\,\rho(\nu\omega^3)^{\frac{1}{2}}\,r\,dr \qquad \text{(B2)}$$

therefore

$$\text{Moment} = -0{\cdot}616\,\pi\rho(\nu\omega^3)^{\frac{1}{2}}(r_2^4 - r_1^4) \ . \qquad \text{(B3)}$$

The moment of the driving torque due to an arc current I along a radius and a uniform magnetic field, B, along the axis of the annulus is given by,

$$\text{Moment} = \int_{r_1}^{r_2} BI\,r\,dr \qquad \text{(B4)}$$

therefore

$$\text{Moment} = BI(r_2^2 - r_1^2)/2 \ . \qquad \text{(B5)}$$

Equating (B3) and (B5) and rearranging,

$$\omega = \left(\frac{0{\cdot}258}{\rho\nu^{\frac{1}{2}}}\right)^{2/3}\left(\frac{BI}{r_2^2 + r_1^2}\right)^{2/3} \ . \qquad \text{(B6)}$$

By substituting values for B, I, r_2 and r_1 from experimental results for arcs rotating on carbon electrodes [1] and assuming values for ρ and v for air at 300°K the angular velocity ω may be shown to be more than one order of

magnitude less than the measured angular velocity of the arc. However, when an arc is made to rotate in an enclosed annular channel, so that the device behaves like a single blade centrifugal pump, it can be made to accelerate the heated test gas to supersonic speeds [24].

Table 1

VALUES OF K, n_1 AND n_2 IN EQUATION (9)

$$U \doteq K I^{n_1} B^{n_2} \qquad (9)$$

Electrodes				K	n_1	n_2	U (m/s)	B (Wb/m^2)	I (amp)	Distance or time over which U,B and I measured
Configuration and reference	Material	Dimensions (cm)	d (cm)							
Pair of straight open-ended rails (horizontal - Fig.1(b) - D.C. arcs) (See note below)	Graphite	120 x 5·5 x 2·5	3·0	190 to 350	-	(0·7 ±0·1)	10-50	0·01-0·09	~350	50 cm
	Brass	120 x 3·8 x 0·33	1·27	-	(0·50 ±0·01)	-	30-100	0·026-0·037	100-1200	
				(22 ±1)	(0·40 ±0·01)	(0·40 ±0·01)	30-275	0·04-0·49	100-1250	
							70-420	0·12-0·49	200-3700	
				-	-	(0·20 ±0·01)	210-270	0·05-0·15	3700	
Electrodes with long closed path length (horizontal - Fig.1(a) - D.C. arcs)	Brass	Total path length over inner electrode = 219	1·27	(9·0 ±0·5)	(0·58 ±0·01)	-	40-70	0·02-0·12	230-500	Several cycles of arc
							55-205	0·04-0·12	230-1200	
							65-340	0·06-0·12	230-2700	
						(0·42 ±0·01)	40-200	0·02-0·12	230-1200	
Circular electrodes with annular gap (Fig.3(a) and Ref.1 - D.C. arcs)	Graphite	r_1 = 0·65 Outer electrode = 1·9 thick	0·65	(143 ±10)	(0·33 ±0·01)	(0·60 ±0·01)	16-190	0·006-0·094	100-750	Several cycles of arc
	Brass	r_1 = 12·7 and 17·8 Outer electrode = 0·33 thick	1·27	45 approx.	0·35 approx.	0·55 approx.	50-130	0·02-0·13	200-450	
Pair of straight cylindrical electrodes (vertical, arc motion up - D.C. arcs) Eidinger and Reider[5]	Copper	No data	A few tenths ($Bg^3 > 3$)	41	0·61	0·74	50 max	0·032 max	60 max	No data
Pair of straight cylindrical electrodes (horizontal - D.C. arcs) Secker and Guile[2]	Carbon	15 x 0·95 dia	0·32	155	-	0·74	3·5-18	0·006-0·05	40-670	5-13 cm
	Aluminium	15 x 0·95 dia	0·32	34	-	0·43	5-13	0·01-0·1	40-670	
Pair of straight cylindrical electrodes (horizontal - A.C. arcs - ½ cycle) Spink and Guile[3]	Polished brass	30 x 0·96 dia	10·2	-	-	0·55 to 0·563	45-135	0·032-0·16	2500-6000	0·3-0·5 millisec
			0·32	-	-	$0·55-0·43 \times 10^{-5} I$	60-215	0·02-0·128	400-6000	
				(1·5 +86B)	(0·47-0·96B)	-	26-140	0·021	100-2000	
								0·128	100-800	
				(1·5 +246B)	(0·36-1·18B)	-	80-215	0·032	1200-2000	
								0·128	800-6000	
Ring electrodes with circular arc path (D.C. arcs) Blix and Guile[4]	Brass	Mean rad = 8·1 Thickness = 0·6	0·2	-	-	0·62	25-250	0·034-0·106	20	Many cycles of arc
				-	-	0·60	50-100	0·034-0·106	87	
				-	0·46 to 0·48	-	18-95	0·034-0·106	10-80	
				-	0·96	-	40-130	0·106	100-350	
Ring electrodes with annular gap (A.C. arcs - ½ cycle) Bronfman[11]	Copper	Inner rad = 2·0 Thickness = 0·3	0·1	10·5	0·33	-	20-107	0·046	10-1000	1st cycle of arc
				∝B	0·4	-	80-390	0·03-0·13	200-2000	Several cycles of arc

Note:- (1) The results for a pair of straight open-ended brass electrodes were measured at fixed values of applied magnetic field which were then corrected for the self-field of the arc current in the electrodes, so that analysis at "constant B" includes a variation in B of up to ±12%, see Fig.21.

(2) Later results with the same electrodes indicate that the same empirical relation applies for magnetic fields up to 1·0 Wb/m^2 and arc velocities up to 580 m/s.

Table 2

VALUES OF $2/K^2$, $(1-2\ n_1)$ AND $(1-2\ n_2)$ IN EQUATION (10)

$$\rho A = 2/K^2\ I^{(1-2n_1)}\ B^{(1-2n_2)} \qquad (10)$$

Electrodes			$2/K^2$	$(1-2\ n_1)$	$(1-2\ n_2)$	U (m/S)	B (Wb/m^2)	I (amp)
Configuration	Material	d(cm)						
Pair of straight open-ended rails (Fig.1(b))	Graphite	3·0	-	-	(-0·4 ±0·2)	10-50	0·01-0·09	~350
	Brass	1·27	-	0 ±0·02)	-	30-100	0·026-0·037	100-1200
			0·0038 to 0·0045	(0·20 ±0·02)	(0·20 ±0·02)	30-275	0·04-0·49	100-1250
						70-420	0·12-0·49	200-3700
			-	-	(0·60 ±0·02)	210-270	0·05-0·15	∞
Electrodes with long path length	Brass	1·27	0·022 to 0·028	-0·16 ±0·02)	-	40-70	0·02-0·12	230-500
						55-205	0·04-0·12	230-1200
						65-340	0·06-0·12	230-2700
				-	(0·16 ±0·02)	40-200	0·02-0·12	230-1200
Circular electrodes with annular gap	Graphite 1	0·65	0·000083 to 0·00011	(0·34 ±0·02)	(-0·20 ±0·02)	16-190	0·006-0·094	100-750
	Brass	1·27	~0·0001	~0·3	~ -0·1	50-130	0·02-0·13	200-450

Table j

VALUES OF n_3, n_4 IN THE EQUATIONS :-

$$E \propto B^{n_3}$$

$$E/U \simeq (\text{const})\,(IU)^{-n_4}$$

	Pair of open-ended rail electrodes	Circular electrodes with annular gaps		Electrodes with long path length (Fig.1(a))
	Brass	Carbon[1]	Brass	Brass
n_3	0·3 approx.	0·27 approx.		0·4 approx.
n_4	0·4 ±0·1	0·4 ±0·1	0·4 ±0·1	0·4 ±0·1
U(m/s)	30-180	16-185	50-130	40-340
B(Wb/m^2)	0·02-0·13	0·006-0·10	0·02-0·13	0·02-0·12
I(amp)	100-3700	100-500	200-450	200-2700
E(v/cm)	16-26	28-60	14-30 (assumed same as col.5)	14-30
d(cm)	2·54-3·8	0·65-3·2	1·27	1·27-2·54

SYMBOLS

A	effective drag area	(m^2)
B	magnetic field	(Wb/m^2)
C_D	drag coefficient	
D	effective arc width	(m)
d	electrode gap width	(m)
E	voltage gradient	(V/m)
f_1 to f_{12}	functions	
I	arc current	(amp)
K	constant of proportionality	
M	Mach number	
n_1 to n_4	indices in simple power relations	
P	pressure	
Re	Reynolds number	
r	radius	
$\hat{r}$	radius of conducting boundary of cylindrical arc column	
T	temperature	(°K)
U	arc velocity	(m/sec)
V	total arc voltage	(volts)
v	sum of arc electrode fall voltages and of non-uniform parts of arc column	(volts)
ρ	density	(Kg/m^3)
ν	kinematic viscosity	(m/sec)
μ_o	magnetic permeability of free space	(Henry/m)
ω	angular velocity	(radians/sec)

Subscripts (apply only to section 4.1.1)

i	denotes value for initial motion of arcs
r	denotes value *for* arcs rotating in annular gaps

A	±14%
B	±5%
E	±10%
g	±0.05 cm
I	±10%
U	±5%
V	±10%

Estimated Experimental Errors

E/U	±11%
Iu	±11%
EI	±14%
U^2 I/E	±16%
BI/U	±12%

REFERENCES

No.	Author	Title, etc
1	V. W. Adams	The influence of gas streams and magnetic fields on electric discharges, (Parts 1 and 2). A.R.C. C.P. No.743, June 1963
2	P. E. Secker, A. E. Guile	Arc movement in a transverse magnetic field at atmospheric pressure. Proc. I.E.E., 106A, 28, 311. 1959
3	H. C. Spink, A. E. Guile	The movement of high current arcs in transverse external and self-magnetic fields *in* air at atmospheric pressure. (University of Leeds, 1964.) A.R.C. C.P. No.777, May 1964
4	E. D. Blix, A. E. Guile	The magnetic deflection of short arcs rotating between annular electrodes above and below atmospheric pressure. (University of Leeds, 1964.) A.R.C. C.P. No.843, October 1964
5	A. Eidingcr, W. Rieder	Das Verhalten des Lichtbogens in transversalen magnetfeld. Archiv. für Elektrotechnik, 43, 94. 1957
6	D. Hesse	Über den EinfluB des laufschienen-feldes auf dio ausbildung und bewegung von lichtbogenfuBipunkten. Archiv. für Elektrotechnik, 45, 188. 1960
7	J. R. Jedlicka	The shape of *a magnetically* rotated electric arc column in an annular gap. NASA TN D-2155. October 1964

REFERENCES (Contd)

No.	Author	Title, etc
8	W. T. Lord	Some magneto-fluid-dynamic problems involving electric arcs. R.A.E. Tech Note No. Aero 2909, August 1963
9	W. T. Lord	Effects of a radiative heat sink on arc voltage-current characteristics. Proceedings of a Specialists Meeting on arc heaters and MHD accelerations for Aerodynamic purposes, AGARD Fluid Dynamics Institute, Belguim, 1964. AGARDograph 84, Part 2, 673.
10	A. H. Mitchell	Unpublished Mintech work
11	A. I. Bronfman	Arc travel in the annular clearances of spark gaps in magnetic rotating arc arrestors. Elektrichestvo, No.8, 56. 1963
12	A. I. Bronfman	Vestnik elektroprom., No.7, 1960
13	A. H. Mitchell	Unpublished Mintech work
14	H. C. Early, W. N. Lawrence	Transient, high current arcs in extremely dense air. AEDC 02792-1-T. Dept. of Electrical Engineering, University of Michigan. 1960
15	A. A. Wells	Unpublished Mintech work
16	E. G. Broadbent	A theoretical exploration of the flow about an electric arc transverse to an airstream using potential flow methods. R.A.X. Tech Report No.65056, A.R.C. 26,848, March 1965

REFERENCES (Contd)

No.	Author	Title, etc
17	S. F. Hoerner	Fluid dynamic drag. Published by the Author. 1958
18	W. T. Lord, E. G. Broadbent	An electric arc across an airstream. R.A.E. Tech Report No.65055, A.R.C. 26,847, March 1365
19	H. Z. Maecker	Plasma streams in arcs due to self-magnetic compression. z. für Phys, 141, 198. 1955
20	H. W. Emmons, R. I. Land	Poiseuille plasma experiment. Physics of Fluids 5, 12. 1962
21	M. M. Chen	Theoretical investigations of a high pressure fully developed laminar column. Theoretical and experimental investigations of arc plasma - generation technology, Part II, Vol.2, 5. ASD-TDR-62-729. 1963
22	M. Strutt	Das magnetische feld eines reckteckigen von gleichstrom. Archiv. für Elektrotechnik XVii, 535 and Xviii, 282. 1927
23	V. L. Streeter	Handbook of Fluid Mechanics, 5-20. McGraw Hill. 1961
24	W. B. Boatright, R. R. Stenart, D. I. Sebacher, M. A. Wallio	Summary of some of the arc-heated hypersonic wind tunnel development effort underway at the Langley Research Center. Proceedings of a Specialists Meeting on arc heaters and MHD accelerators for aerodynamic purposes, AGARD Fluid Mechanics Institute, Belguim, 1964. AGARDograph 84, Part 2, 353

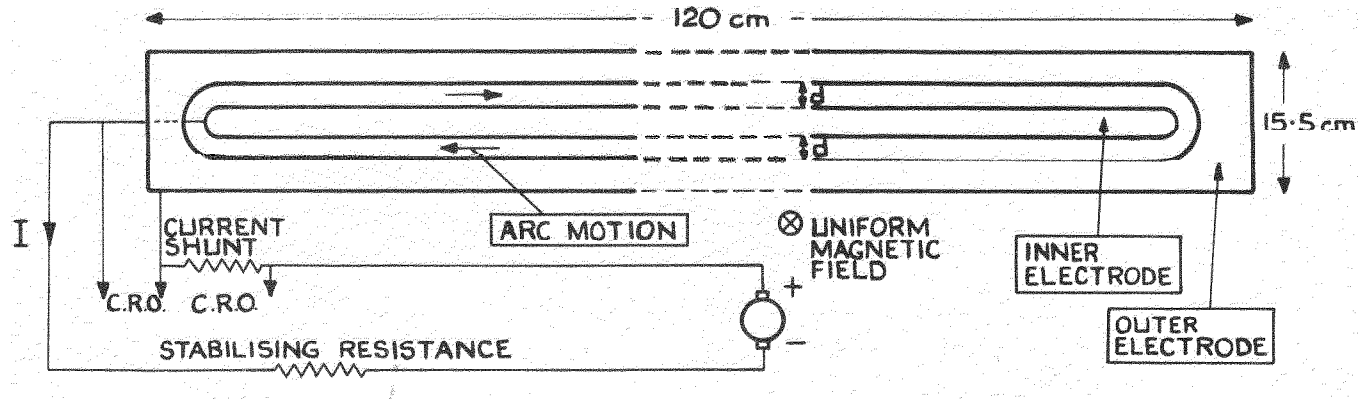

FIG. 1(a) ELECTRODES FOR CONTINUOUSLY OPERATED ARCS (BRASS) (INSULATED ON TOP AND BOTTOM SURFACES WITH THIN ALUMINIUM OXIDE COATING OR "SINDANYO" 0·6cm THICK)

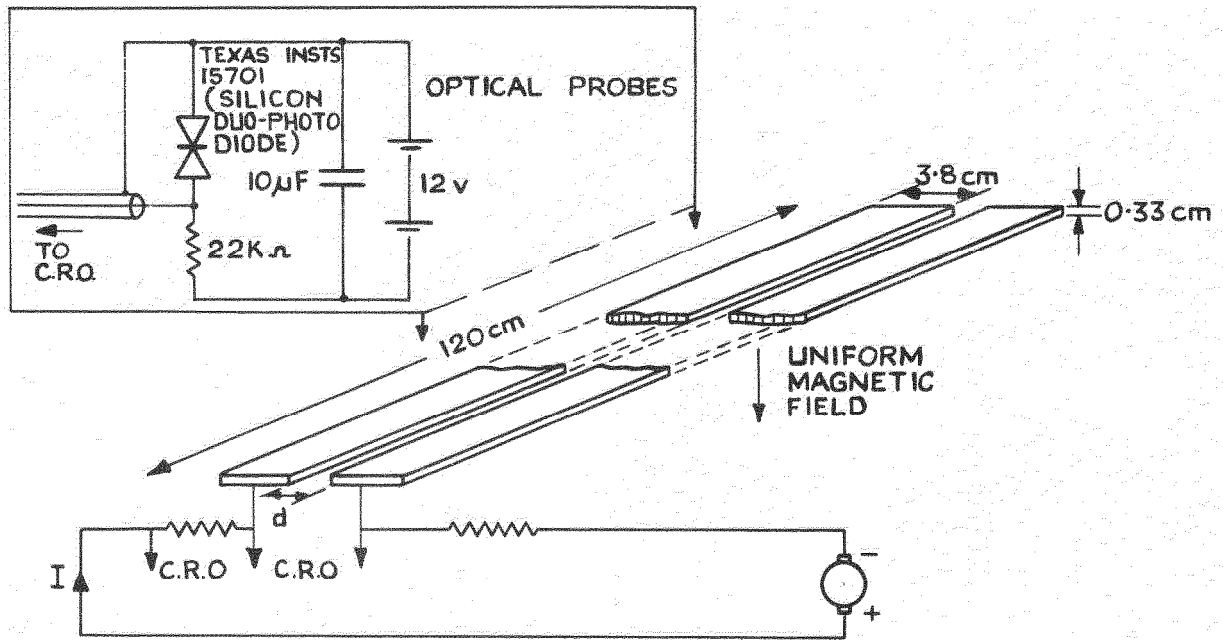

FIG. 1(b) PAIR OF STRAIGHT OPEN ENDED BRASS RAIL ELECTRODES (INSULATED ON TOP AND BOTTOM SURFACES WITH "SINDANYO" 0·6 cm THICK)

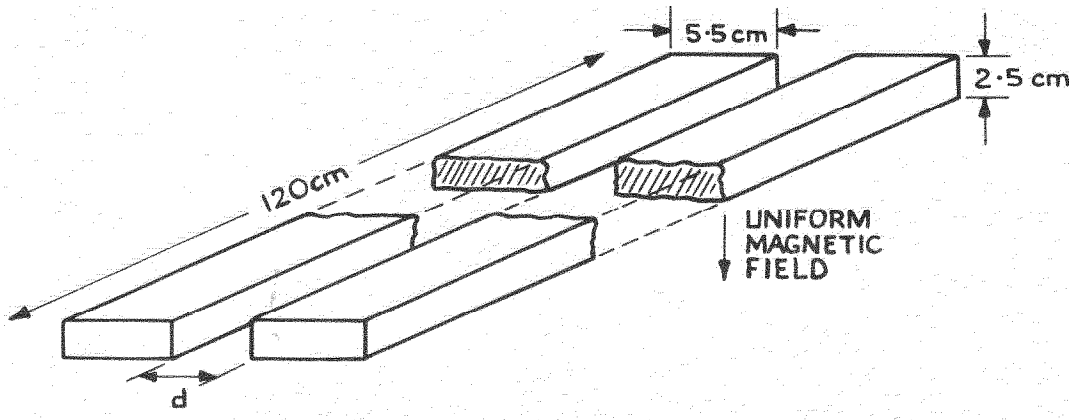

(ELEC. CIRCUIT AS (b) ABOVE)

FIG. 1(c) PAIR OF STRAIGHT OPEN ENDED CARBON ELECTRODES

FIG. 1 ELECTRODES WITH STRAIGHT ARC PATHS

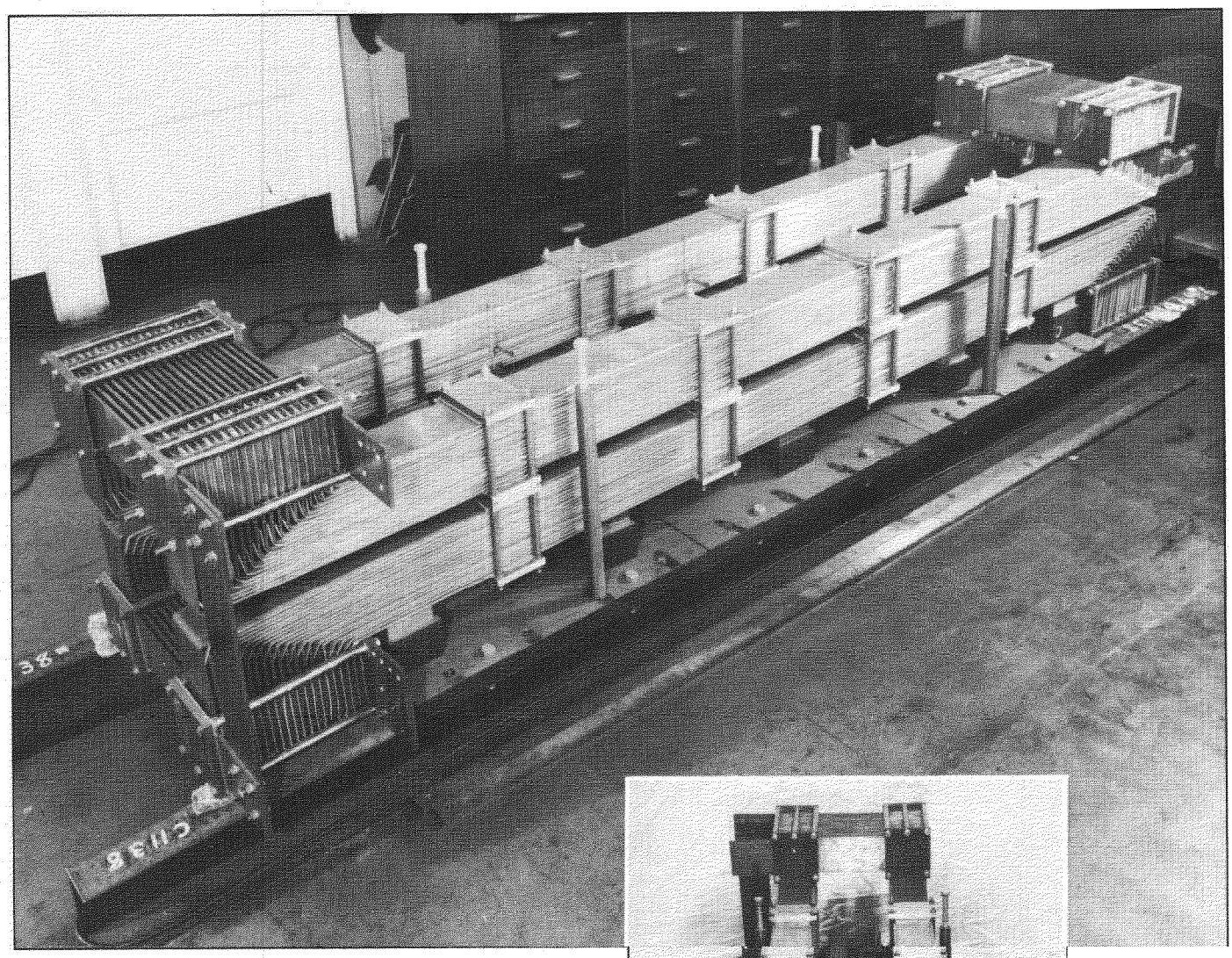

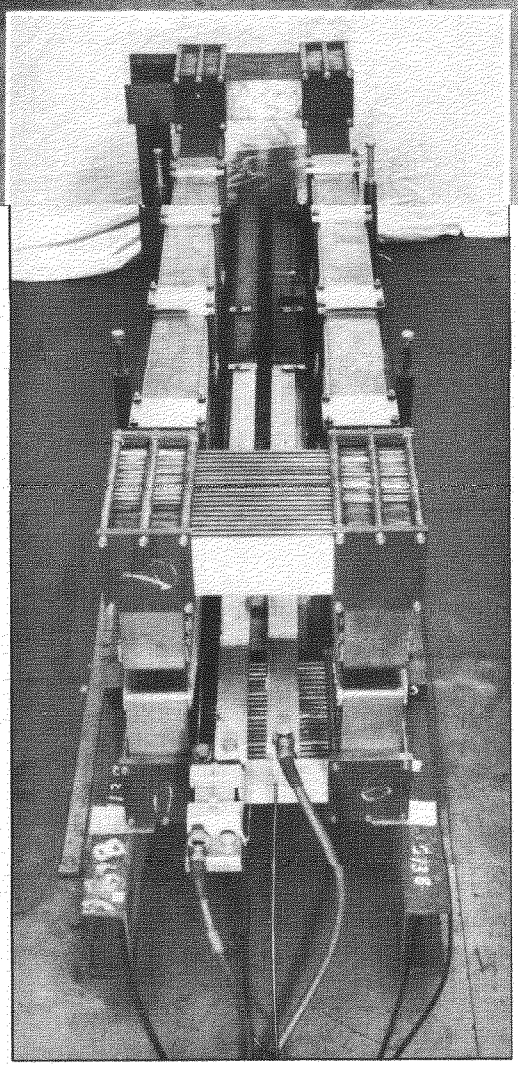

Fig.2. Magnet for arc experiments in a transverse magnetic field (Showing carbon electrodes, connecting bars and current shunt in position)

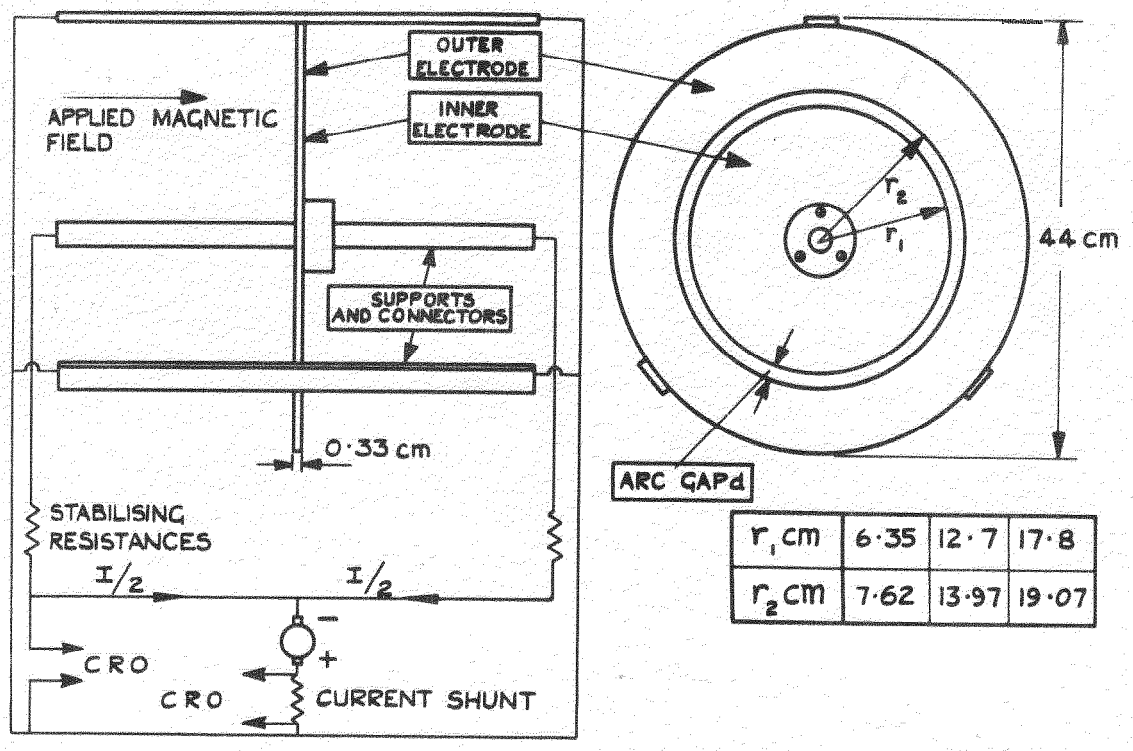

r_1 cm	6·35	12·7	17·8
r_2 cm	7·62	13·97	19·07

FIG 3(a) UNCOOLED CIRCULAR BRASS ELECTRODES (SPRAYED ON BOTH SIDES WITH REFRACTORY INSULATOR)

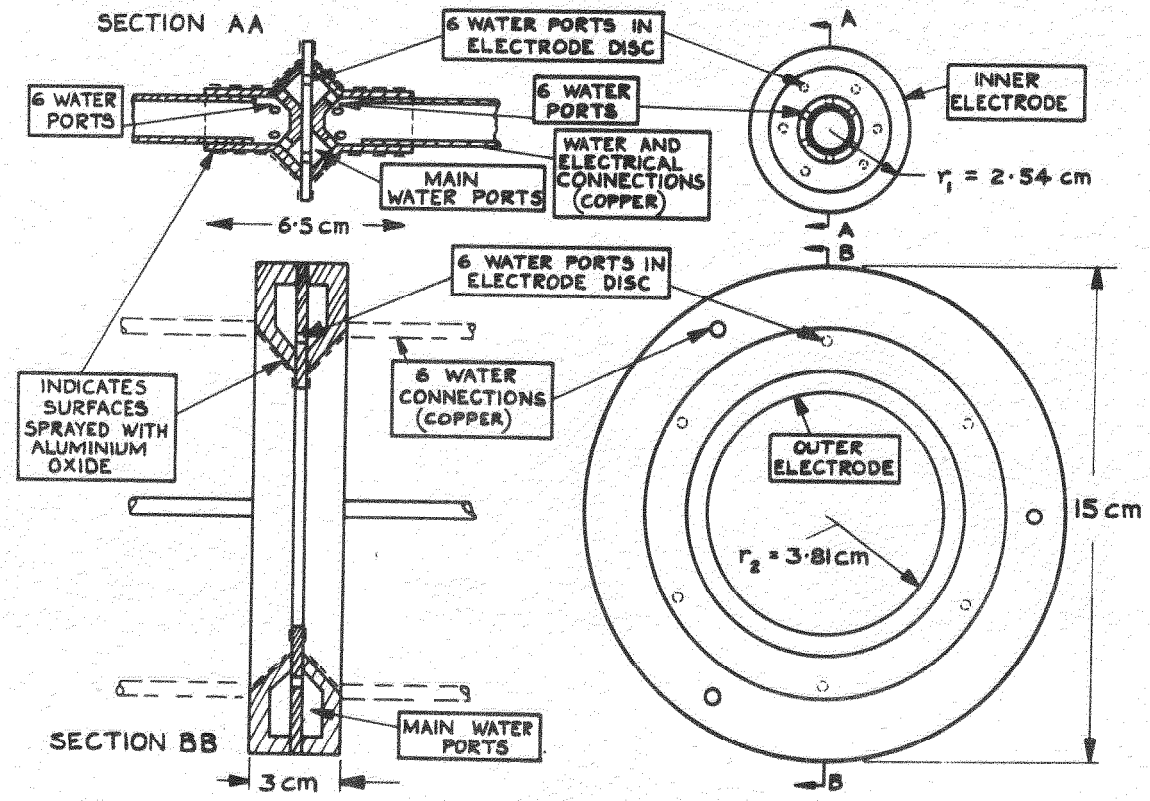

FIG 3(b) WATER-COOLED CIRCULAR BRASS ELECTRODES (ALL JOINTS SOFT-SOLDERED) (ELEC CIRCUIT AS (a) ABOVE)

FIG 3 CIRCULAR BRASS ELECTRODES

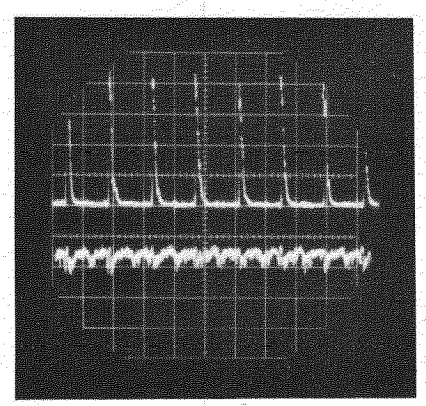

UPPER TRACE : PROBE SIGNALS
LOWER TRACE : VOLTAGE (50V/DIV.)

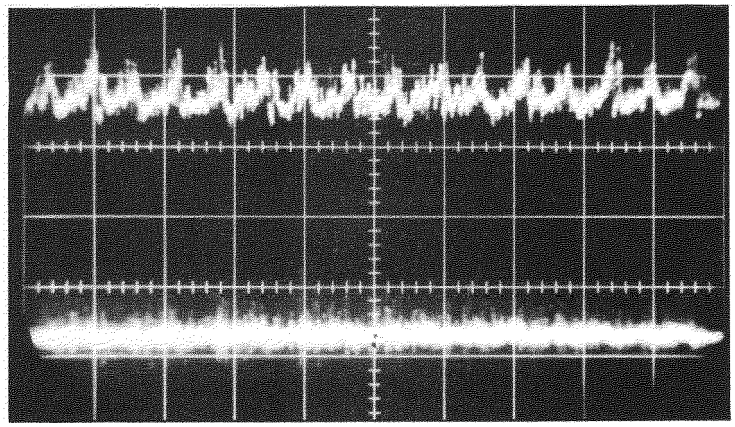

UPPER TRACE : VOLTAGE (50V/DIV.)
LOWER TRACE : CURRENT (600A/DIV.)

RECORDS FOR ARC ON ELECTRODES OF FIG.1(a) 10 MSEC/DIV.

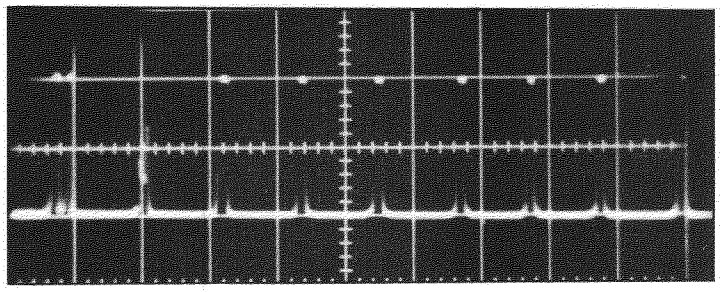

PROBE SIGNALS

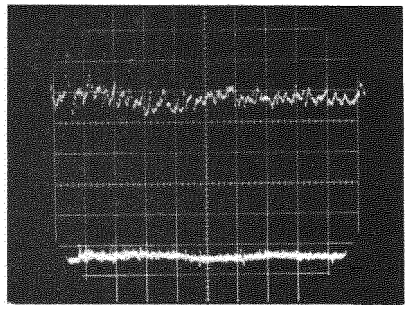

UPPER TRACE : VOLTAGE (50V/DIV.)
LOWER TRACE : CURRENT (100A/DIV.)

RECORDS FOR ARC ON WATER-COOLED BRASS ELECTRODES OF FIG.3(b)
2 MSEC/DIV.

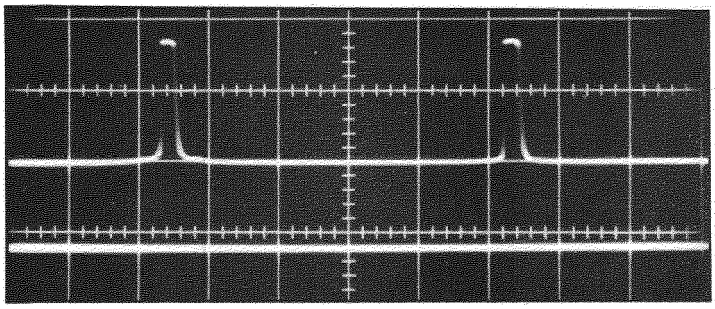

PROBE SIGNALS

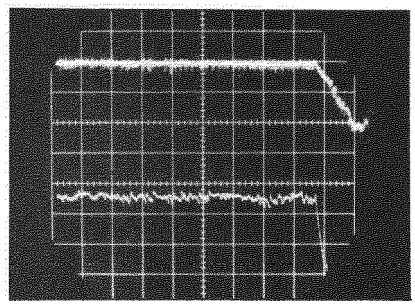

UPPER TRACE : CURRENT 400A/DIV.)
LOWER TRACE : VOLTAGE (50V/DIV.)

RECORDS FOR ARC ON PAIR OF BRASS RAILS (FIG.1(b))
1 MSEC/DIV. U = 102 M/S

Fig.4. Examples of oscilloscope records (Zero at scale centres)

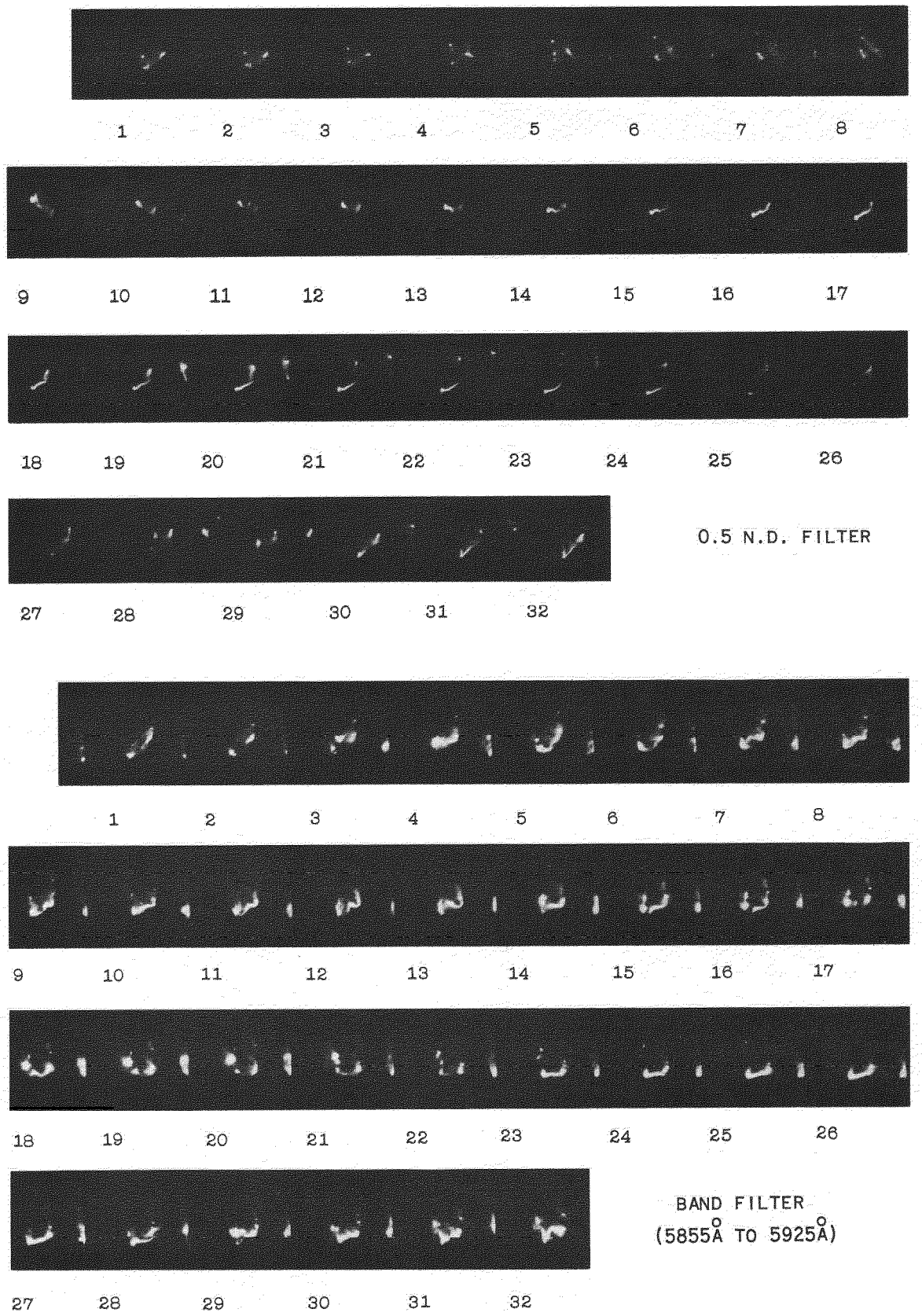

Fig.5. High speed photographs of arcs on graphite electrodes (I=300A, U=31.3m/s, d=3cm.) The left hand image of each frame was taken looking horizontally across the top surfaces of the electrodes and the right hand image looking vertically down onto the electrode gap; the arc motion is down the paper

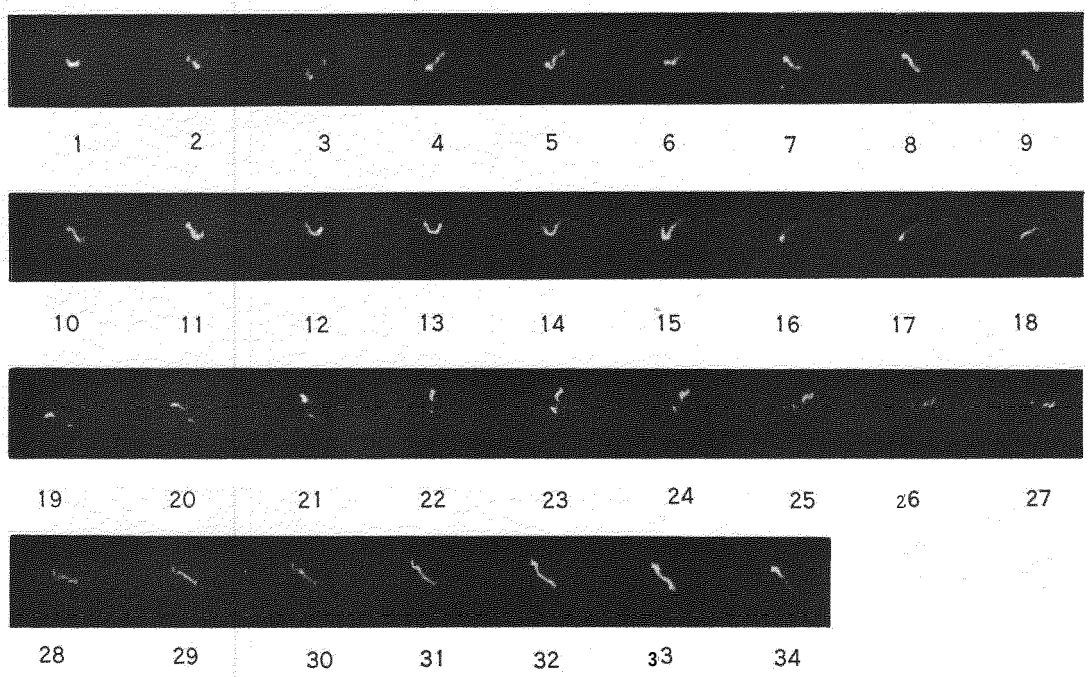

ARC MOTION AS SHOWN BELOW:-

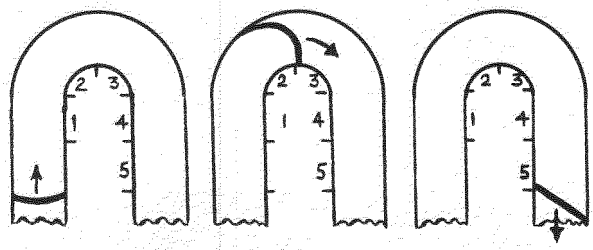

FRAME 1 FRAME 18 FRAME 34

0.5 N.D. FILTER
I = 430A
d = 2.54 CM
U = 100 M/S
ELECTRODE THICKNESS = 0.33 CM

FIG.6(a) TAKEN WITH CAMERA POINTING VERTICALLY DOWN ONTO ELECTRODE GAP

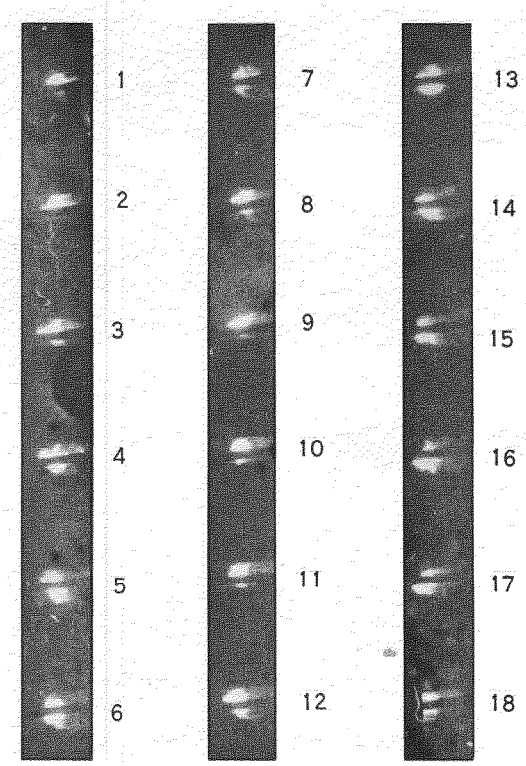

0.5 N.D. FILTER
I = 500A
d = 1.27 CM
U = 130 M/S
ELECTRODE THICKNESS = 0.63 CM
(ARC MOTION FROM RIGHT TO LEFT)

FIG.6(b) TAKEN WITH CAMERA POINTING ALONG ARC AXIS

Fig.6. High speed photographs of arcs on electrodes of fig.1(a)

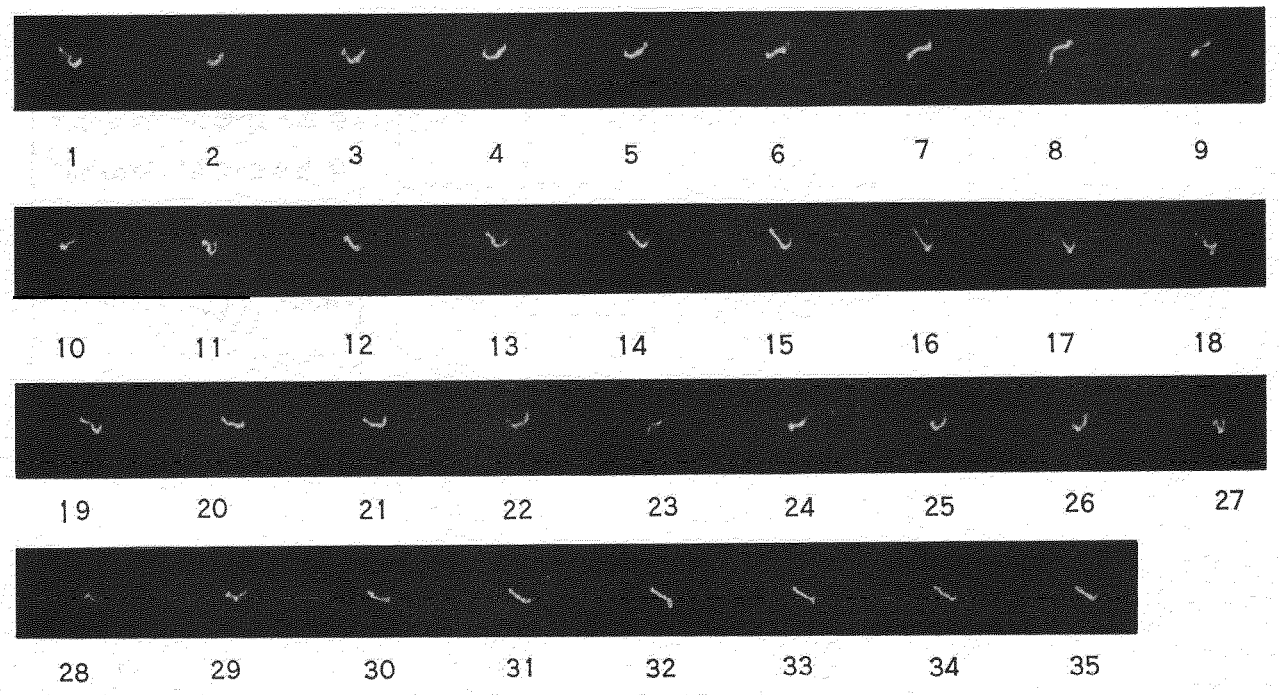

I = 500A
d = 2.54 CM 0.5 N.D. FILTER
U = 90 M/S

FIG.7(a) TAKEN WITH CAMERA POINTING VERTICALLY DOWN ONTO ELECTRODE GAP (ARC MOTION IS UP THE PAPER)

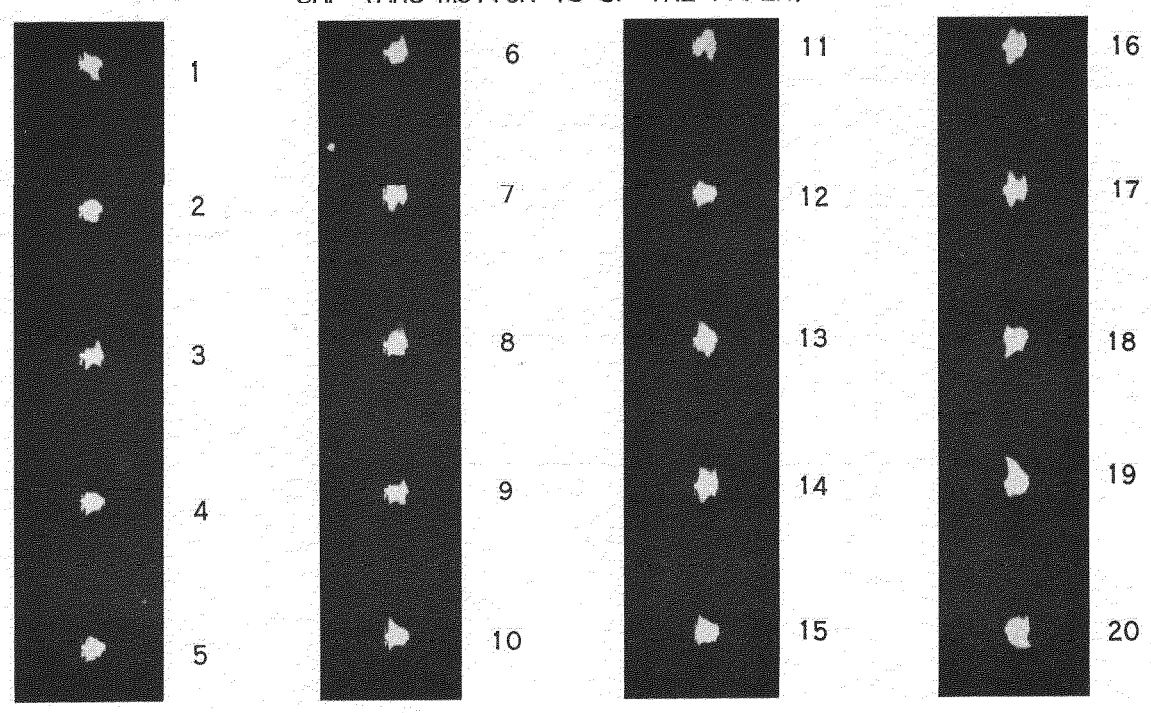

I = 1100A d = 1.27 CM U = 167 M/S
1.0 N.D. FILTER

FIG.7(b) TAKEN WITH CAMERA POINTING ALONG DIRECTION OF ARC MOTION (TOWARDS CAMERA)

Fig.7. High speed photographs of arc on straight brass electrodes

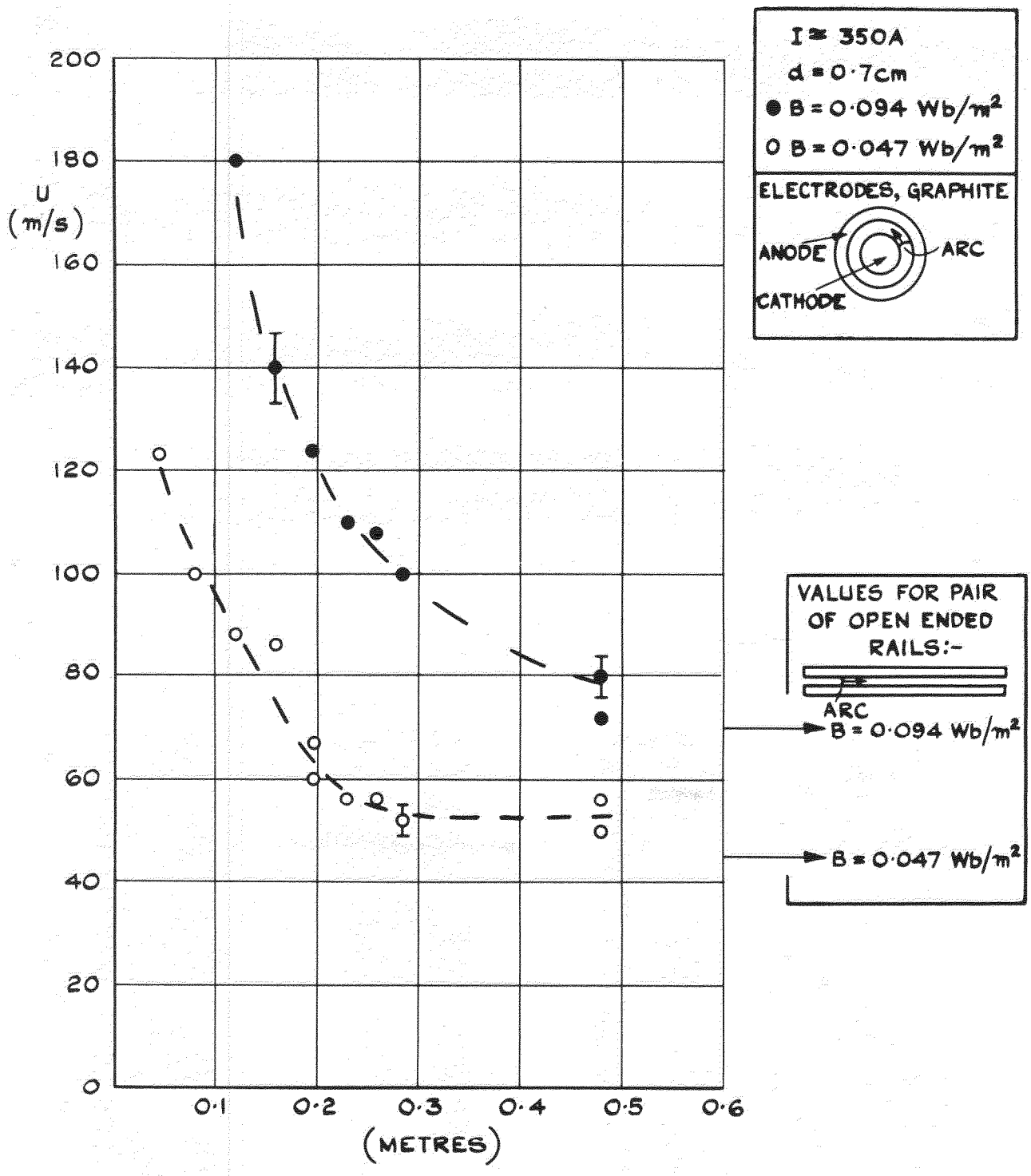

FIG 8 ARC VELOCITY AGAINST ELECTRODE PATH LENGTH (GRAPHITE)

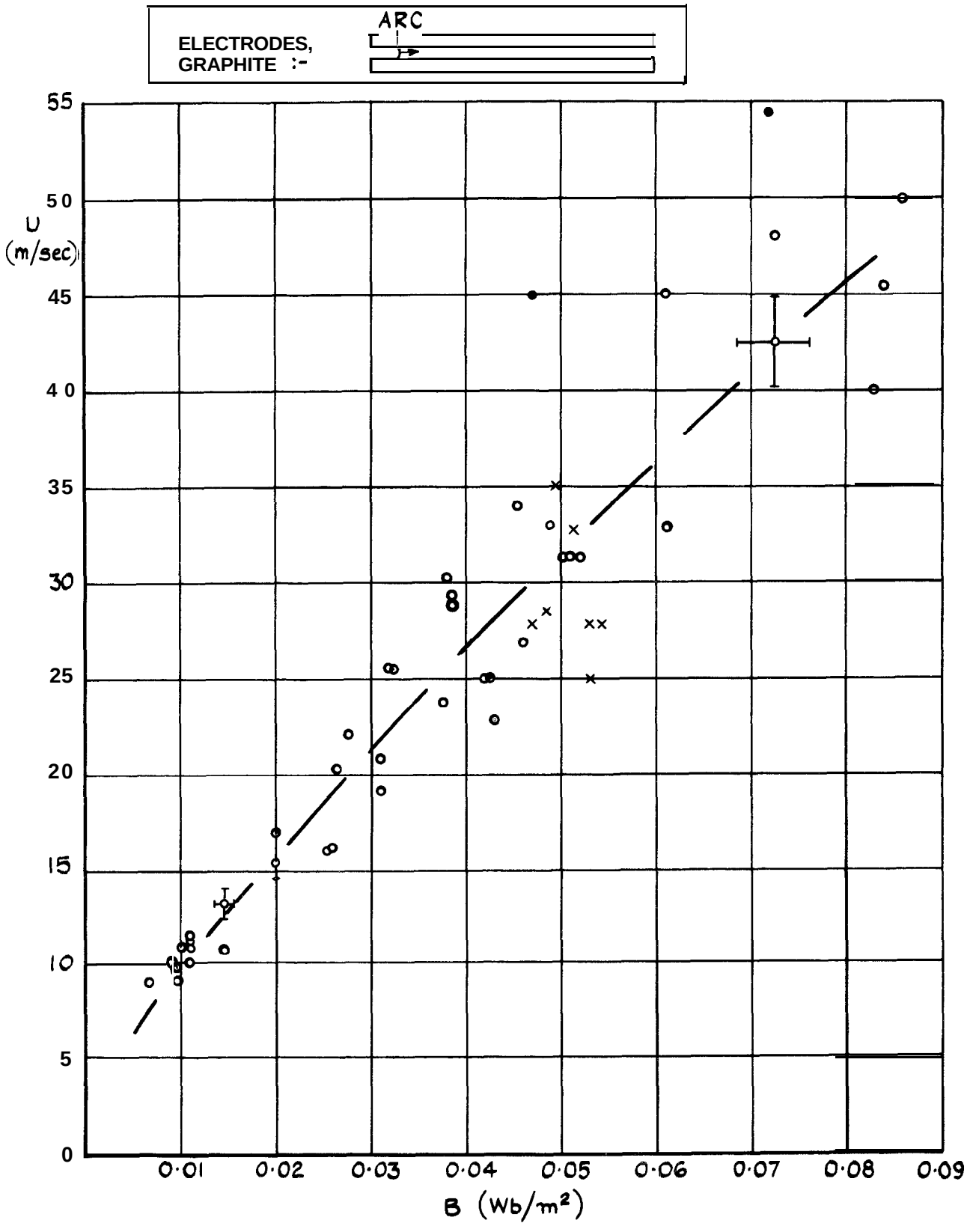

o GAP WIDTH = 3cm. ARC CURRENT = 250 TO 350 amp
x GAP WIDTH = 1·5cm. ARC CURRENT = 150 TO 170 amp
. GAP WIDTH = 0·7cm. ARC CURRENT = 350 amp

FIG. 9 ARC VELOCITY AGAINST APPLIED MAGNETIC FIELD FOR STRAIGHT GRAPHITE ELECTRODES

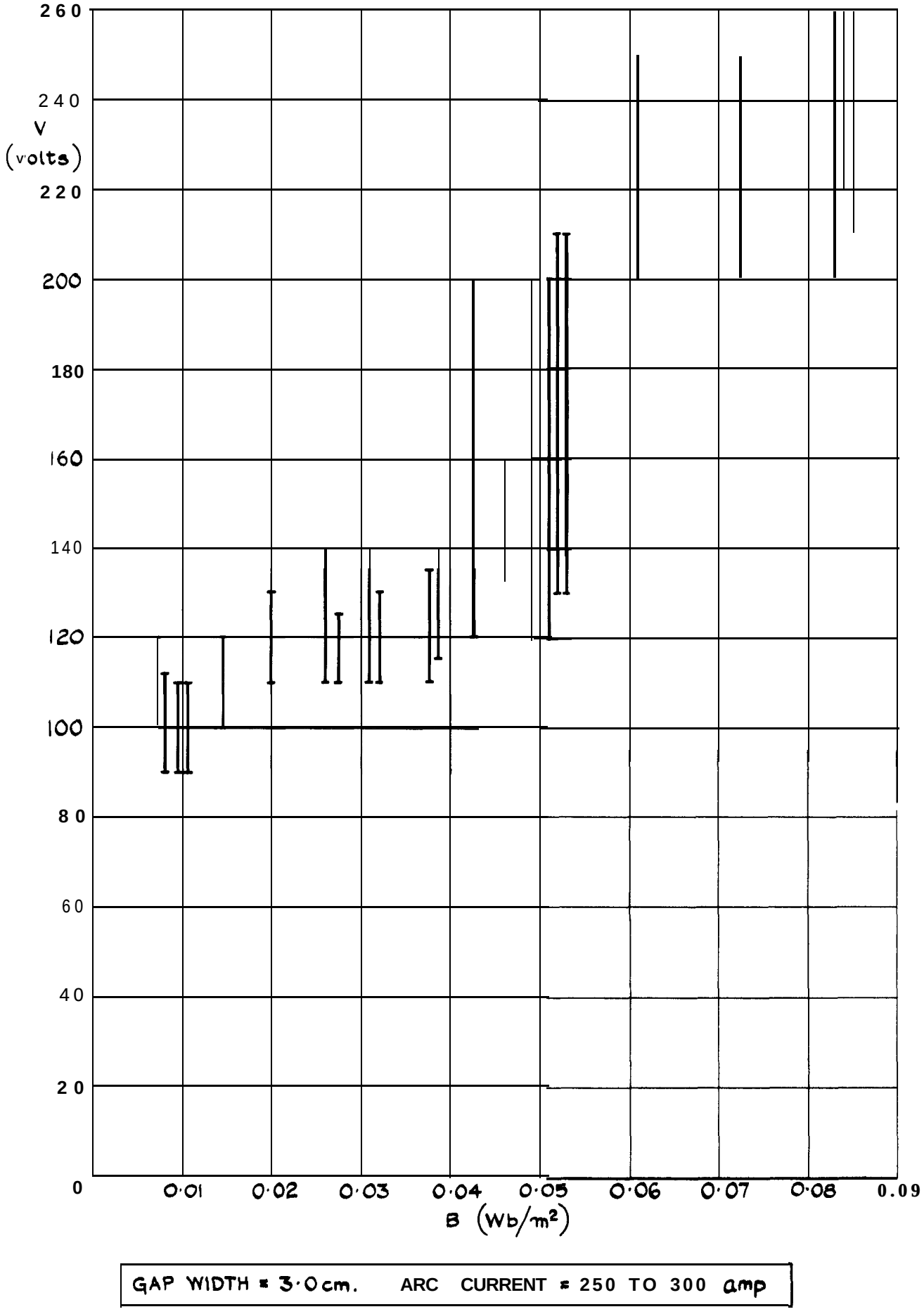

FIG. 10 ARC VOLTAGE AGAINST APPLIED MAGNETIC FIELD FOR STRAIGHT GRAPHITE ELECTRODES

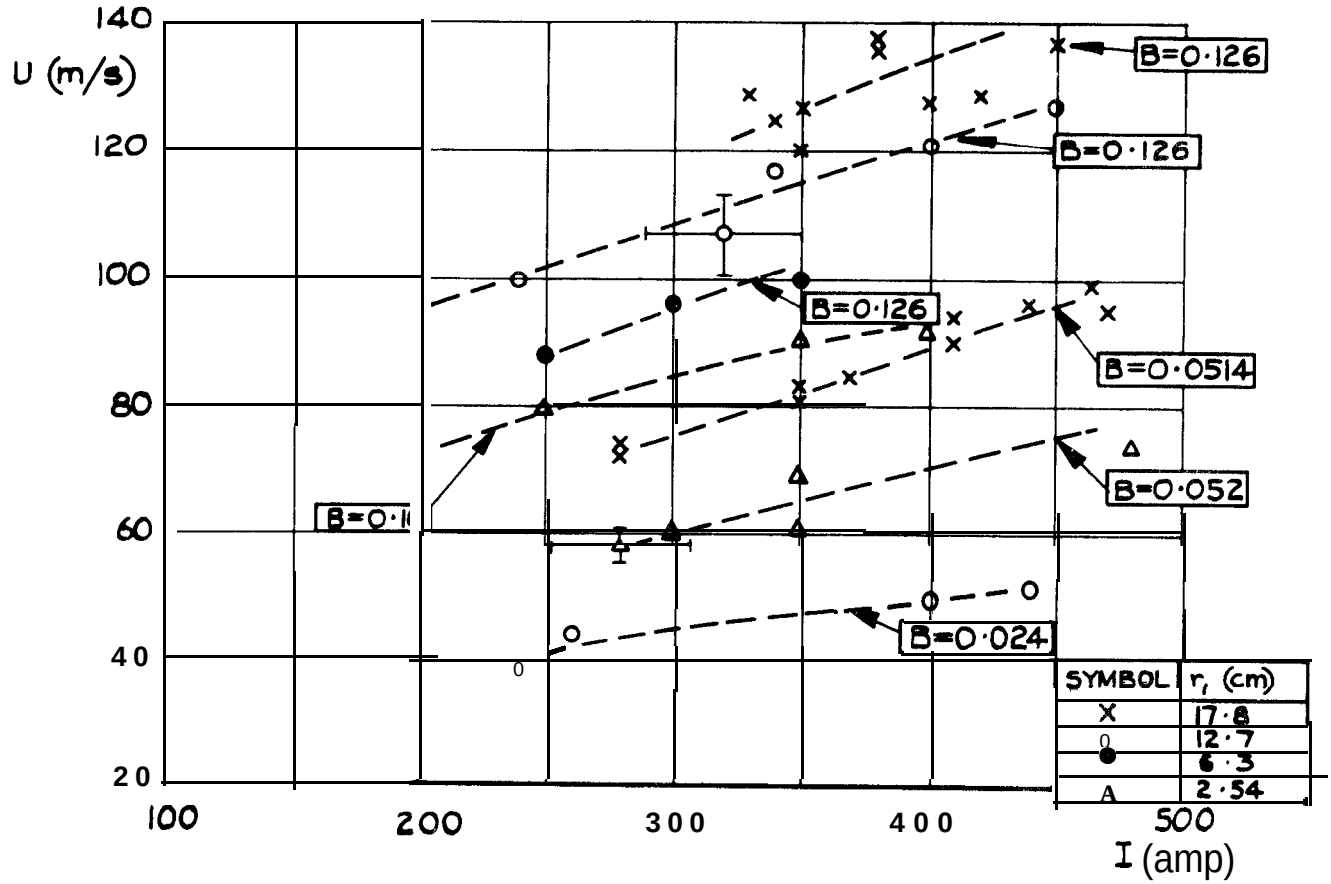

FIG II ARC VELOCITY AGAINST ARC CURRENT FOR CIRCULAR BRASS ELECTRODES ($a = 1{\cdot}27$cm) (B IN Wb/m^2)

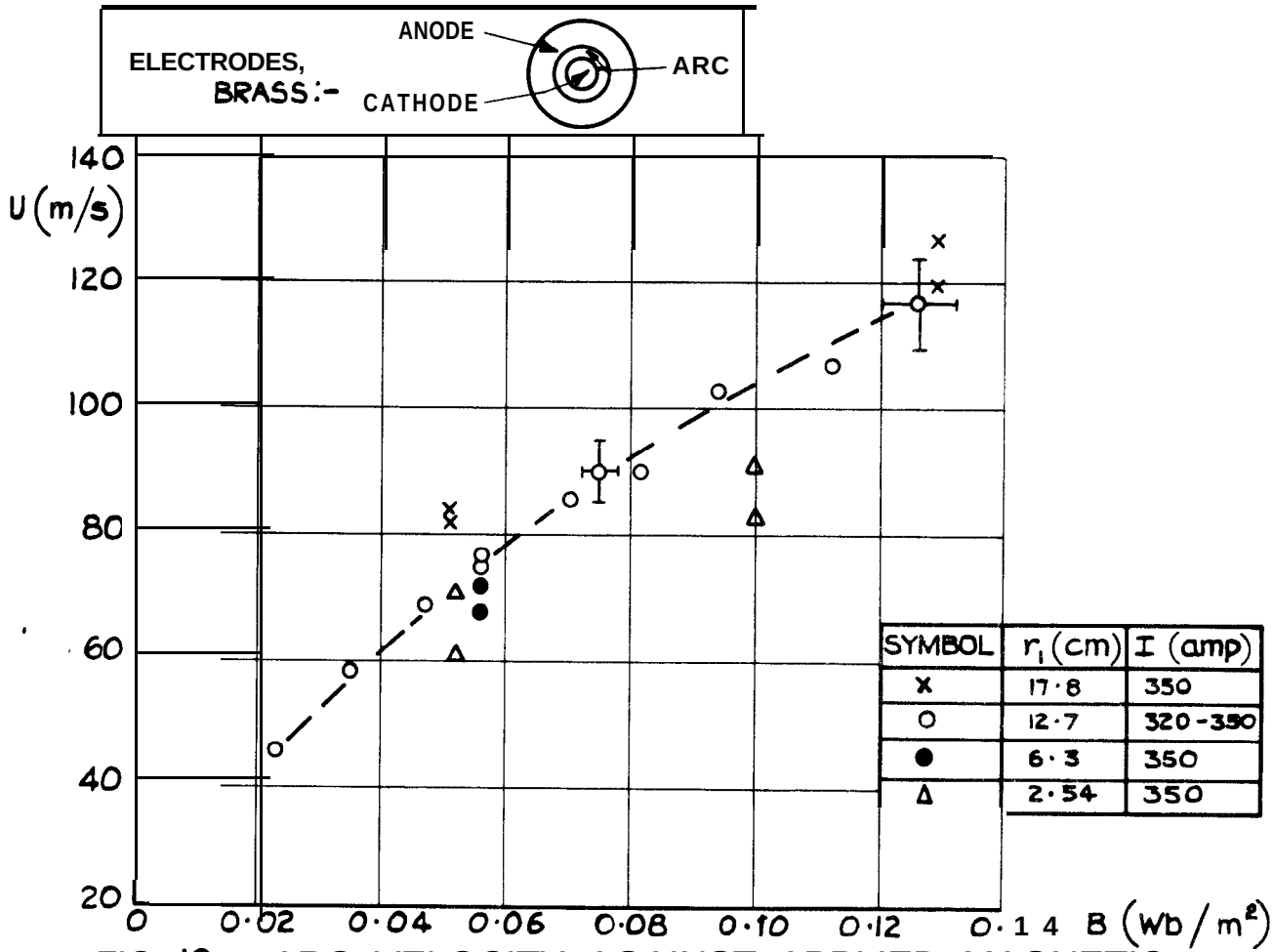

FIG. 12 ARC VELOCITY AGAINST APPLIED MAGNETIC FIELD FOR CIRCULAR BRASS ELECTRODES ($d = 1{\cdot}27$cm)

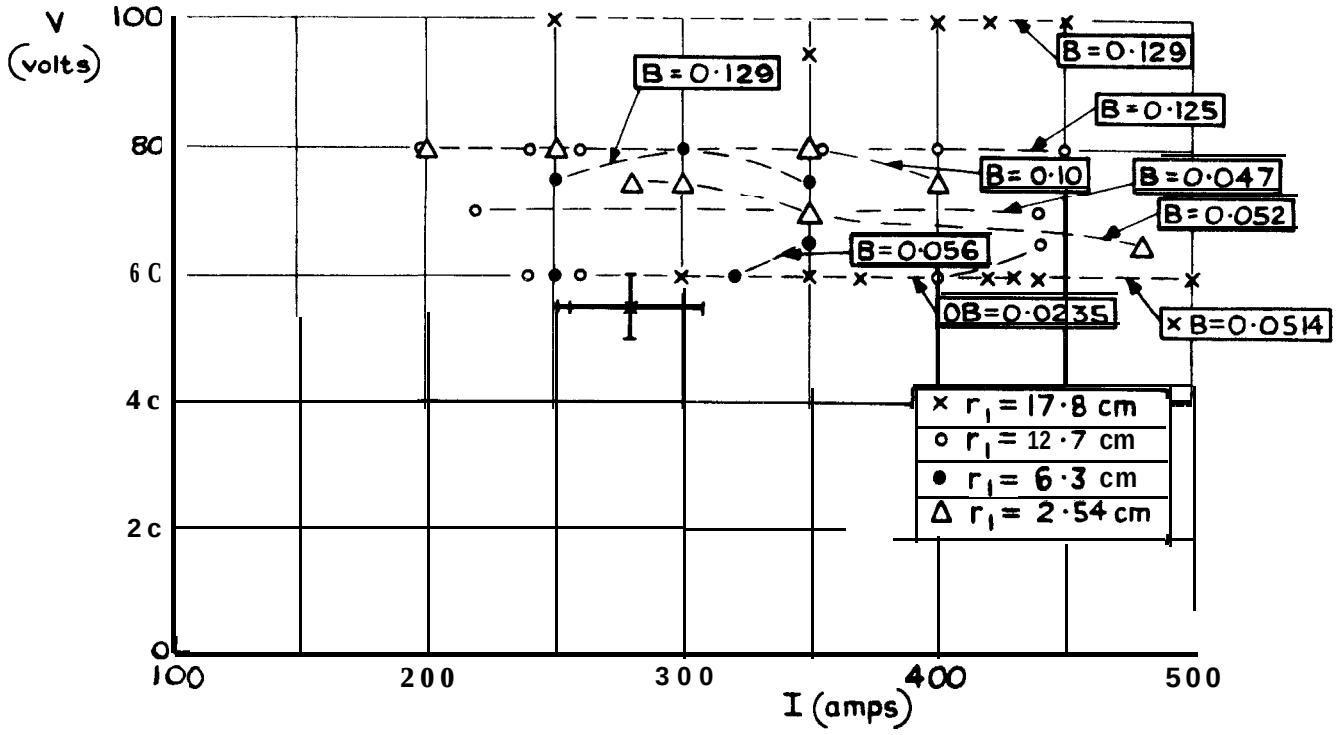

FIG. 13 MINIMUM ARC VOLTAGE **AGAINST ARC CURRENT FOR CIRCULAR** BRASS ELECTRODES (d= 1·27cm) (B IN Wb/m²)

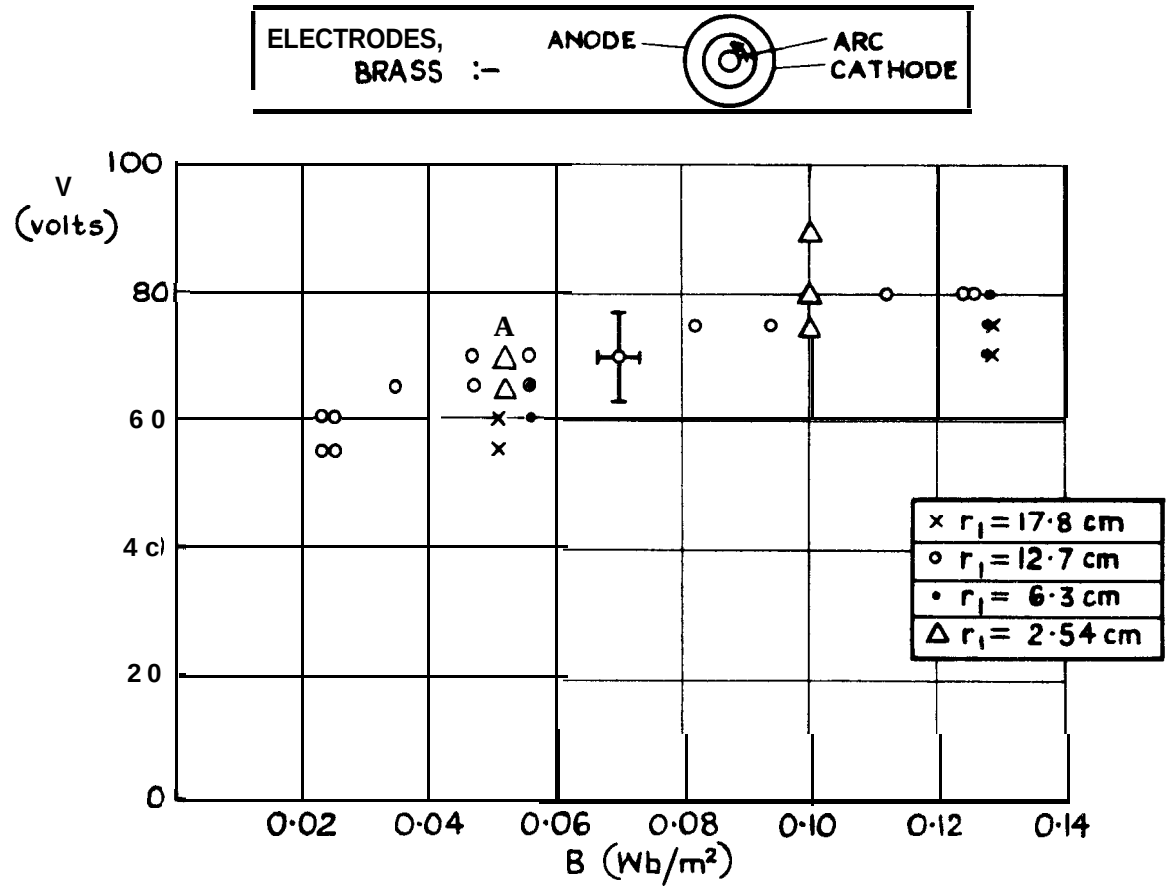

FIG. 14 MINIMUM ARC VOLTAGE AGAINST APPLIED MAGNETIC FIELD FOR CIRCULAR BRASS ELECTRODES (d = 1·27cm)
(V ASSUMED INDEPENDENT OF I)

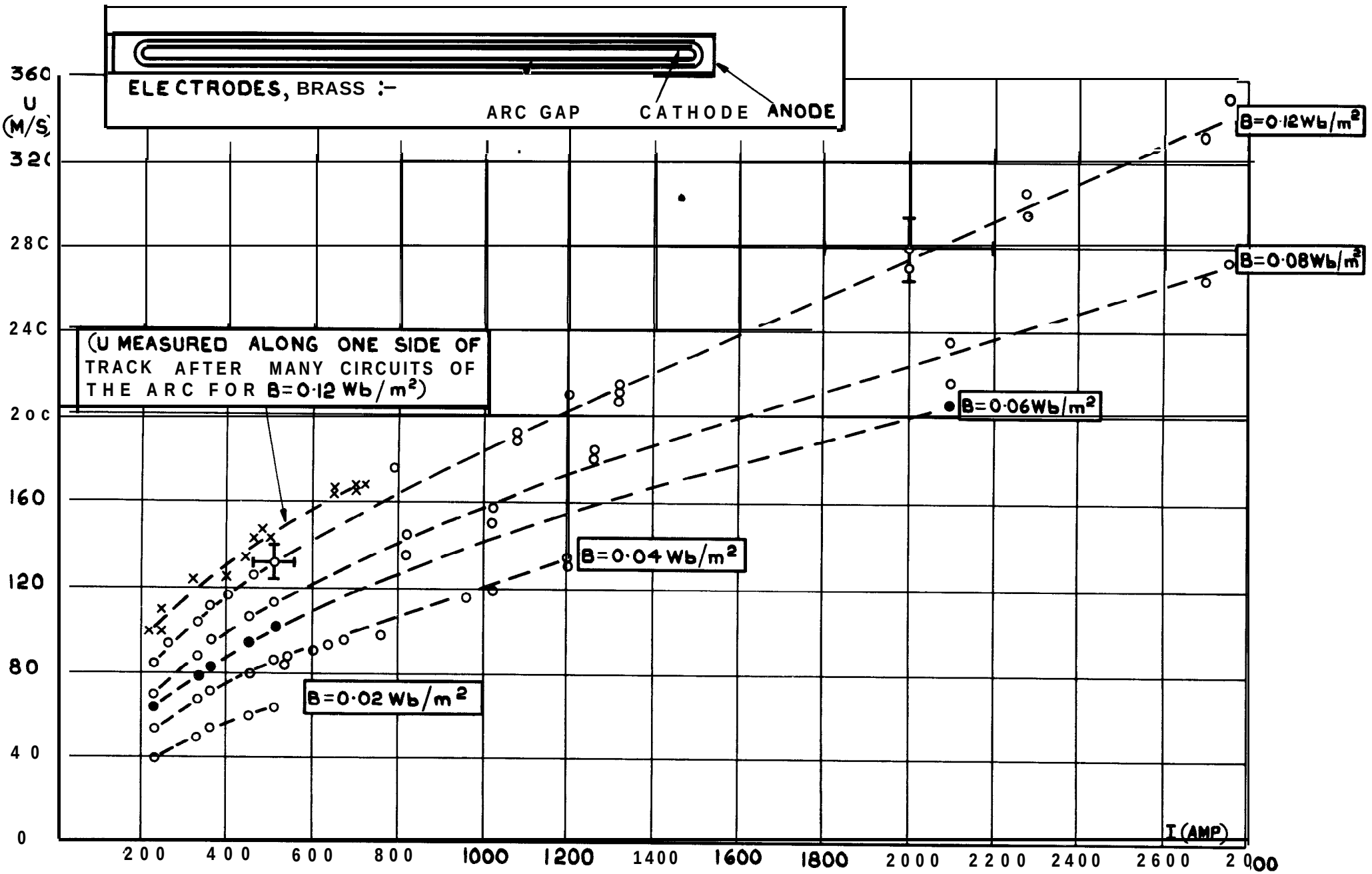

FIG.15 ARC VELOCITY AGAINST ARC CURRENT FOR CONTINUOUSLY OPERATED ARCS ON BRASS ELECTRODES (d=1·27 cm)

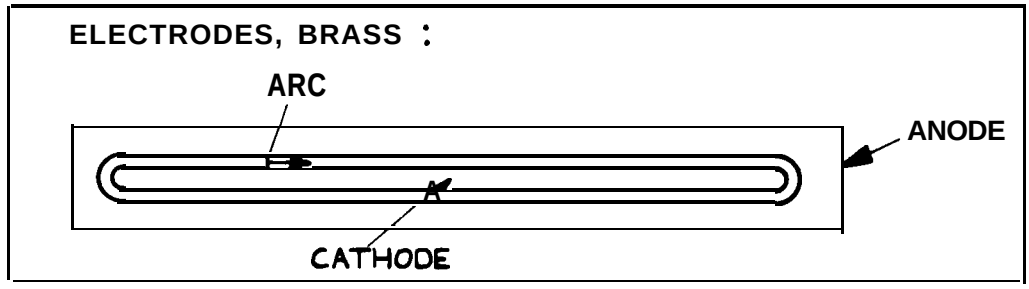

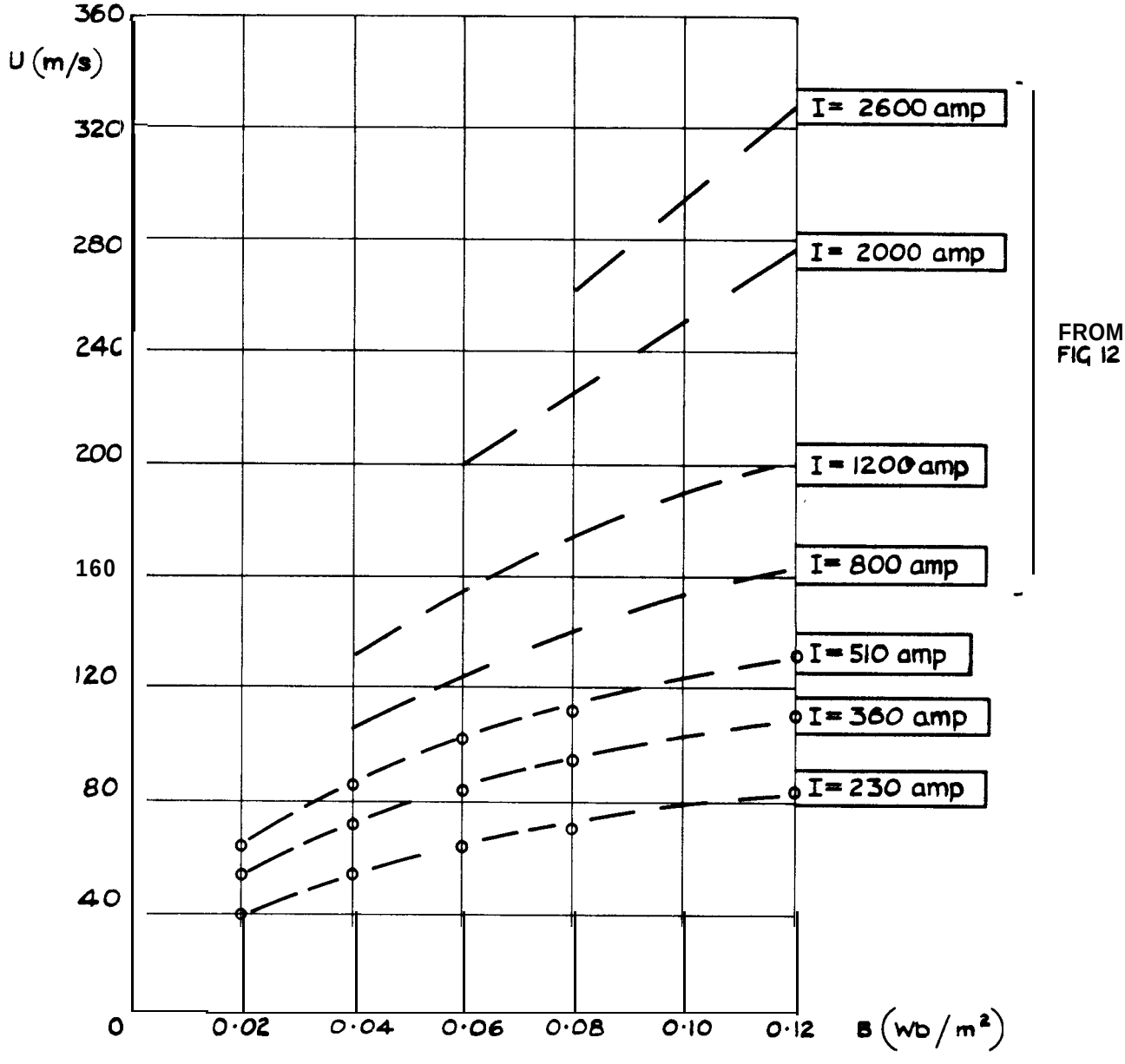

FIG 16 ARC VELOCITY AGAINST APPLIED MAGNETIC FIELD FOR CONTINUOUSLY OPERATED ARCS ON BRASS ELECTRODES (d =1·27cm)

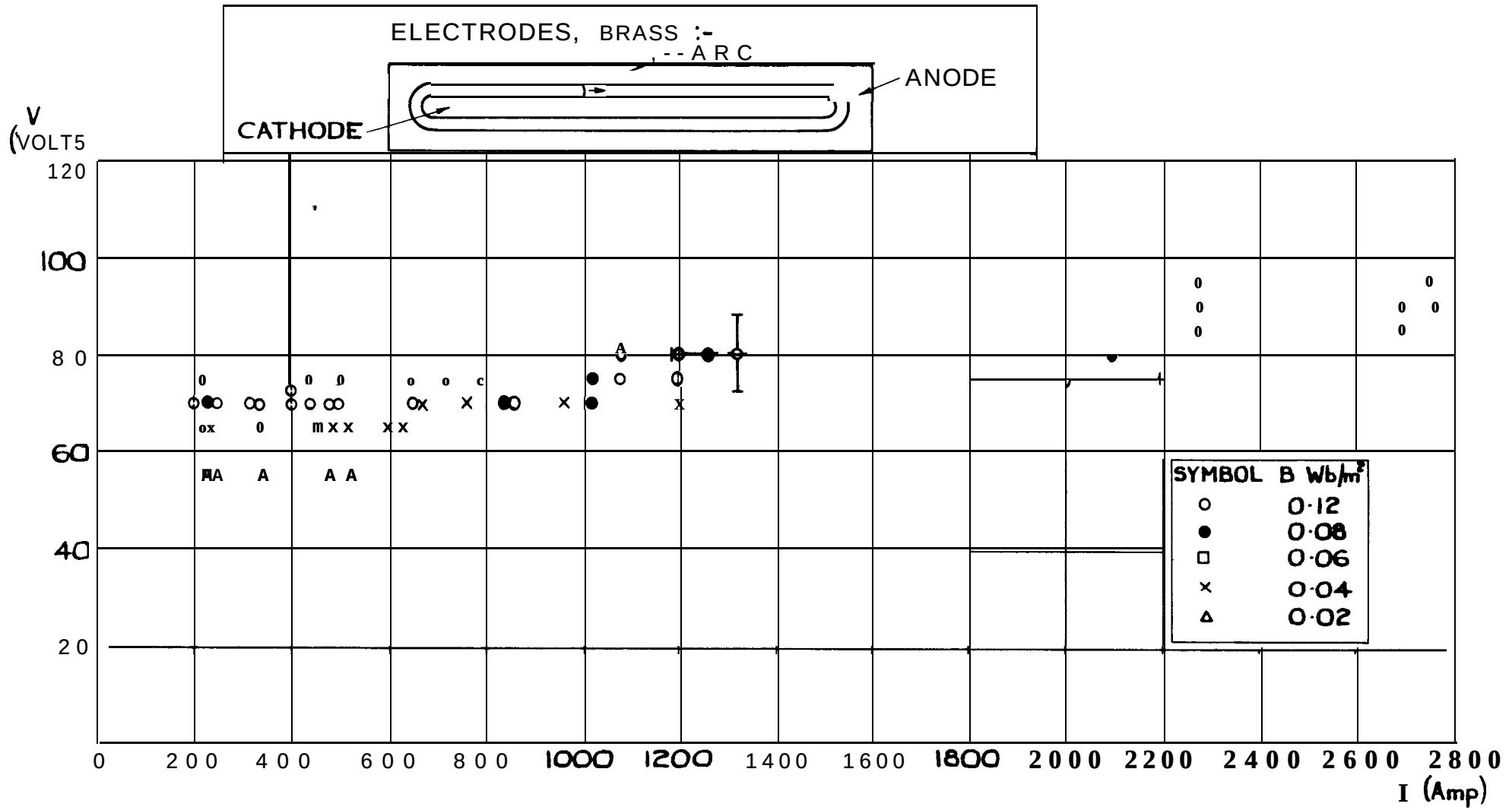

FIG. 17 MINIMUM ARC VOLTAGE AGAINST ARC CURRENT FOR CONTINUOUSLY OPERATED ARCS ON BRASS ELECTRODES (d = 1·27 cm)

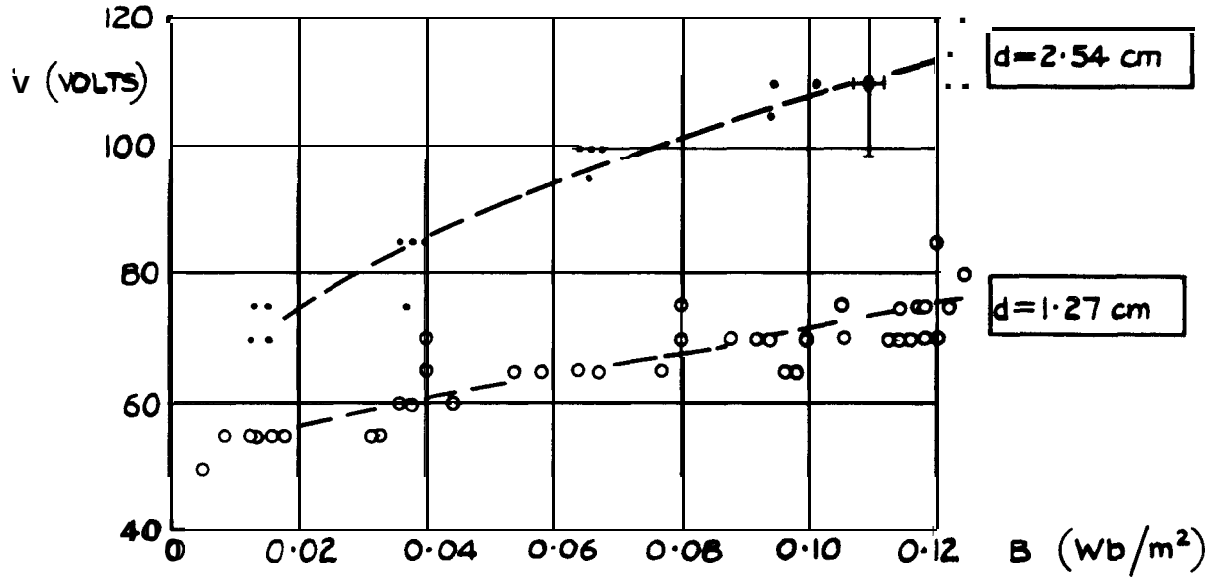

FIG.18 MINIMUM ARC VOLTAGE AGAINST APPLIED MAGNETIC FIELD FOR CONTINUOUSLY OPERATED **ARCS ON BRASS ELECTRODES**
(V ASSUMED INDEPENDENT OF I)

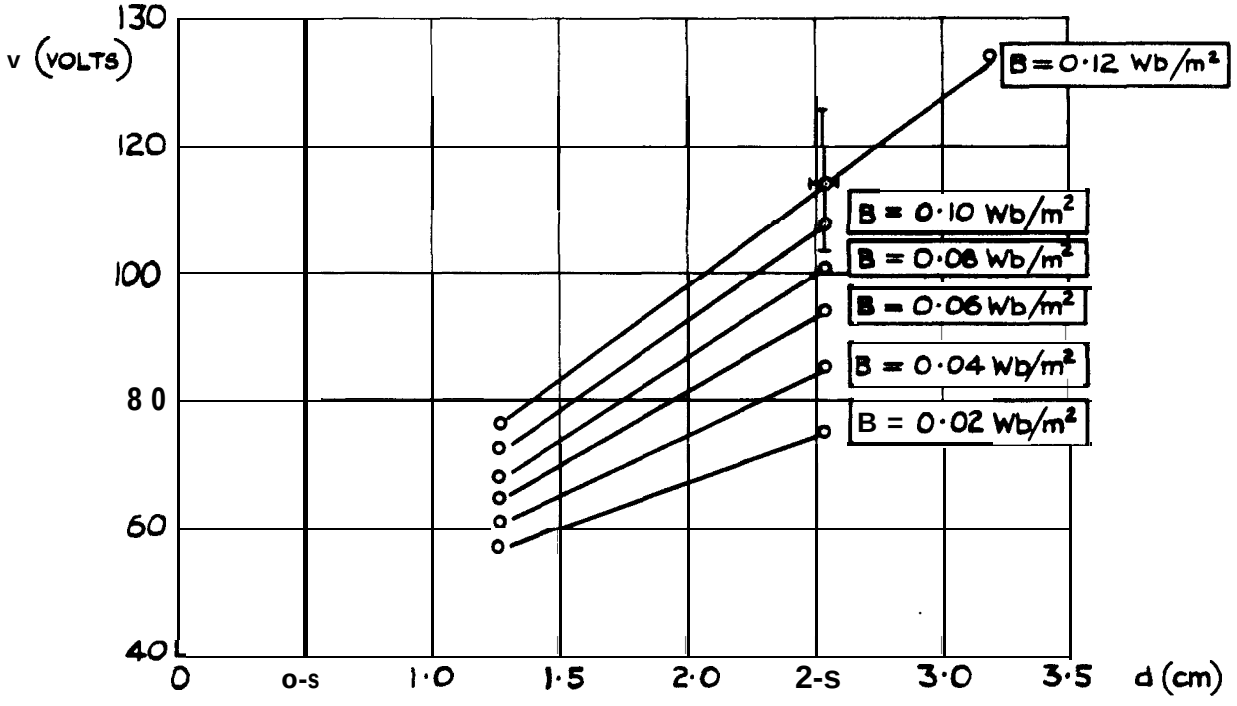

FIG.19 MINIMUM ARC VOLTAGE AGAINST ARC GAP FOR CONTINUOUSLY OPERATED **ARCS** ON BRASS ELECTRODES
(MEAN VALUES OF v FROM FIG. 18)

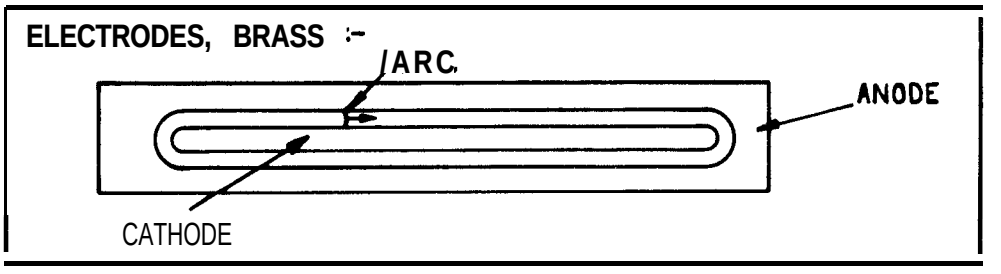

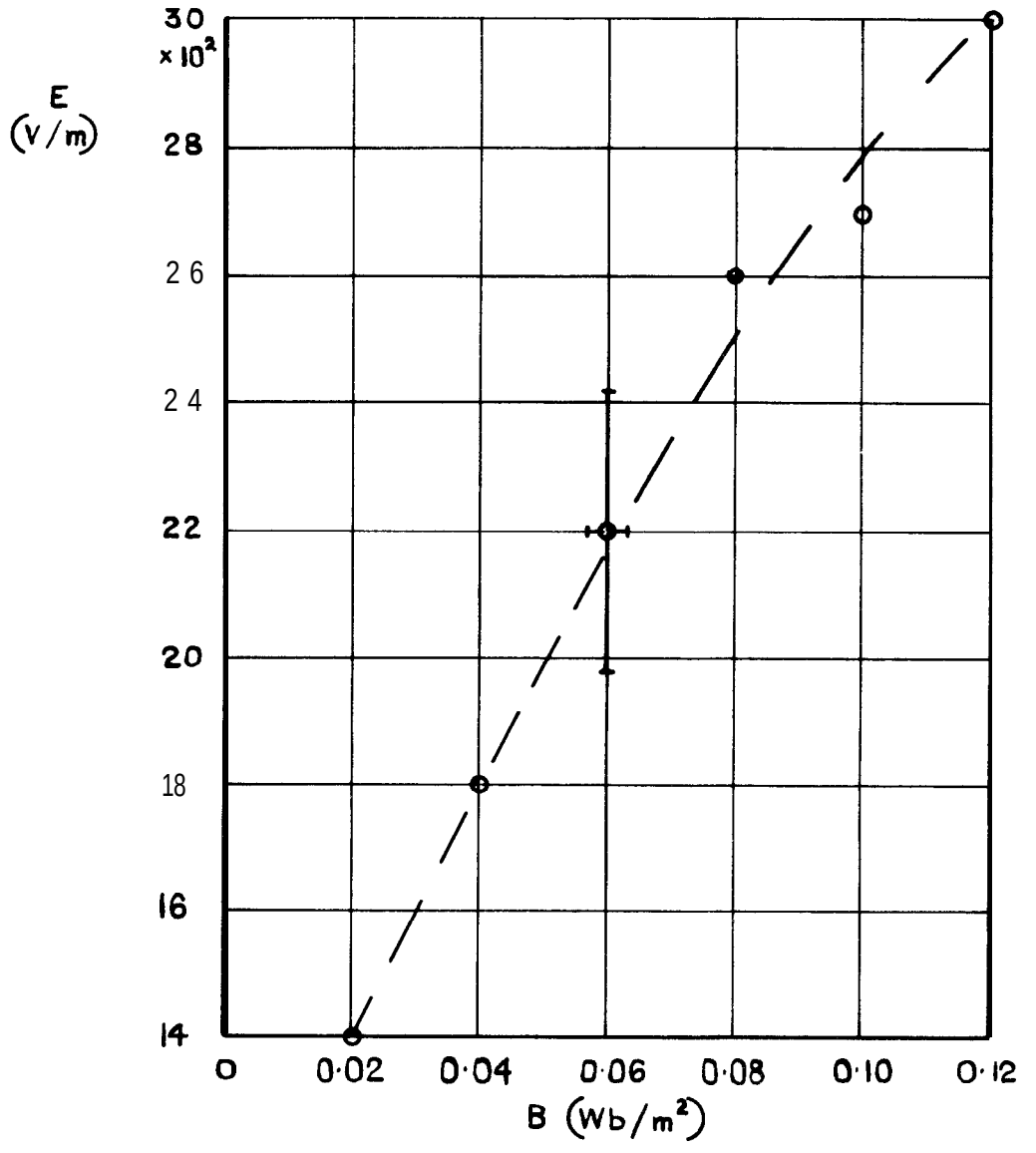

FIG.20 VOLTAGE GRADIENT AGAINST APPLIED MAGNETIC FIELD FOR CONTINUOUSLY OPERATED ARCS ON BRASS ELECTRODES
(E INDEPENDENT OF I)

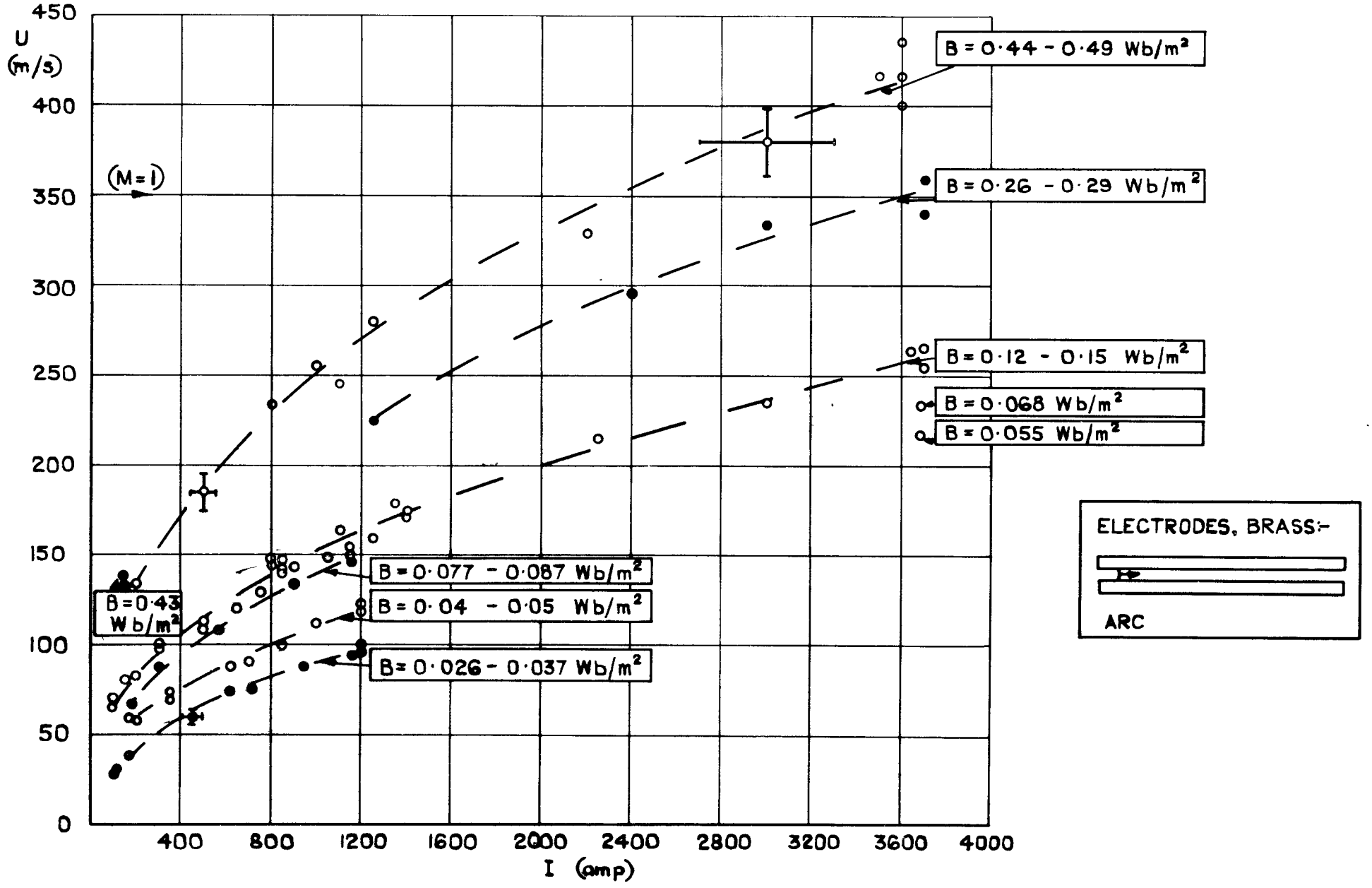

FIG. 21 ARC VELOCITY AGAINST ARC CURRENT FOR STRAIGHT BRASS ELECTRODES
(d = 1·27 cm)

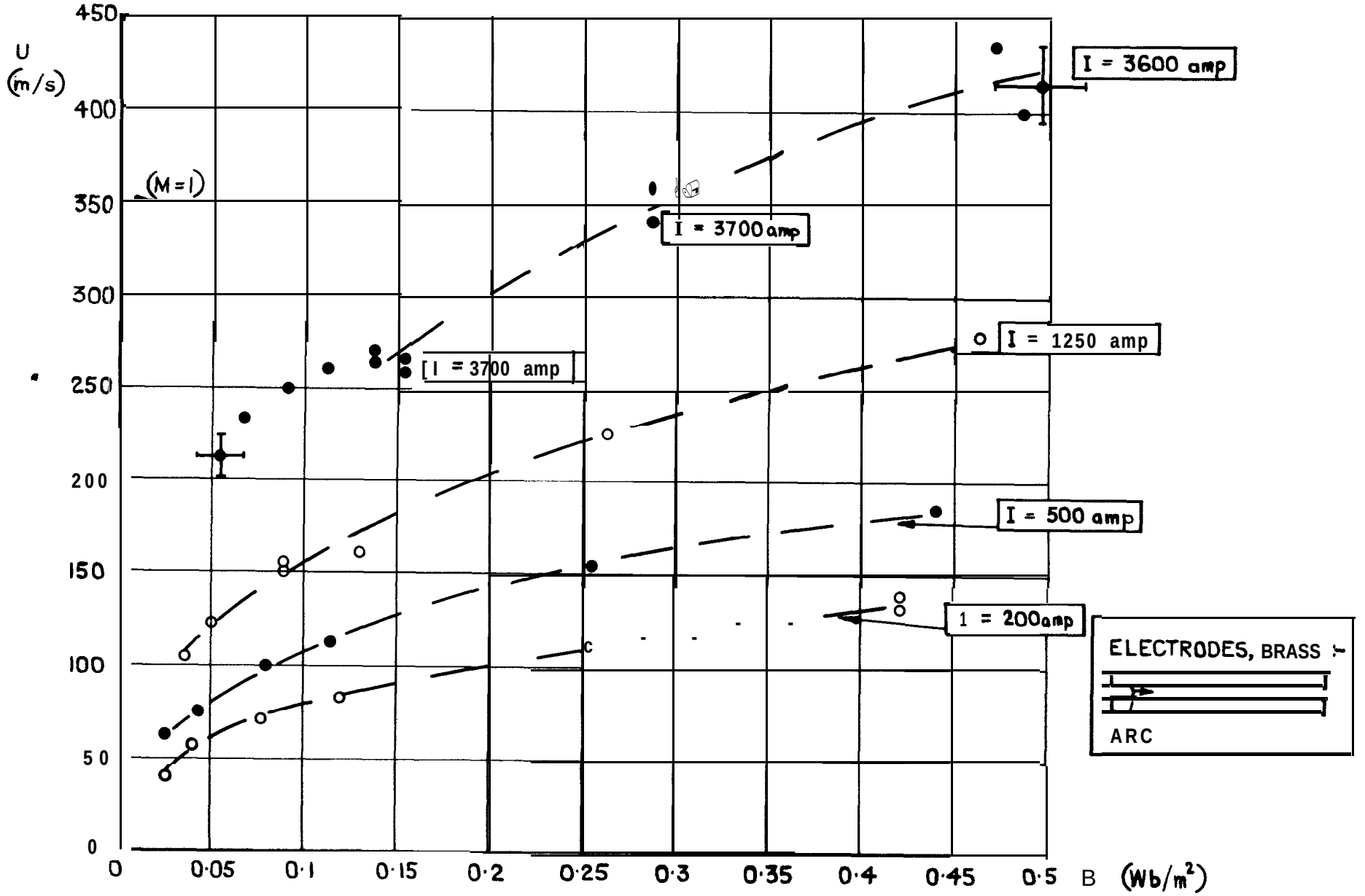

FIG. 22 ARC VELOCITY AGAINST APPLIED MAGNETIC FIELD FOR STRAIGHT BRASS ELECTRODES (d = 1·27 cm)

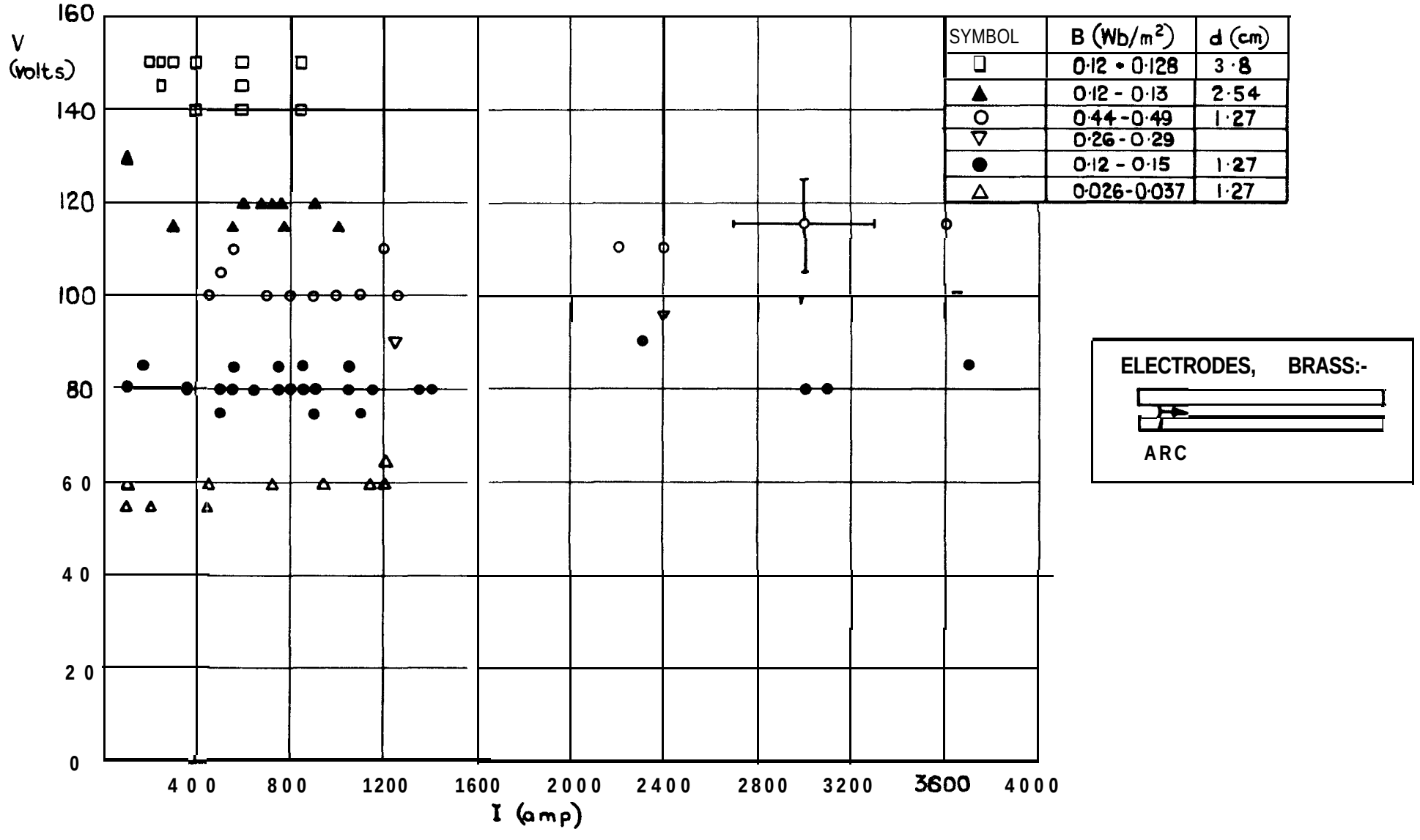

FIG. 23 MINIMUM ARC VOLTAGE AGAINST ARC CURRENT FOR STRAIGHT BRASS ELECTRODES

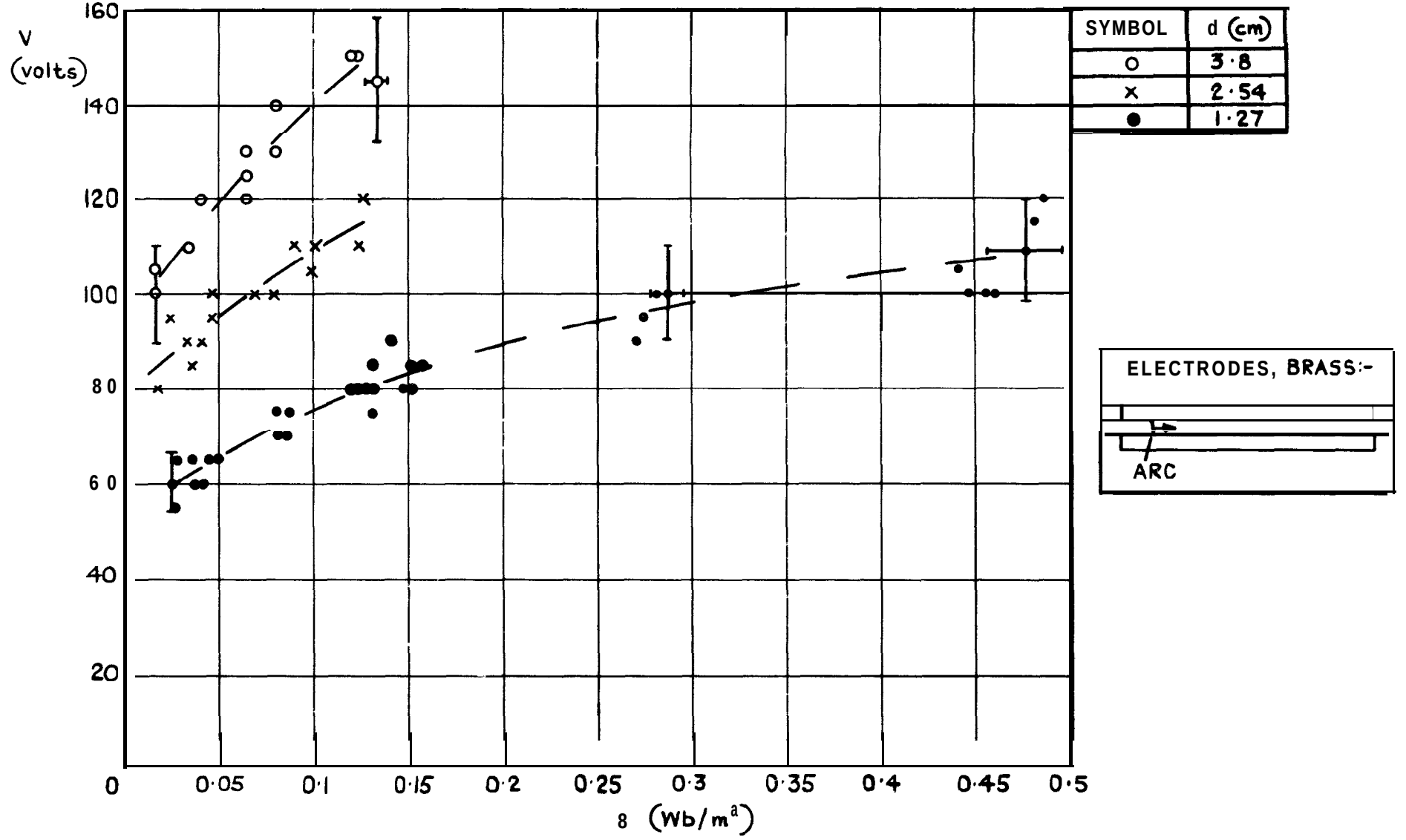

FIG.24 MINIMUM ARC VOLTAGE AGAINST APPLIED MAGNETIC FIELD FOR STRAIGHT BRASS ELECTRODES (V ASSUMED INDEPENDENT OF I)

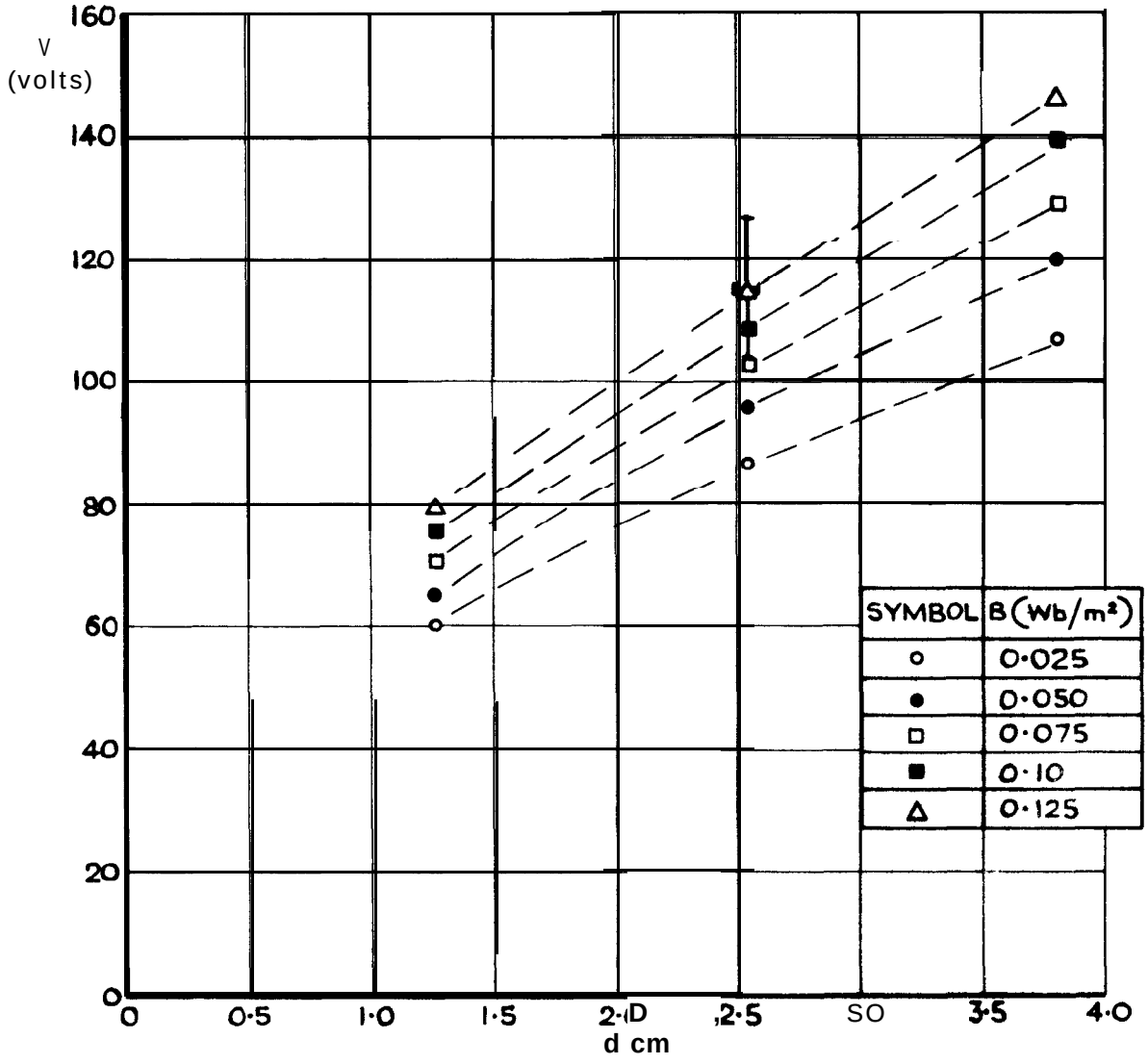

FIG. 25 MINIMUM ARC VOLTAGE AGAINST ARC GAP FOR STRAIGHT BRASS ELECTRODES (MEAN VALUES OF V FROM FIG. 24)

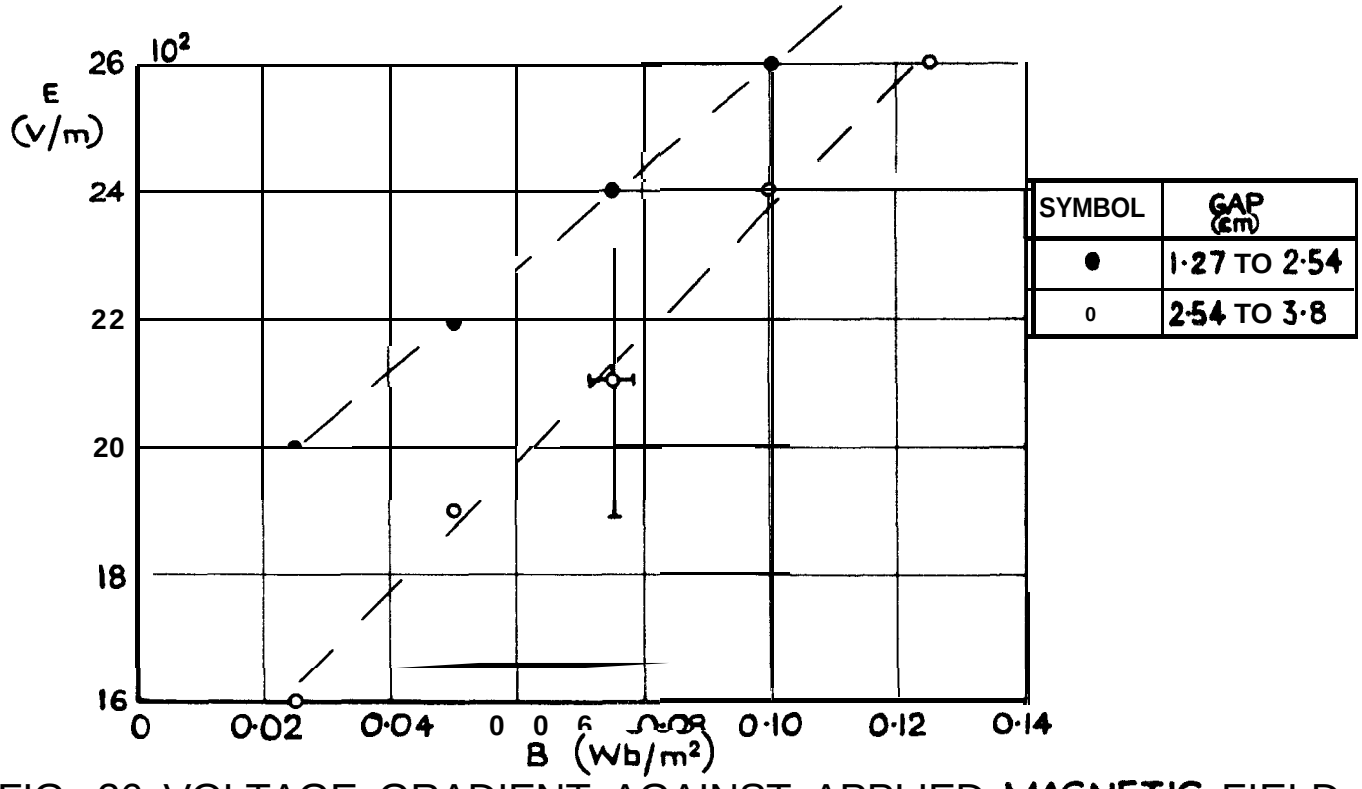

FIG. 26 VOLTAGE GRADIENT AGAINST APPLIED MAGNETIC FIELD FOR STRAIGHT BRASS ELECTRODES

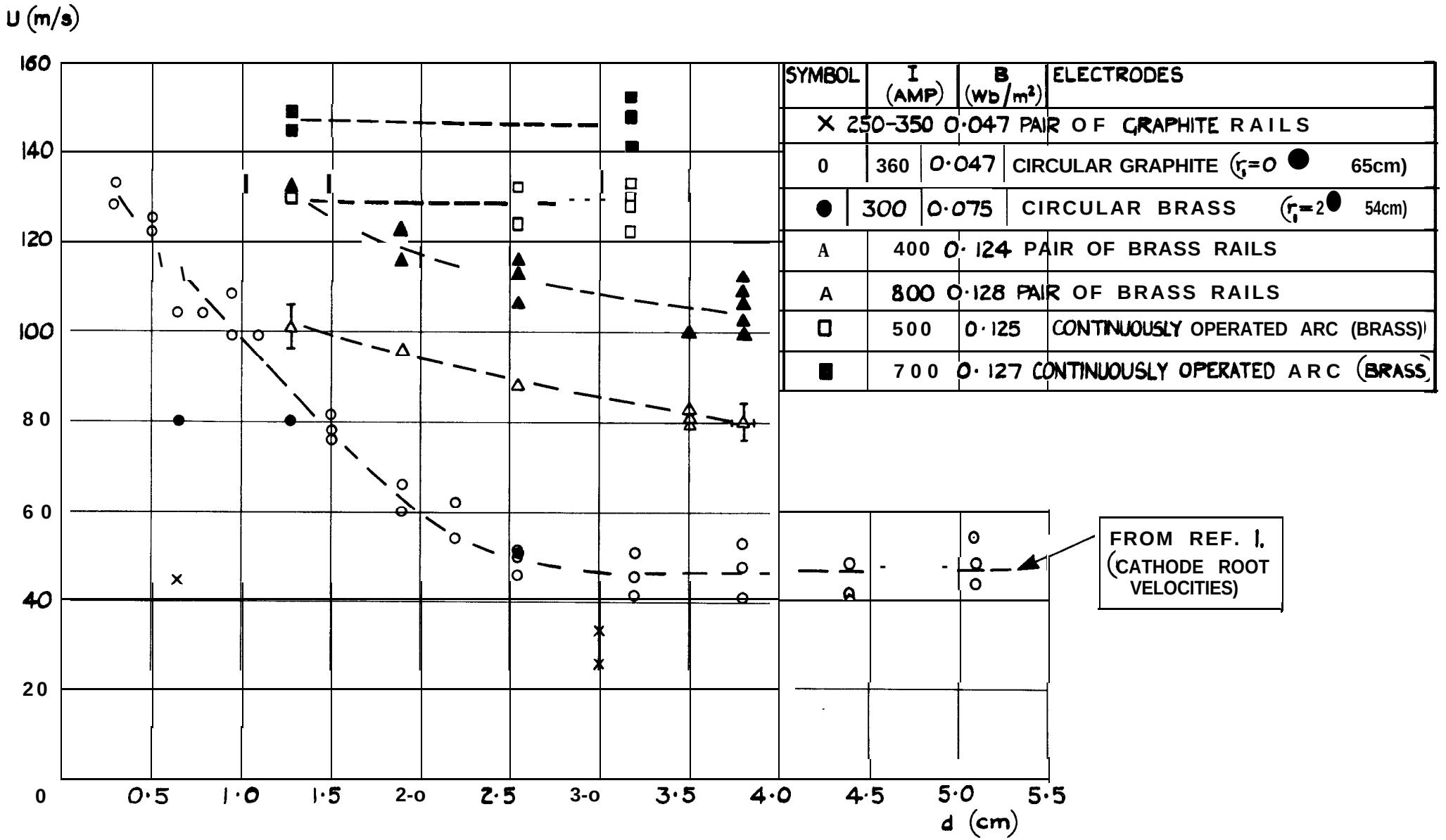

FIG. 27 ARC VELOCITY AGAINST ELECTRODE GAP WIDTH

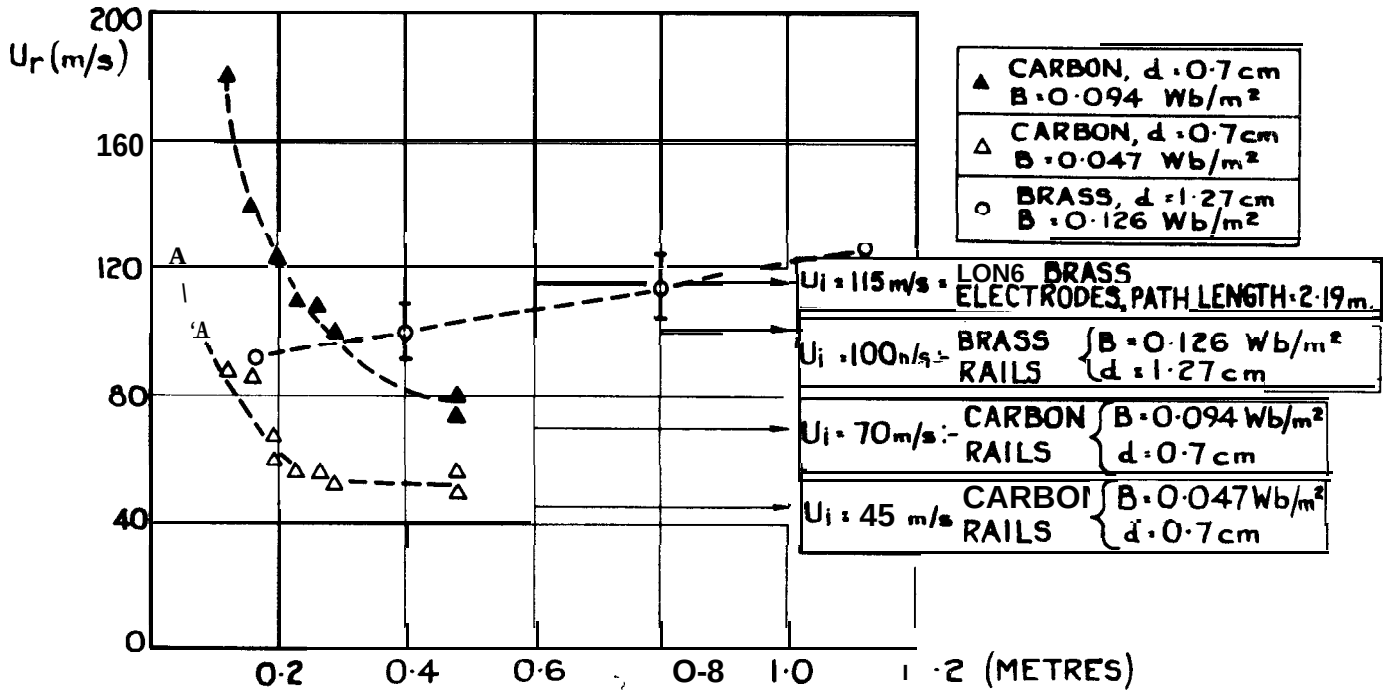

FIG. 28 ARC VELOCITY AGAINST ELECTRODE PATH LENGTH (I = 350 A)

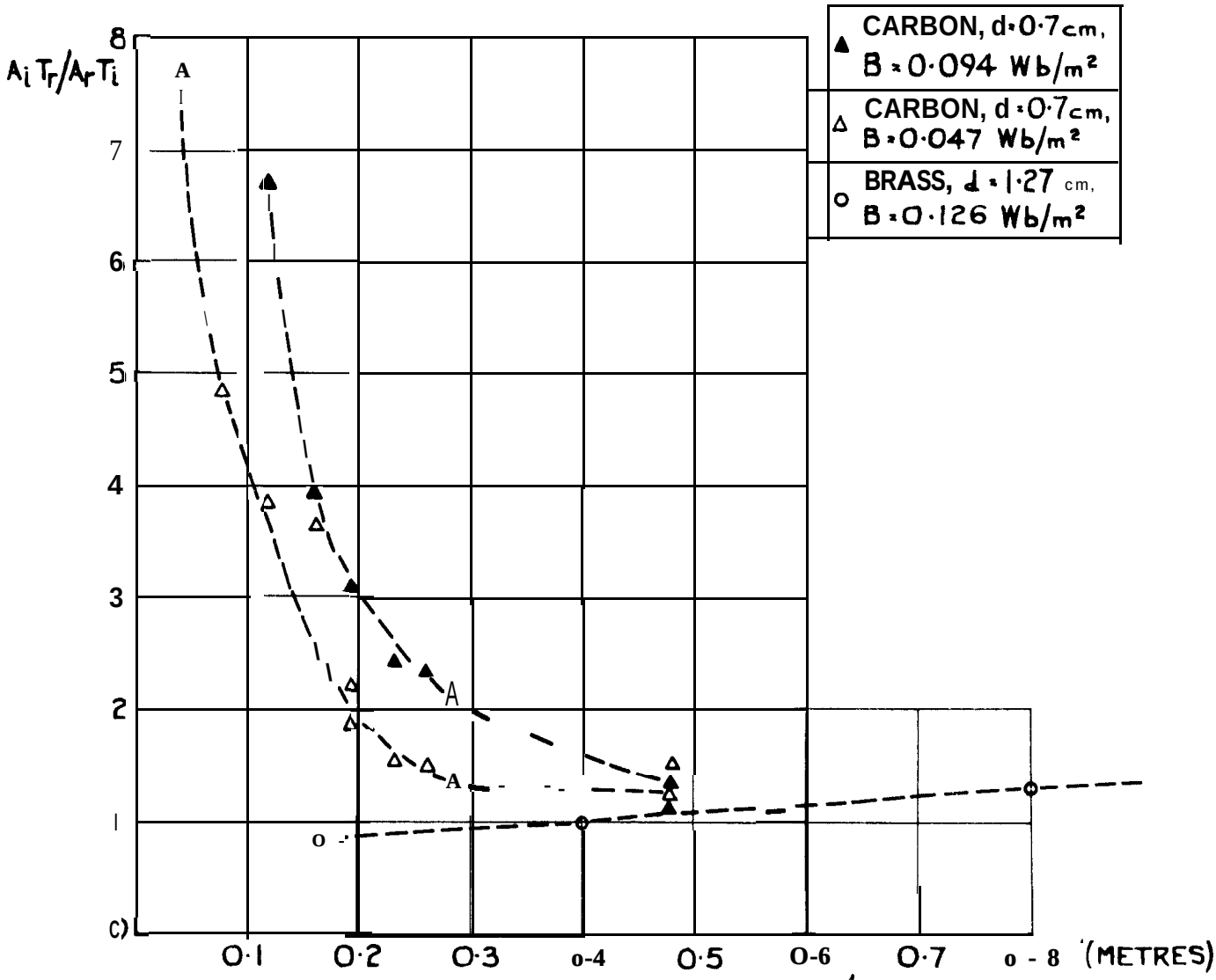

FIG. 29 CALCULATED VALUES OF $A_i T_r / A_r T_i$ AGAINST ELECTRODE PATH LENGTH

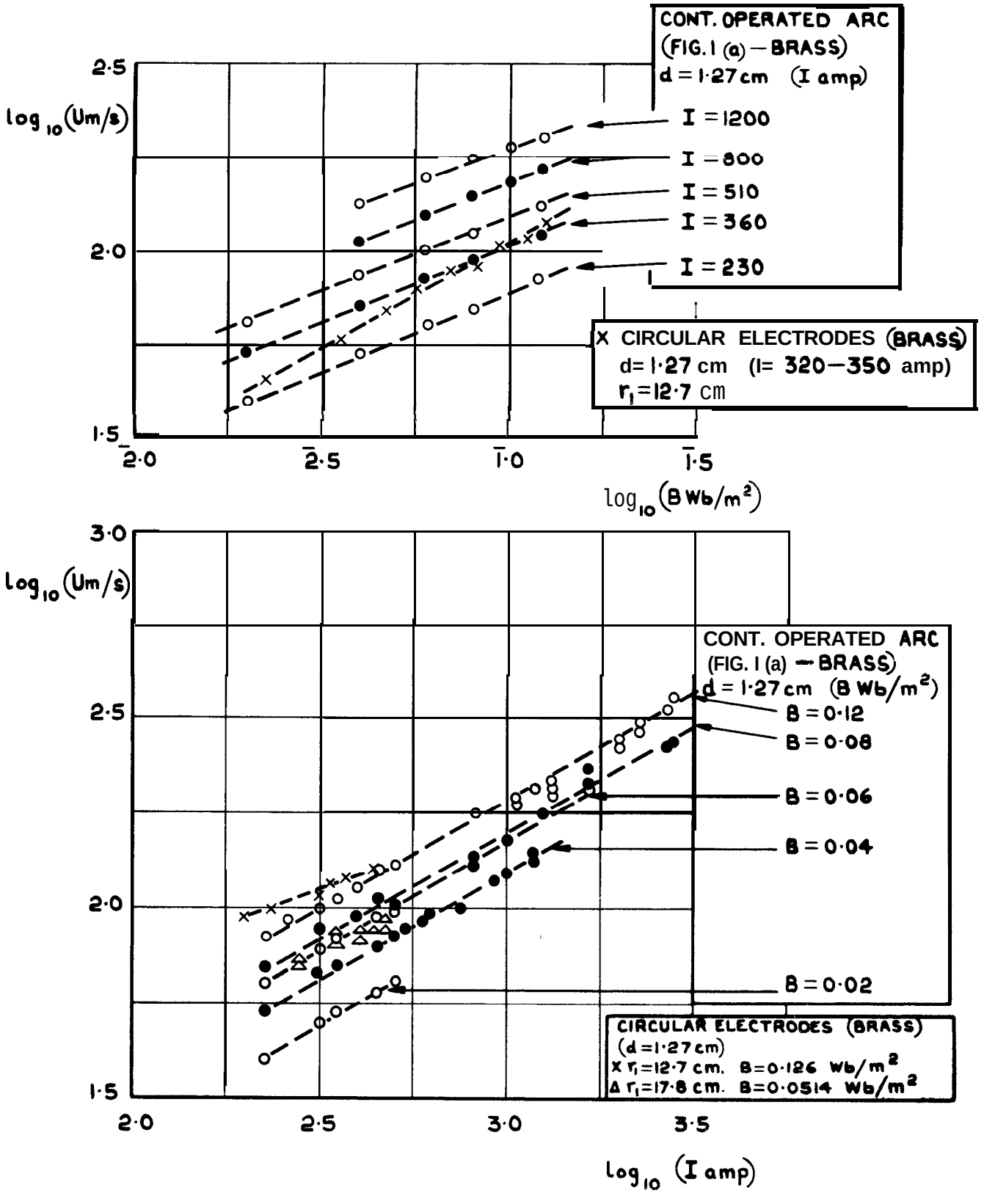

FIG.30 VELOCITIES OF CONTINUOUSLY OPERATED ARCS AND ARCS ROTATING ON CIRCULAR ELECTRODES (BRASS)

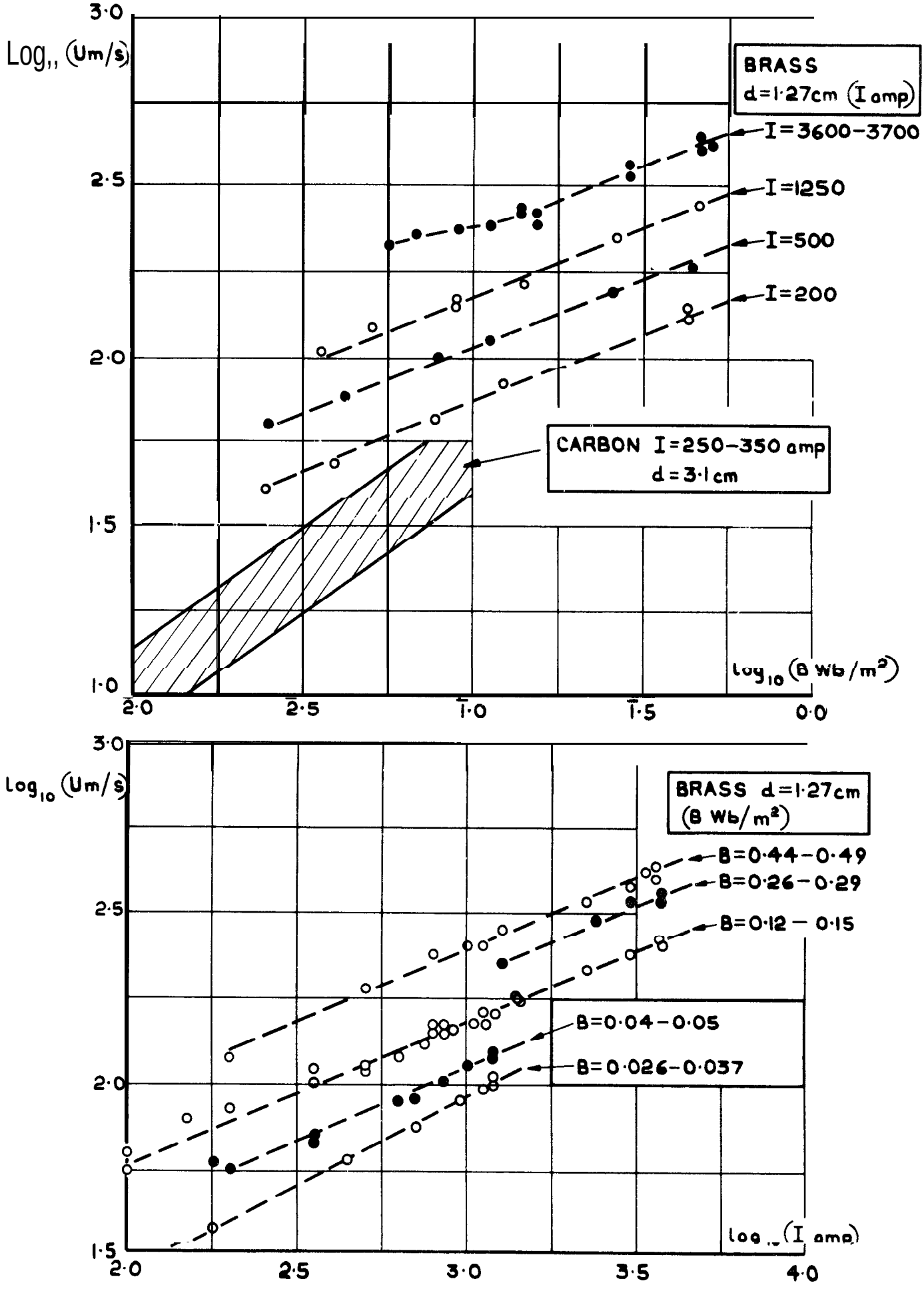

FIG.31 ARC VELOCITIES ON PAIR OF STRAIGHT ELECTRODES

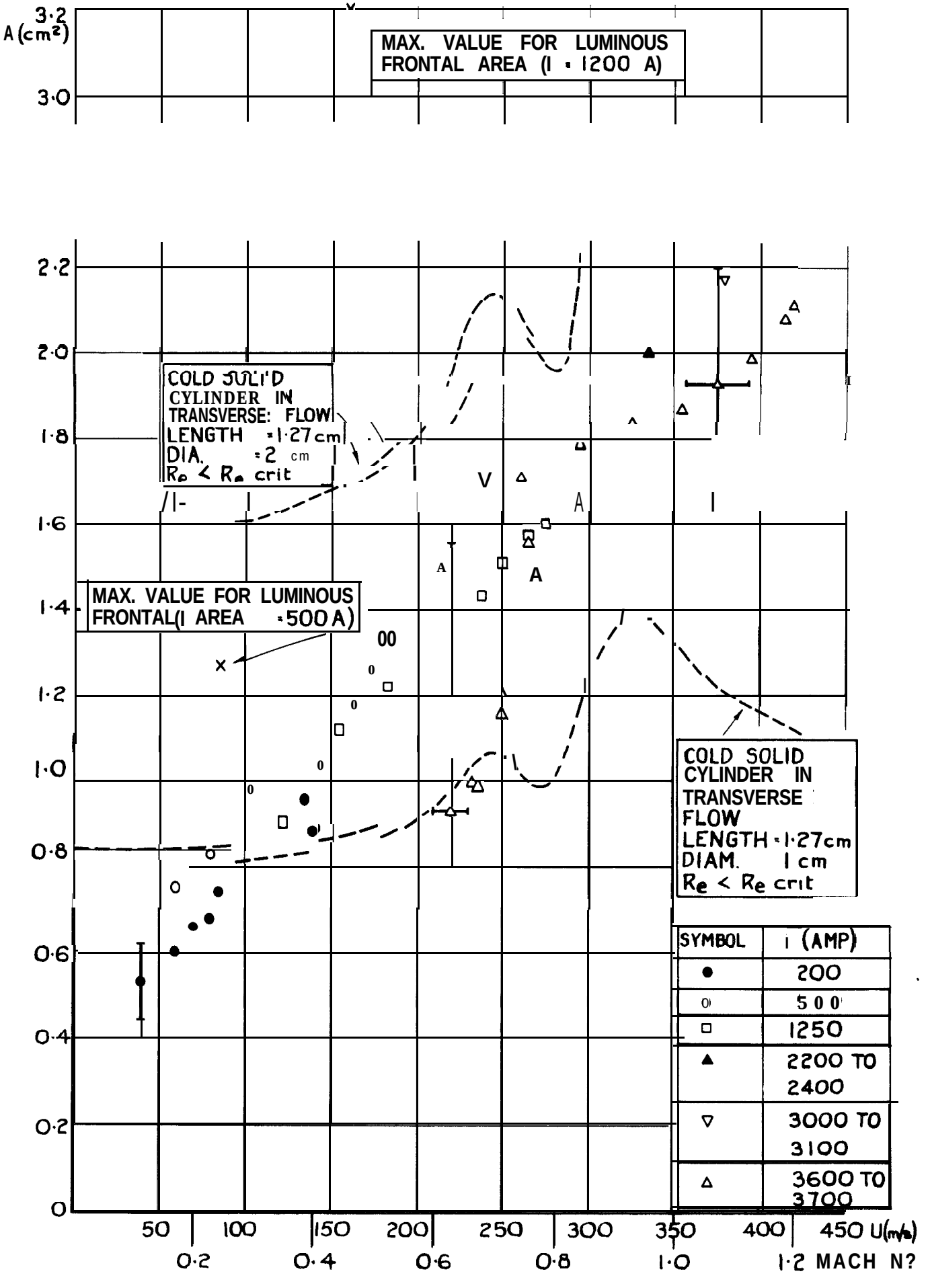

FIG. 32 CALCULATED VALUES OF A AGAINST ARC VELOCITY FOR ARCS QN STRAIGHT BRASS ELECTRODES (d = 1·27 cm)

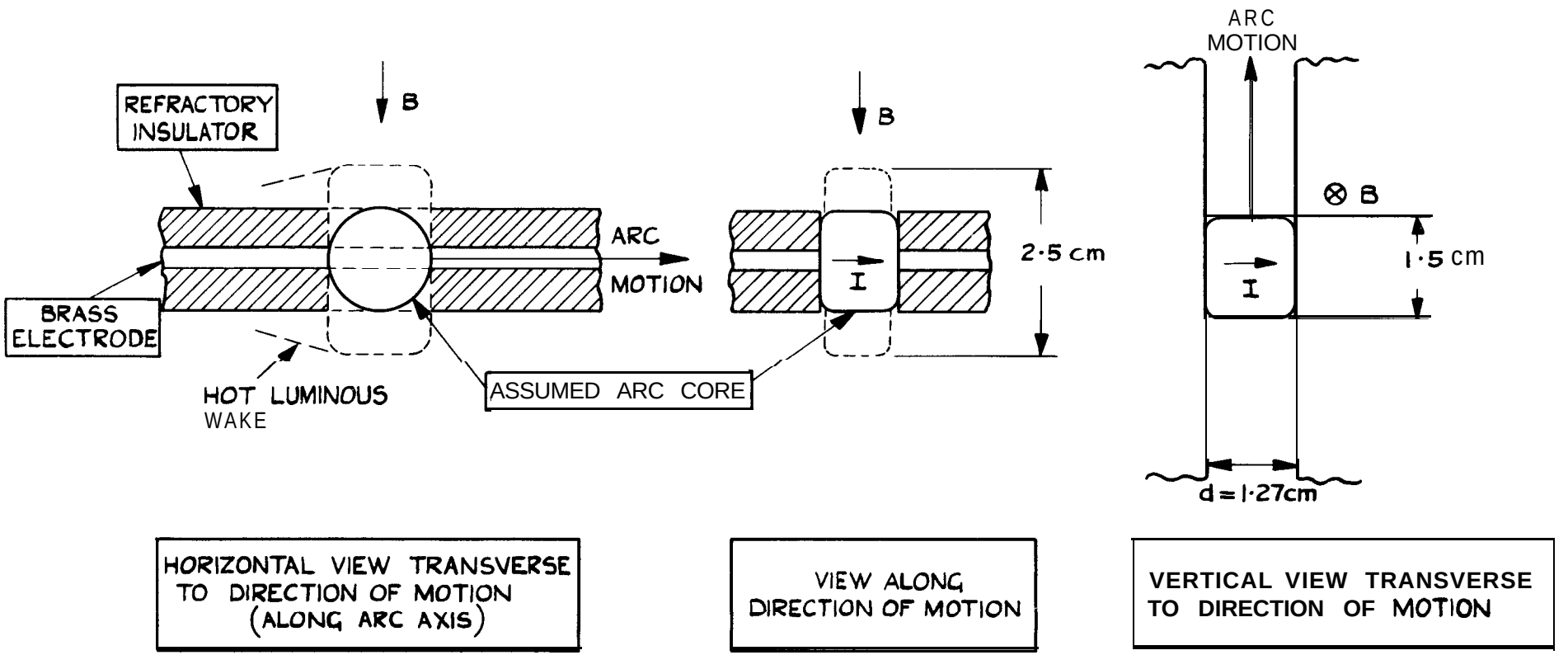

(THE DASHED LINES INDICATE EXTENT OF LUMINOUS GAS AND NOT THE TRUE SHAPE)

FIG.33 SCHEMATIC DIAGRAM OF LUMINOUS ARC SHAPE
$(I = 1200\,A \quad B = 0{\cdot}13 \ Wb/m^2 \quad U = 160 \ m/s)$

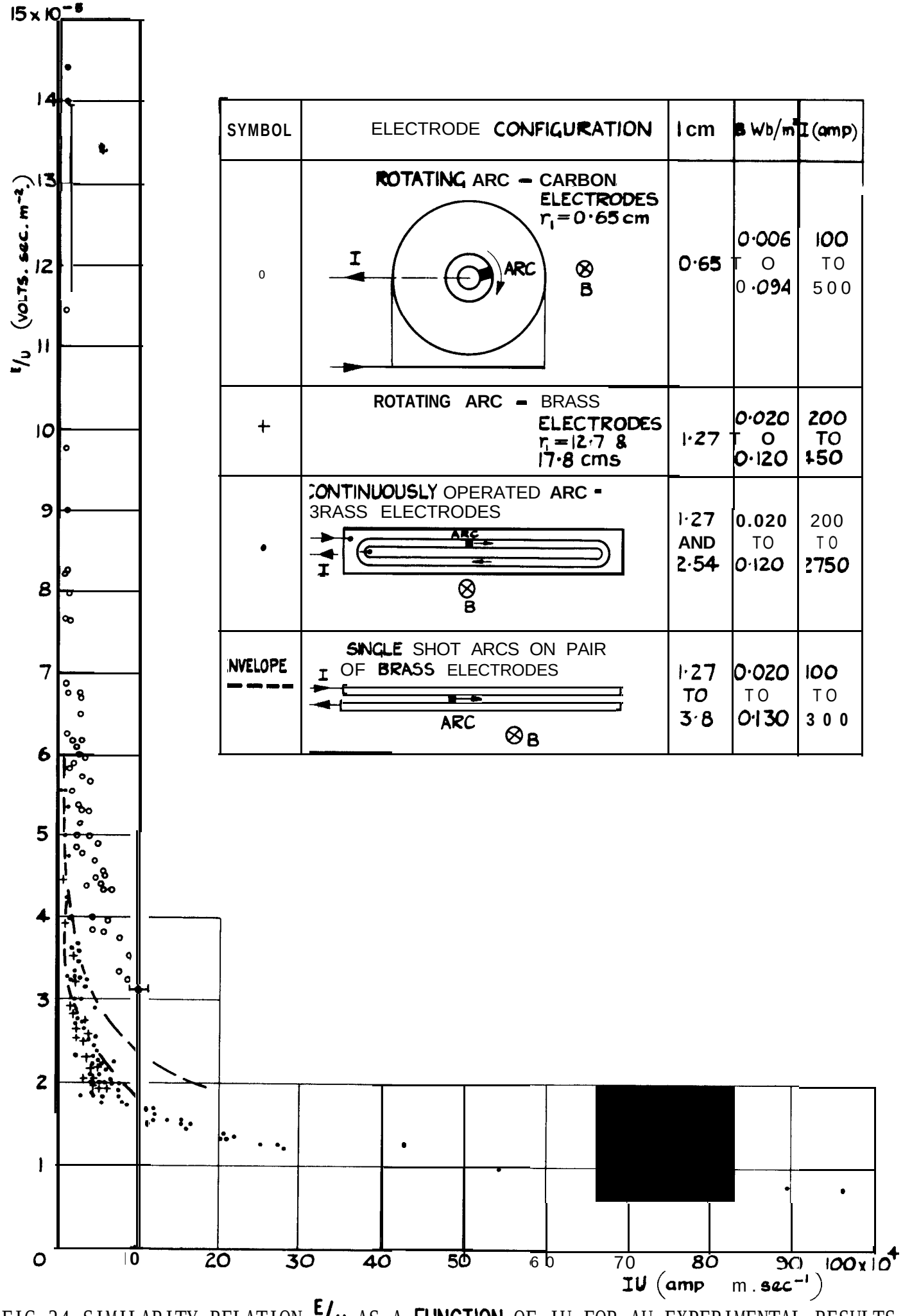

FIG. 34 SIMILARITY RELATION E/U AS A FUNCTION OF IU FOR AU EXPERIMENTAL RESULTS

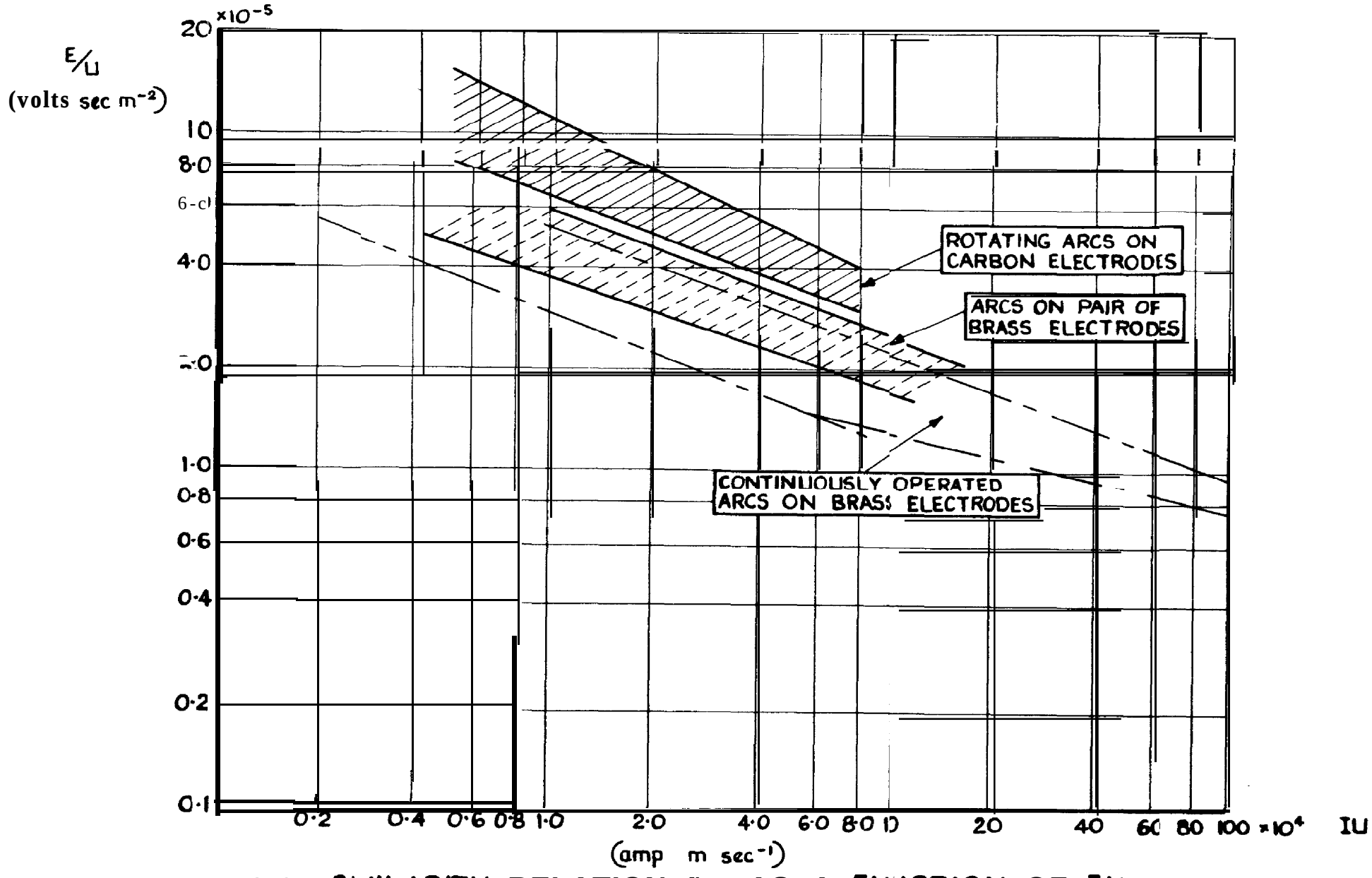

FIG.35 SMILARITY RELATION E/U AS A FUNCTION OF IU

FOR ALL EXPERIMENTAL RESULTS

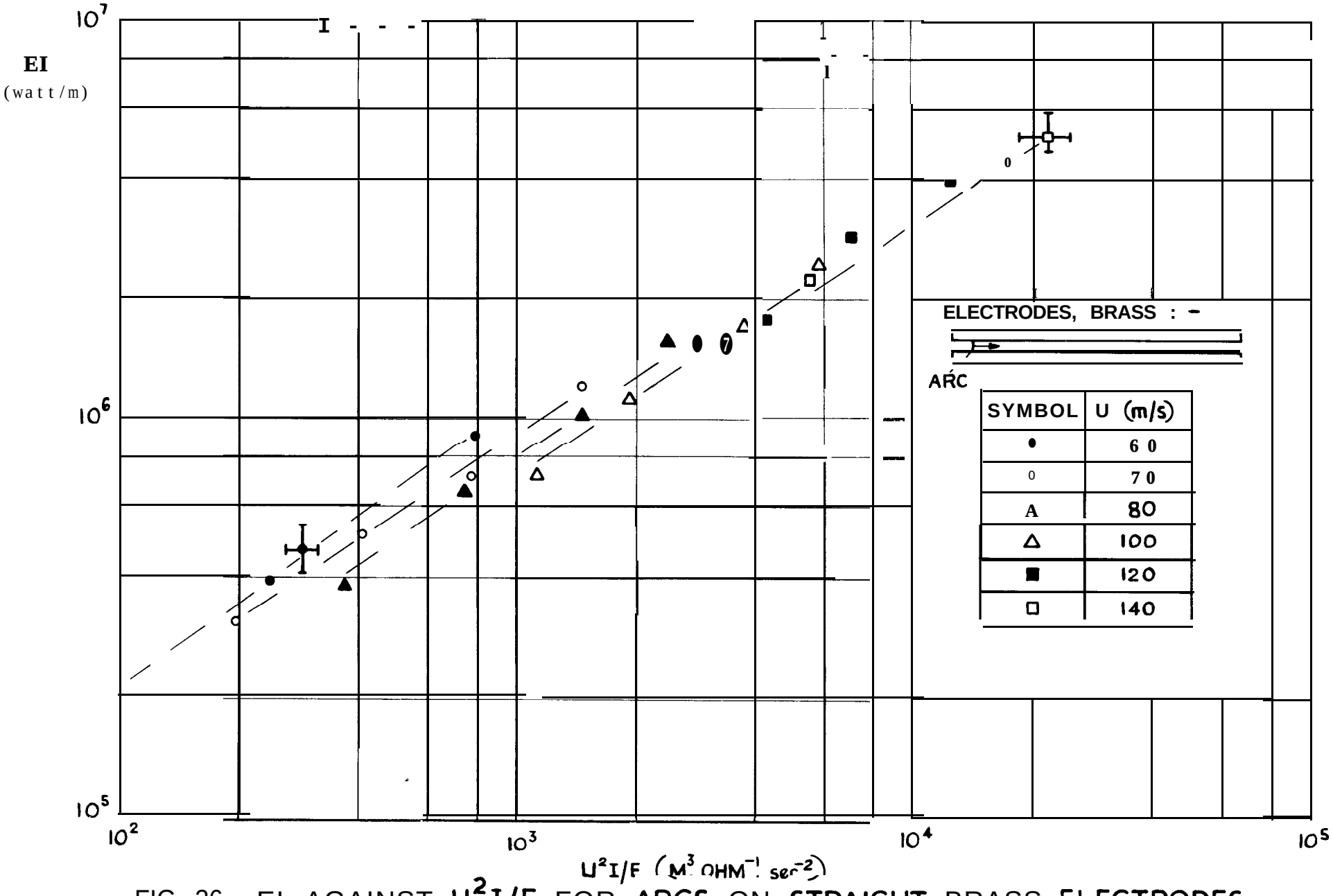

FIG. 36 EI AGAINST U^2I/E FOR ARCS ON STRAIGHT BRASS ELECTRODES – SMOOTHED OUT RESULTS **(USING MEAN VALUES FOR E)**

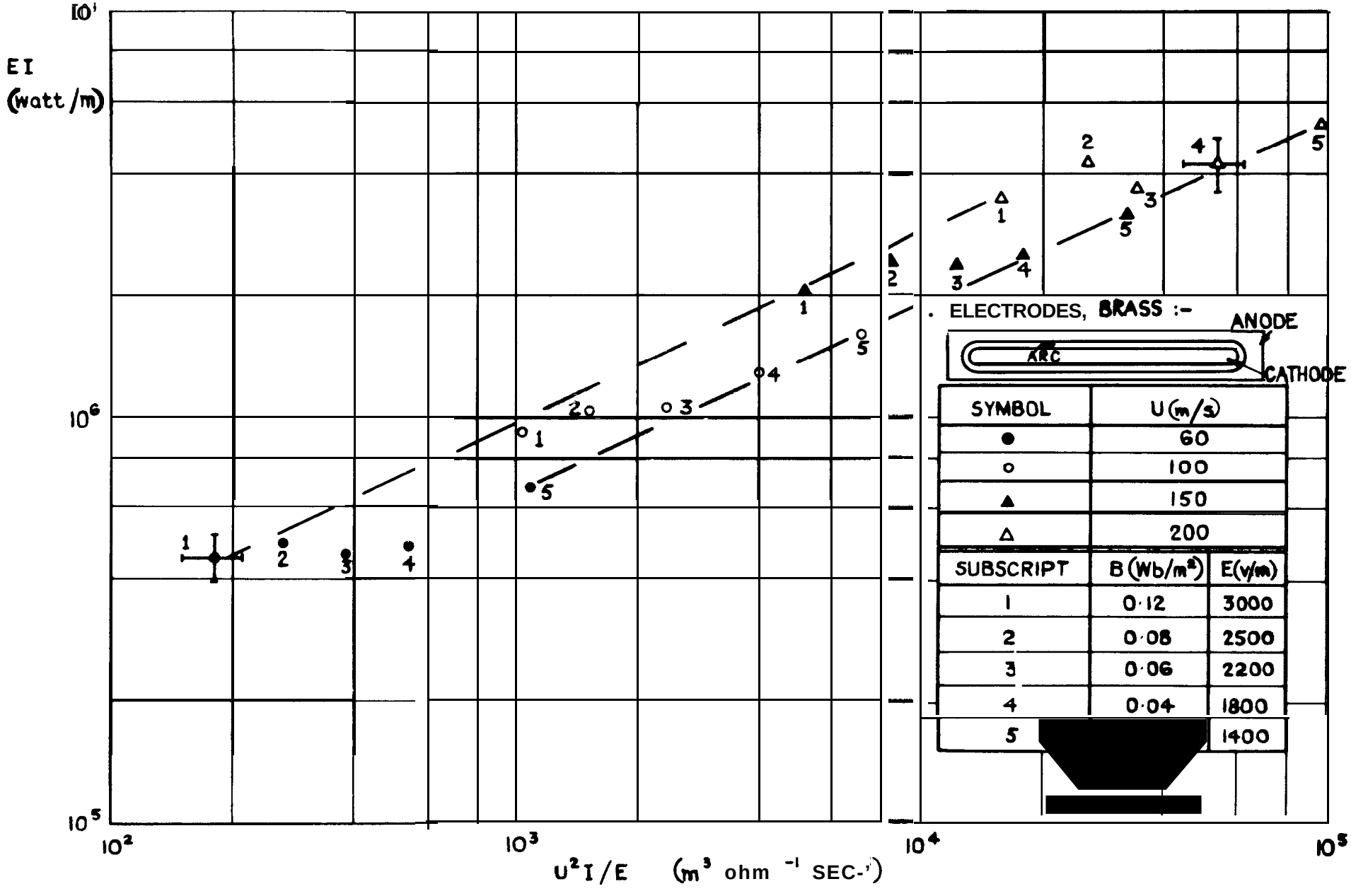

FIG.37 EI AGAINST U^2I/E FOR CONTINUOUSLY OPERATED ARCS ON BRASS ELECTRODES SMOOTHED OUT RESULTS

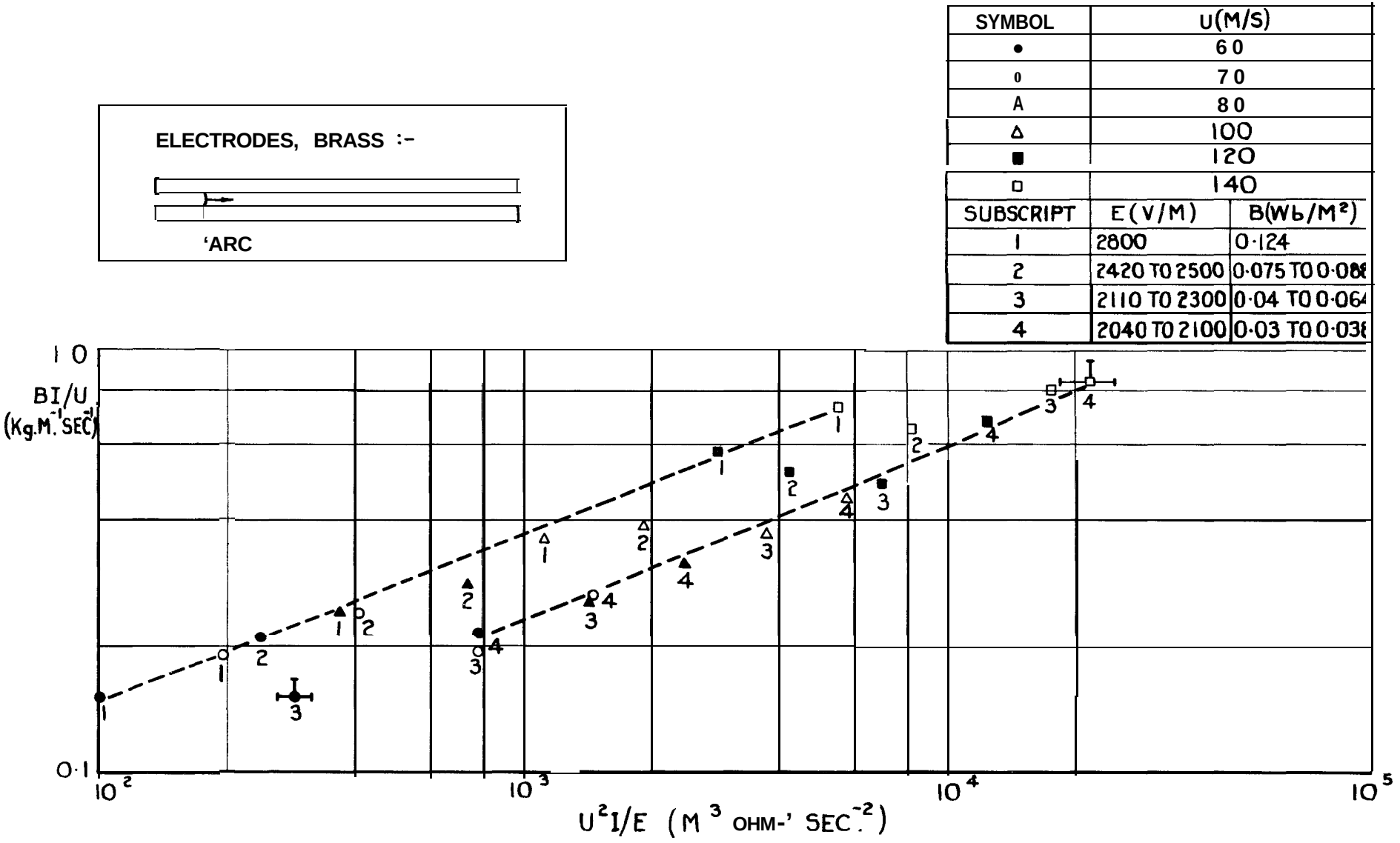

FIG.38 BI/U AGAINST U^2I/E FOR ARCS ON STRAIGHT BRASS ELECTRODES-SMOOTHED OUT RESULTS (USING MEAN VALUES FOR E)

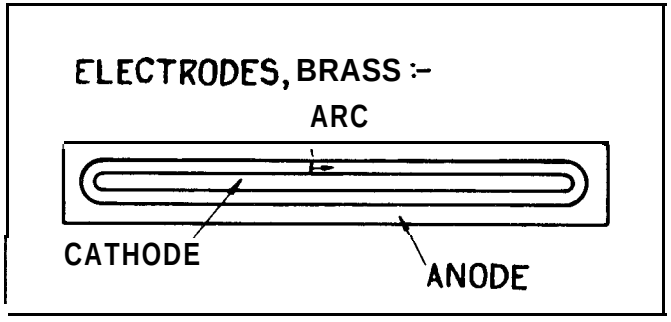

SYMBOL	U(M/S)	
●	60	
o	100	
A	150	
△	200	
SUBSCRIPT	E (v/m)	B (wb m^2)
1	3000	0·12
2	2500	0·08
3	2200	0·06
4	1800	0·04
5	1400	0·02

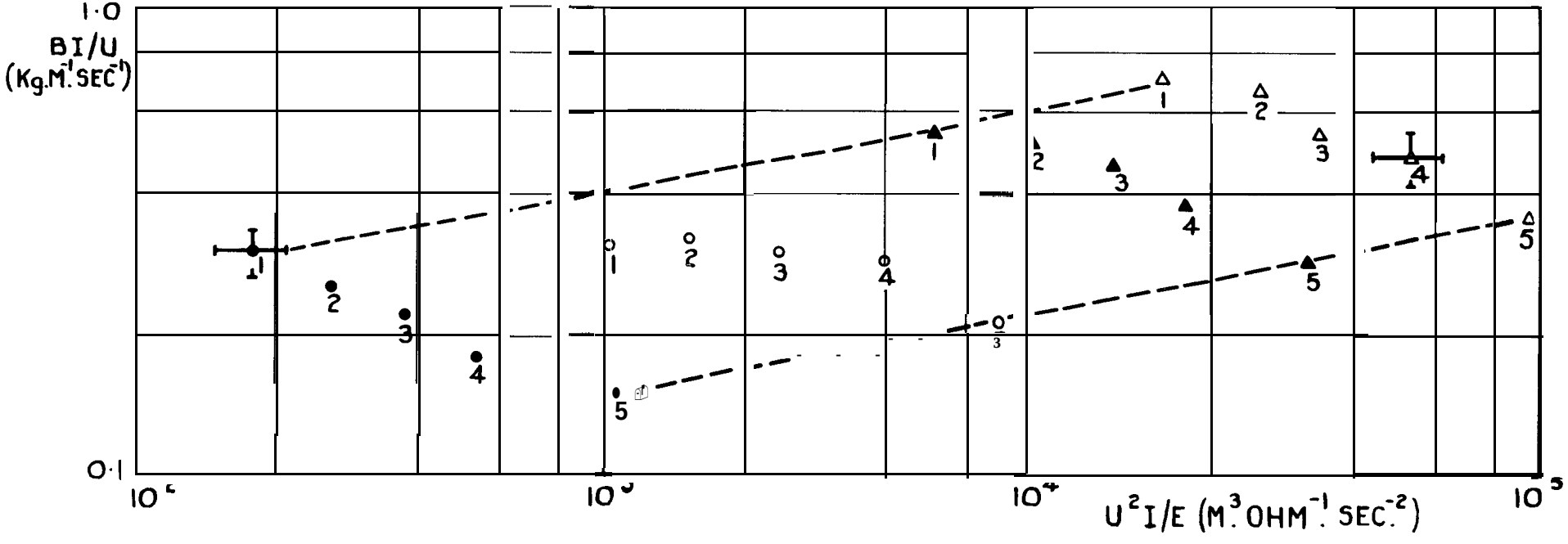

FIG. 39 BI/U AGAINST U^2I/E FOR CONTINUOUSLY OPERATED ARCS ON BRASS ELECTRODES-SMOOTHED OUT RESULTS

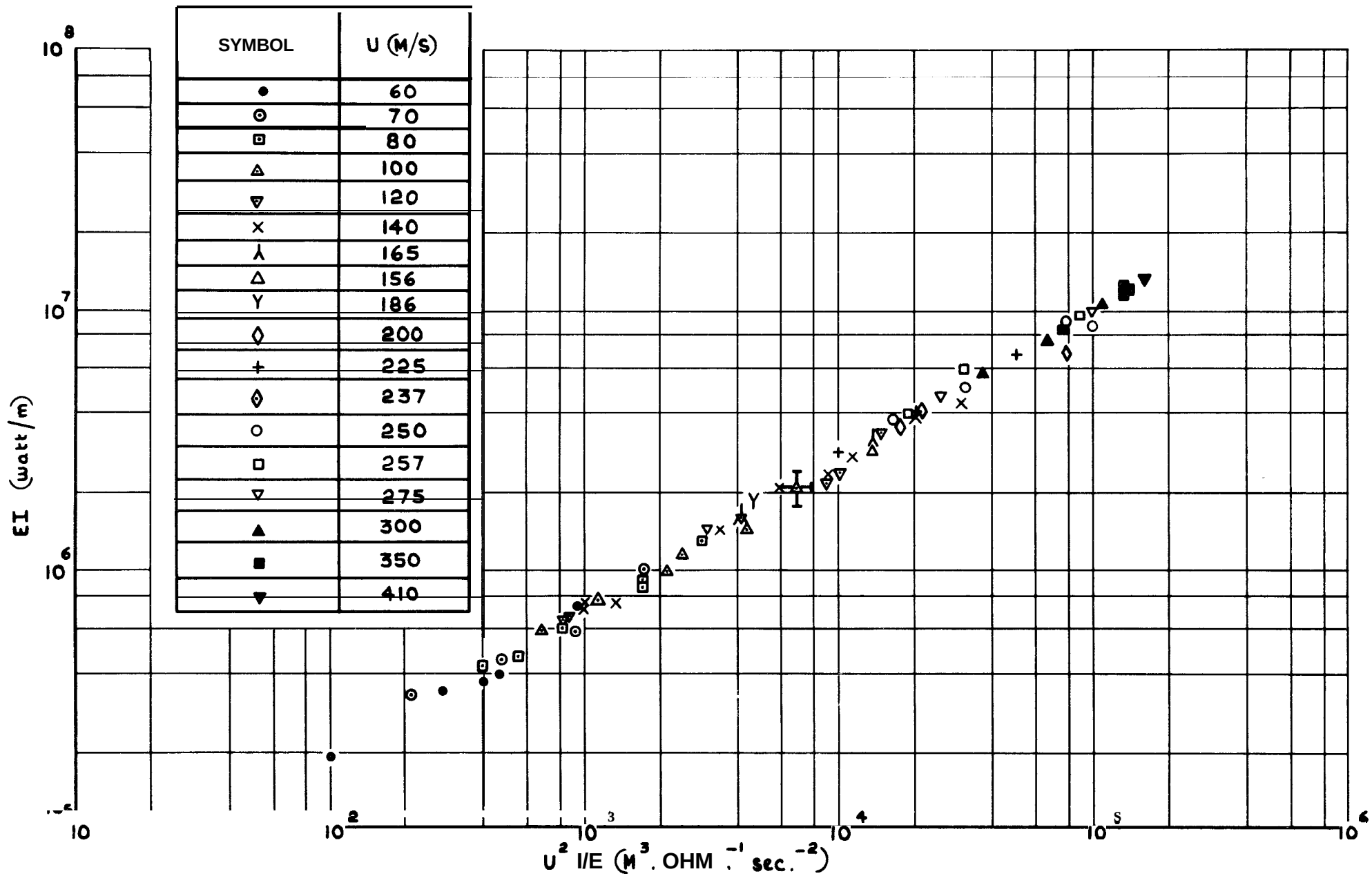

FIG.40 EI AGAINST U^2 I/E FOR ARCS ON STRAIGHT BRASS ELECTRODES— SMOOTHED OUT RESULTS (USING E FOR LARGE GAPS)

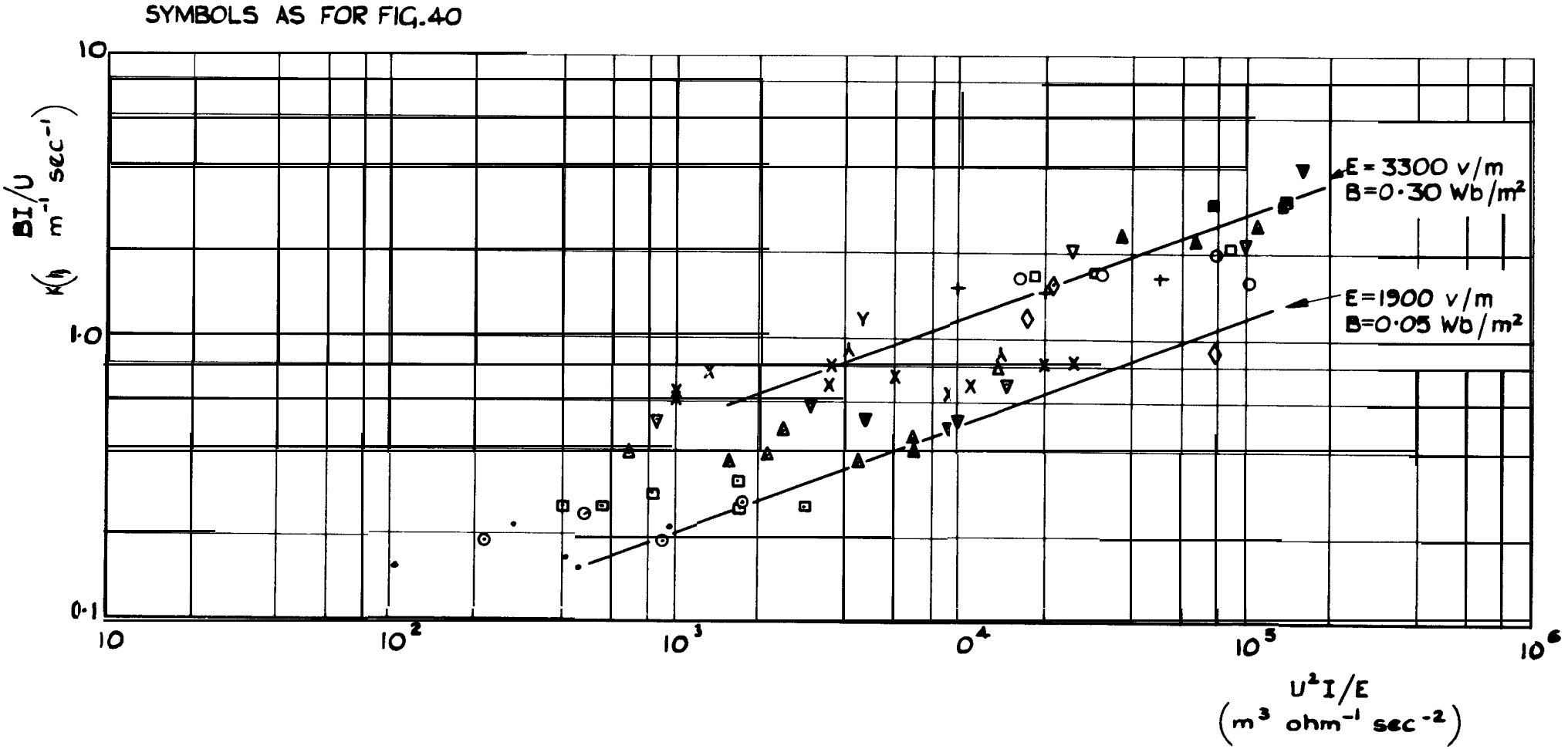

FIG. 41 BI/U AGAINST U^2I/E FOR STRAIGHT BRASS ELECTRODES – SMOOTHED OUT RESULTS (USING E FOR LARGE GAPS)

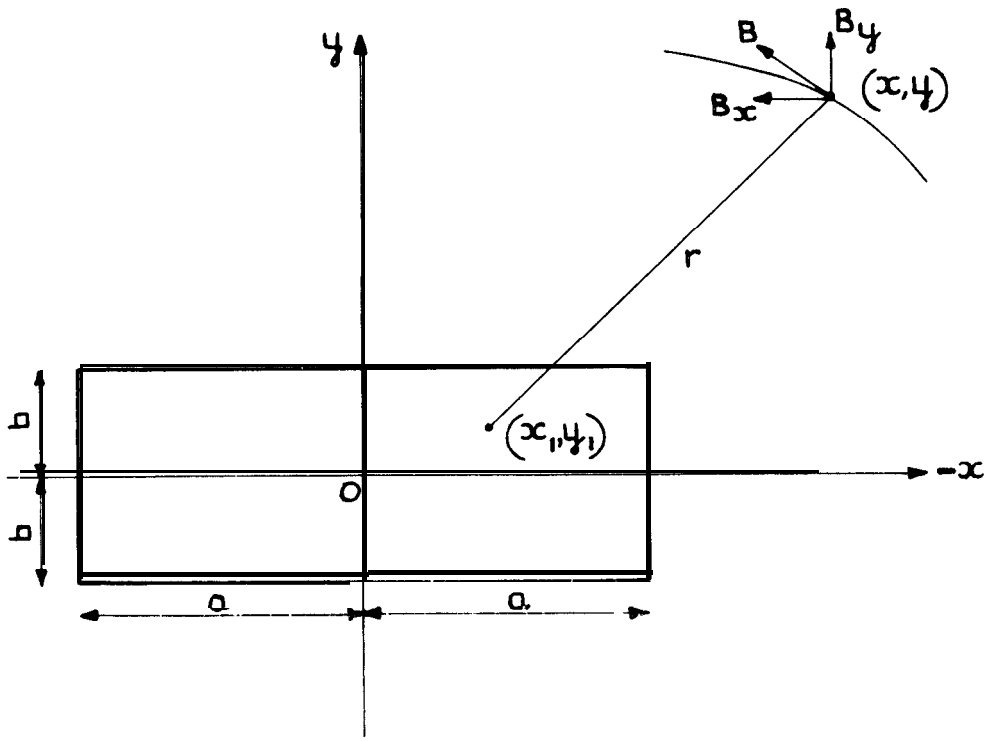

FIG. 42 FIELD DUE TO RECTANGULAR CONDUCTOR **(APPENDIX A]**

Printed in England for Her Majesty's Stationery Office by
the Royal Aircraft Establishment, Farnborough. Dd.125875 K4.

A.R.C. C.P. No.93
December 1965

537.523.5 :
538.63 :
532.5

Adams, V. W.

THE INFLUENCE OF GAS STREAMS AND MAGNETIC FIELDS ON ELECTRIC DISCHARGES
PART 3. ARCS IN TRANSVERSE MAGNETIC FIELDS AT ATMOSPHERIC PRESSURE

Experimental results in air at a pressure of one atmosphere on the behaviour of arcs under the action of applied magnetic fields are given for two electrode materials (graphite and brass) and different electrode configurations. These results extend earlier work, in annular gaps using graphite, to larger electrode path lengths on graphite and brass, and also include results for a pair of long straight electrodes. The range of arc current ins been extended to 3700 amps and the applied magnetic field to 0.49 Wb/m^2 for experiments on a pair of straight electrodes.

The results are analysed using a simple model for the arc motion assuming that the arc behaves in the Same way as a body in a gas stream. Some

(Over)

A.R.C. C.P. No.959
December 1965

537.523.5 :
538.63 :
532.5

Adams, V. W.

THE INFLUENCE OF GAS STREAMS AND MAGNETIC FIELDS ON ELECTRIC DISCHARGES
PART 3. ARCS IN TRANSVERSE MAGNETIC FIELDS AT ATMOSPHERIC PRESSURE

Experimental results in air of a pressure of one atmosphere on the behaviour of arcs under the action of applied magnetic fields are given for two electrode materials (graphite and brass) and different electrode configurations. These results extend earlier work, in annular gaps using graphite, to larger electrode path lengths on graphite and brass, and also include results for a pair of long straight electrodes. The range of arc current has been extended to 3700 amps and the applied magnetic field to 0.49 Wb/m^2 for experiments on a pair of straight electrodes.

The results are analysed using a simple model for the arc motion assuming that the arc behaves in the same way as a body in a gas stream. Some

(Over)

A.R.C. C.P. No.993
December 1965

537.523.5 :
538.63 :
532.5

Adams, V. W.

THE INFLUENCE OF GAS STREAMS AND MAGNETIC FIELDS ON ELECTRIC DISCHARGES
PART 3. ARCS IN TRANSVERSE MAGNETIC FIELDS AT ATMOSPHERIC PRESSURE

Experimental results in air at a pressure of one atmosphere on the behaviour of arcs *under the action of applied magnetic fields are given for two electrode materials (graphite and brass) and different electrode configurations. These results extend earlier work, in annular gaps using graphite, to larger electrode path lengths on graphite and brass, and also include results for a pair of long straight electrodes. The range of arc current has been extended to 3700 amps and the applied magnetic field to 0.49 Wb/m^2 for experiments on a pair of straight electrodes.

The results are analysed using a simple model for the arc notion assuming that the arc behaves in the same way as a body in a gas stream. Some

(Over)

comments are made on a major difference between results for bras3 and graphite electrodes in experiments where the arc wake might affect tne arc motion (annular gaps). Arc drag areas are calculated for results where the arc wake does not affect the motion (pair of open-ended rail electrodes) and are found to be about one half of the maximum luminous frontal area3 of the arc determined photographically. A tentative picture of the arc's cross-sectional shape is also given.

Finally, the results are analysed according to a theory for convection-stabilised arc column3 and snoothed-out results for arcs moving through stationary air at constant temperature are shown to agree qualitatively with this theory.

However, a direct analogy between an arc and a heated solid body in a transverse gas flow 1s shown to be inadequate.

comments are made on a major difference between results For brass and graphite electrodes in expriments where the arc wake might affect the arc motion (annular gaps). Arc drag areas are calculated for results where the arc wake does not affect the motion (pair of open-ended rail electrodes) and are round to be about one half or the maximum luminous frontal areas or the arc determined photographically. A tentative picture of the arc's cross-sectional shape is also given.

Finally, the results are analysed according to a theory for convection-stabilised arc columns and snoothed-out results for arcs moving through stationary air at constant temperature are shown to agree qualitatively with this theory.

However, a direct analogy between an arc and a heated solid body in a transverse gas flow is shown to be inadequate.

comments an made on a major difference between results for brass and graphite electrodes in expriments where the arc wake might affect the arc motion (annular gaps). Arc drag areas are calculated for results where the arc wake does not arfect the motion (pair of open-ended rail electrodes) and are found to be about one half of the maximum luminous frontal areas of the arc determined photographically. A tentative picture of the arc's cross-sectional shape is also given.

Finally, the results are analysed according to a theory for convection-stabilised arc columns and snoothed-out results for arcs moving through stationary air at constant temperature are shown to agree qualitatively with this theory.

However, a direct analogy between an arc and a heated solid body in a transverse gas flow is shown to be inadequate.

Published by
HER MAJESTY'S STATIONERY OFFICE.

To be purchased from
49 High Holborn, London W.C.1
423 Oxford Street, London W.1
13A Castle Street, Edinburgh 2
109 St. Mary Street, Cardiff
Brazennose Street, Manchester 2
50 Fairfax Street, Bristol 1
35 Smallbrook, Ringway, Birmingham 5
7-11 Linenhall Street, Belfast 2
or through any bookseller

C.P. No. 959

S.O. CODE No. 23-9017-59